POLYMER NANOCOMPOSITES

Crystallization, Reinforcement and Conductivity through SWNTs

Thesis submitted to

Cochin University of Science and Technology

in partial fulfillment of the requirements for the award of the degree of

Doctor of Philosophy

under the

Faculty of Technology

by

Anoop Anand K

Department of Polymer Science and Rubber Technology
Cochin University of Science and Technology
Cochin- 682 022, Kerala, India
http://cusat.ac.in/

December 2006

Certificate

Certified that, the thesis entitled **'POLYMER NANOCOMPOSITES: Crystallization, Reinforcement and Conductivity through SWNTs'** submitted to Cochin University of Science and Technology under the Faculty of Technology, by Mr. Anoop Anand K, is an authentic record of the original research carried out by him under my supervision and guidance. The thesis has fulfilled all the requirements as per regulations and no part of the results embodied has been submitted to any other institution for any other degree/diploma.

Cochin
20th Dec 2006

Dr. Rani Joseph
Professor
Dept. of Polymer Science and Rubber Technology
Cochin University of Science and Technology
Cochin-22, Kerala

Declaration

I hereby declare that, the thesis entitled **'POLYMER NANOCOMPOSITES: Crystallization, Reinforcement and Conductivity through SWNTs'** submitted to Cochin University of Science and Technology, under the Faculty of Technology, is based on the original research carried out by me under the supervision of Dr. Rani Joseph, Professor, Dept. of Polymer Science and Rubber Technology, and further, no part of the results presented has been submitted to any other institution for any other degree/diploma.

Cochin
20th Dec 2006

Anoop Anand K

...to the one who always treasured my life, for her unstinted support,

unconditional love and care

Acknowledgements

At this moment of great happiness, I would like to express my heartfelt thanks to all people who have directly or indirectly contributed to the successful completion of this thesis in every possible way.

First and foremost, I am beholden to my Professor, Dr. Rani Joseph for her constant support and guidance. Teacher, I wish to record my sincere gratitude for providing me all the facilities and freedom throughout the course of my research.

Uday, I honestly appreciate the motivation, support and care, that you have given me allthrough my Ph.D. You are very special to me, made me enjoy the perfection in carrying out the experiments/ interpreting the results/ writing the articles... After all, you are the real source of my inspiration, thank you so much.

I profoundly thank Dr. K.E. George, former Head of PSRT for his kind concern. I extend my thanks to all the faculty members of PSRT: Dr. Thomas Kurian (Head of the Dept.), Dr. Philip Kurian, Dr. Eby Thomas Thachil, Dr. Sunil KN Kutty and Ms. Jayalatha Gopalakrishnan. I am also thankful to Dr. A.P. Kuriakose, former Head of PSRT and Dr. K.N. Ninan (ISRO), Visiting professor, for their support.

I express my deep sense of gratitude to all my beloved colleagues who were always encouraging and helpful, in particular, my group mates. I owe a lot to all of you: Dr. Honey John for your love and compassion (especially at the critical moments); Dr. Lovely Mathew for your support and concern; Dr. Rinku Mariam for your enthusiasm in my work; Dr. Ushamani for your imperative suggestions; Dr. Vipin Rajan for your timely tips; Abhilash for being a good lab partner; Aswathy for being a 'PET/nano mate'; Dhanya for your amiable company; Joshy sir for your pleasing approach and Maya teacher for being perceptive with my ups and downs. I am extremely thankful to Sunil Jose for introducing me to the wonderful world of *Macromolecules* and helping me in all the possible ways. A special word of thanks to Nisha for her special love and care...I was really enjoying the funny fights with you dear, thanks a lot. I would also like to acknowledge the valuable suggestions, affection

and support of my senior colleagues, Dr. Jacob, Ms. Lity and Dr. Thomas. I am profoundly thankful to Saritha for being an unforgettable (!) companion. A special word of thanks to Sinto for his assistance during the tedious Haake experiments. I express my heartfelt gratitude to rest of the 'PSRTians' especially Bipin, Newsun, and Sreekanth and to the 'FIP' teachers for their inspiration. Parameswaran sir, our *upper class* train journeys back home were just pleasing and relaxing... I also value the support from the secretarial and technical staff of PSRT. Special thanks to Mr. Bakker and Ms. Jyothy for their immense help with the administrative part of the projects.

I am grateful to Jayaram (Sathyabhama University), Jomy (IIT Roorkey), Justin (C-MET), Dr. Radhika (DAC, CUSAT), Sreelekha (IIT B) and Vikram (VSSC) for their support. I would also like to extend my thanks to my friends from the Departments of Physics, Applied Chemistry and Biotechnology of CUSAT for their help. Special thanks to Antony for his inspiration in the initial stage of my research, Jaison for being with me always for a support and Jayakrishnan for his constant encouragement, for making my weekends relaxed and funny... I also remember my school and college teachers, for their wishes and advices.

A major part of my project was completed in the Department of Chemical Engineering and Chemistry of Technical University of Eindhoven (TU/e), the Netherlands. Financial support was offered from the '**Netherlands organisation for international cooperation in higher education (NUFFIC)**' within the framework of the 'Joint financing programme for cooperation in higher education (MHO)'. I am particularly grateful to Prof. Dr. P.J. Lemstra for allowing the use of several laboratory facilities and Ir. Patrick van Schijndel, the pioneer of the programme for his support and help.

I would like to thank Ir. M.M.R.M Hendrix, for WAXD experiments, Prof. Dr. G. de Wit, for thermal expansion studies and Ir. Luiji Bolzano, for helping me with ARES measurements. I appreciate the support from Ir. Wouter Gerritsen and Ir. Pauline Schmit. My heartfelt thanks to Dr. Soney Varghese for his affection and support (and ofcourse, for the utmost patience with SEM/AFM!), and Dr. Merina Rajan, my only Indian office mate for the wonderful friendship she had with me. My sincere thanks to all my group mates at TU/e: Dr. Lijing Xue, Dr. Yunquian Ma, Cees Weijers and

Irina Cotiuga: I had a very pleasing time sharing a group with you my dear friends, thanks for the warm memories; the coffee breaks, the nice Dutch parties...! A very special thanks to my dear friend Jimmy and his family and to Salman Naimat, Pakistani colleague of mine, for his concern. My heartiest thanks to all my Indian friends at Eindhoven; Dr. Jojo, Dr. Prasanth, Dilna, Lopa, Rajesh and Sivaji for their encouragement and help. I extend my gratitude to Mrs. Charvi Agarwal, for a very nice friendship during my stay at Eindhoven.

A very special word of thanks to Dr. T.V. Sreekumar, Asst. Director, Defence Materials and Stores Research and Development Establishment (DMSRDE), Kanpur, for the support and guidance I received from him during the fiber drawing experiments. I am grateful to Dr. K.U. Bhasker Rao, Director, DMSRDE and Dr. Anurag Srivastava, Head of the Dept. of Fiber, Fabric and Interactive Textiles for permitting me to carry out the experiments. I am particularly thankful to Ms. Priyanka Katiyar, Scientist, for her constant assistance with the fiber spinning/drawing processes.

I extend my heartfelt gratitude to Dr. Arup Bhattacharyya (IIT Bombay), Dr. Rosamma Alex (RRII, Kottayam) and Dr. S.N. Potty (C-MET, Thrissur). I sincerely appreciate their unconditional support during the last phase of my Ph.D. I also wish to record my sincere thanks to Reliance Industries Ltd. for helping with several experiments.

I am indebted to the **Department of Science and Technology (DST), Government of India**, for financially supporting the project, '*Nanocomposites: Reinforcement and Conductivity in Natural Rubber through Carbon Nanotubes*', the findings of which contribute one chapter of this thesis. Thanks to **All India Council for Technical Education (AICTE), Government of India**, for the financial support received at the early stages of this research.

I am grateful to Indian Institute of Science (IISc), 'Nanotechnology Initiative' of DST, Indian Institute of Chemical Engineers (IIChE), Indian Association for the Cultivation of Science (IACS), Materials Research Society of India (MRSI), Kerala State Council for Science, Technology and Environment (KSCSTE), Society of Polymer Technologists

(SPOT), Mahatma Gandhi University, University of Calicut, and Rubber Technology Centre (RTC) of IIT KGP for creating platforms for fruitful interactions with eminent scientists all over the world.

I bow my head to my beloved parents and my uncle (and his family) for their constant motivation and support; this dissertation is the fulfillment of a great dream they had. I dedicate this thesis for their wholehearted love and prayers without which this venture would not have materialized.

...and... I am gratified to His Almighty, on the successful completion of my research in an incredible department with two of the best Ph.D coaches!

Thank You!

Contents

Preface

Carbon nanotubes (CNTs) have been widely considered as attractive candidates for use as fillers in composite materials due to their distinctly superior mechanical, thermal, electrical and electronic properties. The CNT can be thought of as the ultimate carbon fiber with breaking strengths reported as high as 200 GPa, and elastic modulii in the 1 TPa range. This, coupled with their enormous surface area per gram and large aspect ratios, has triggered a revolution in using CNTs as a reinforcing phase for polymer matrices.

The current research investigates the possibility of using single walled carbon nanotubes (SWNTs) as filler in polymers to impart several properties to the matrix polymer. SWNTs in a polymer matrix like poly(ethylene terephthalate) induce nucleation in its melt crystallization, provide effective reinforcement and impart electrical conductivity. We adopt a simple melt compounding technique for incorporating the nanotubes into the polymer matrix. For attaining a better dispersion of the filler, an ultrasound assisted dissolution-evaporation method has also been tried. The resulting enhancement in the materials properties indicates an improved disentanglement of the nanotube ropes, which in turn provides effective matrix-filler interaction. PET-SWNT nanocomposite fibers prepared through melt spinning followed by subsequent drawing are also found to have significantly higher mechanical properties as compared to pristine PET fiber.

SWNTs also find applications in composites based on elastomers such as natural rubber as they can impart electrical conductivity with simultaneous improvement in the mechanical properties.

This thesis is divided into seven chapters:

Chapter 1 presents a concise introduction to the subject. Carbon nanotubes, their synthesis, growth mechanism, structure, properties and applications are briefly reviewed. The state-of-art research in polymer-carbon nanotube nanocomposites is discussed. The principal objectives of the work are mentioned at the end of the chapter.

Chapter 2 deals with the preparation and crystallization characteristics of nanocomposites of poly(ethylene terephthalate) and single walled carbon nanotubes. The composites have been prepared by a simple melt compounding technique and their crystallization characteristics have been investigated using differential scanning calorimetry and wide angle X-ray diffraction analysis.

Chapter 3 includes the evaluation of mechanical properties of PET-SWNT nanocomposites. The viscoelastic characteristics of the nanocomposites are presented here. Thermal and dimensional stability as well as electrical conducting properties are also investigated.

Chapter 4 presents the method of preparing nanocomposites through ultrasound assisted dissolution-evaporation. Crystallization, mechanical, dynamic mechanical, thermal and electrical properties of these nanocomposite samples are studied.

Chapter 5 comprises the fabrication of PET-SWNT nanocomposite fibers through melt spinning. The effect of fiber formation conditions on the development of their mechanical properties is studied.

Chapter 6 deals with the preparation and characterization of nanocomposites based on natural rubber with carbon nanotubes. The nanotubes have been incorporated into the elastomer matrix through conventional mill mixing as well as latex stage mixing. The mechanical, electrical, thermal and ageing characteristics of NR-SWNT nanocomposites are presented in this chapter.

Chapter 7 presents summary and conclusions of the investigations.

Chapter 1

General introduction

Our ability to engineer novel structures has led to unprecedented opportunities in materials design. It has fueled rapid development in nanoscience and nanotechnology for the past one decade leading to the creation of new materials with interesting nanoscale features. In the framework of this rapid development, the domain of nanocomposite materials is attracting more and more researchers; both academic and industrial. The field of nanocomposites involves the study of multiphase materials where atleast one of the constituent phases has atleast one dimension of the order of nanometers.[1] The use of these nanoscale fillers to augment the properties of polymers has provided a radical alternative to conventional composites and modified polymers. The promise of nanocomposites lies in their multifunctionality, the possibility of realising unique combinations of properties unachievable with traditional materials.

The current research aims to investigate the possibility of use of carbon nanotubes for fabricating polymer-based nanocomposites and thereby imparting several properties to the matrix polymer. In this chapter, a concise introduction to the subject is presented. Carbon nanotubes, their synthesis, growth mechanism, structure, properties and applications are briefly reviewed. The state-of-art research in polymer-carbon nanotube nanocomposites is also discussed. An outline of the principal objectives of the work is given at the end of the chapter.

1.1 Carbon nanotubes

The ground breaking discovery of carbon nanotubes (CNTs), in 1991 followed by the realisation of their amazing properties led scientists all over the world to focus their research efforts on these fascinating structures. Carbon nanotubes (also known as bucky tubes) are long thin cylinders of carbon that are unique for their size, shape, and

remarkable physical and electrical properties.[2-5] They can be thought of as layers of the conventional graphite structure rolled up into a cylinder such that the lattice of carbon atoms remains continuous around the circumference. Their name is derived from their size, since the diameter of a nanotube is of the order of a few nanometers (approximately 50,000 times smaller than the width of a human hair), while they can be upto several micrometres in length.

The number of carbon shells in CNTs varies from one to as many as fifty, the former being single walled carbon nanotubes- SWNTs and the latter, multi walled carbon nanotubes- MWNTs. These intriguing structures have sparked much excitement in recent years and a large amount of research has been dedicated to their understanding.[6-8] They are potentially useful in a wide variety of applications in nanotechnology, electronics, optics, and other fields of materials science.[9-14]

1.1.1 The discovery

The discovery of carbon nanotubes dates back to the 1985-legendary sequence of experiments by Harry Kroto, of the University of Sussex, and Richard Smalley, of Rice University, Houston.[15,16] During the vaporisation of graphite, Kroto and Smalley were struck by a surprising outcome: in the distribution of the resulted gas-phase carbon cluster, detected by mass spectroscopy, C_{60} was by far the most dominant species. Later they realised that a *closed* cluster containing precisely 60 carbon atoms would have a structure of unique stability and symmetry, as shown in figure 1.1. Although they had no direct evidence to support this structure, subsequent work has proved them correct. The discovery of C_{60} published in *Nature* in November 1985, had an impact, which extended the way beyond the confines of academic chemical physics, and marked the beginning of a new era in carbon science.[17,18]

In the beginning, however, the progress was slow mainly because of the small quantity of C_{60} produced in the Kroto-Smalley experiments. Eventually, more than a laboratory curiosity, the bulk production of C_{60} was achieved by a technique developed by Wolfgang Krätschmer of the Max Planck Institute at Heidelberg, and Donald Huffman of the University of Arizona. They used a simple carbon arc to vaporize graphite

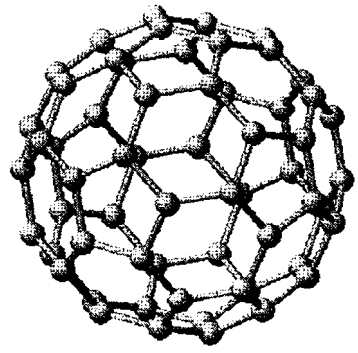

Fig. 1.1 C_{60}: Buckminster Fullerene

in an atmosphere of helium and collected the soot, which settled on the walls of the vessel. Dispersing the soot in benzene produced a red solution, which could be dried down to produce beautiful plate like crystals of 'fullerite': 90 %, C_{60} and 10 %, C_{70}. This report appeared in *Nature* in 1990.[19]

Sumio Iijima of the NEC laboratories in Japan, was fascinated by the Krätschmer-Huffman *Nature* paper, and decided to embark on a detailed study of the soot produced by their technique. The initial High-Resolution Transmission Electron Microscopic (HRTEM) studies were disappointing: the soot collected from the walls of the arc-evaporation vessel appeared almost completely amorphous, with little obvious long-range structures.

Eventually, Iijima turned his attention to the hard cylindrical deposit, which formed on the graphite cathode after arc evaporation. This cathodic soot contained a whole range of novel graphitic structures, the most striking of which were hollow fibers, finer and more perfect than any previously seen. Iijima's beautiful images of carbon nanotubes, shown first at a meeting at Richmond, Virginia in October 1991, and published in *Nature* a month later (figure 1.2).[20]

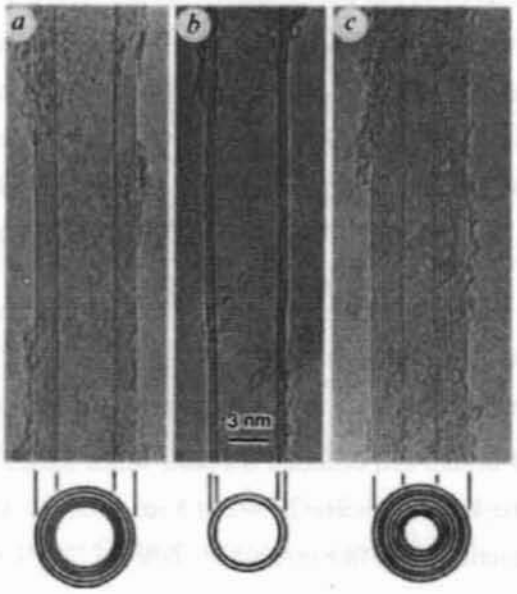

Fig. 1.2 Iijima's electron micrographs of carbon nanotubes (from reference 20)

1.1.2 Preparation methods and growth mechanisms

Carbon nanotubes are generally produced by three main techniques; arc discharge, laser ablation and chemical vapour deposition. In arc discharge method, a vapour is created by an arc discharge between two carbon electrodes with or without catalyst and nanotubes self-assemble from the resulting carbon vapour. In the laser ablation technique, a high-power laser beam impinges on a volume of carbon-containing feedstock gas (CH_4 or CO_2). Laser ablation produces a small amount of clean nanotubes, whereas arc discharge methods generally produce large quantities of impure material. Chemical vapour deposition (CVD) results in MWNTs or poor quality SWNTs. The SWNTs produced by CVD method have a large diameter range, which can be poorly controlled. But on the other hand, this method is very easy to scale up, what favours commercial production.

1.1.2.1 Arc discharge

The carbon arc discharge method, initially used for producing C_{60} fullerenes, is the most common and perhaps the easiest way to produce carbon nanotubes as it is rather simple to undertake. However, it is a technique that produces a mixture of components and requires separating nanotubes from the soot and the catalytic metals present in the crude product.

This method creates nanotubes through arc-vaporisation of two carbon rods placed end to end, separated by approximately 1 mm, in an enclosure that is usually filled with an inert gas (He, Ar) at low pressure (between 50 and 700 mbar). Recent investigations have shown that it is also possible to create nanotubes with the arc method in liquid nitrogen.[21] A direct current of 50 to 100 A driven by approximately 20 V creates a high temperature discharge between the two electrodes. The discharge vaporises one of the carbon rods and forms a small rod shaped deposit on the other rod. Producing nanotubes in high yield depends on the uniformity of the plasma arc and the temperature of the deposit form on the carbon electrode.[22]

Depending on the exact technique, it is possible to selectively grow SWNTs or MWNTs, which is shown in figure 1.3. Two distinct methods of synthesis can be performed with the arc discharge apparatus. If SWNTs are preferable, the anode has to be doped with metal catalyst, such as Fe, Co, Ni, Y or Mo. A lot of elements and mixtures of elements have been tested by various authors and it is noted that the results vary a lot, even though they use the same elements.[23] This is not surprising as the experimental conditions differ. The quantity and quality of the nanotubes obtained depend on various parameters such as the metal concentration, inert gas pressure, kind of gas, the current and system geometry. Usually the diameter is in the range of 1.2-1.4 nm.

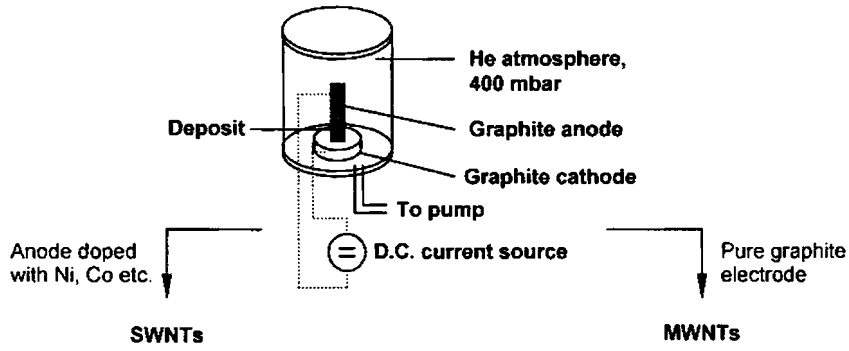

Fig. 1.3 Experimental set-up of an arc discharge process

1.1.2.2 Laser ablation

In 1995, Smalley's group at Rice University reported the synthesis of carbon nanotubes by laser vaporisation (figure 1.4).[24] A pulsed, or continuous laser is used to vaporise a graphite target in an oven at 1200 °C. The oven is filled with He or Ar gas in order to keep the pressure at 500 Torr. A very hot vapour plume forms, then expands and cools rapidly. As the vaporised species cool, small carbon molecules and atoms quickly condense to form larger clusters, possibly including fullerenes. The catalysts also begin to condense, but more slowly at first, and attach to carbon clusters and prevent their closing into cage structures.[25] Catalysts may even open cage structures when they attach to them. From these initial clusters, tubular molecules grow into single walled carbon nanotubes until the catalyst particles become too large, or until conditions have cooled sufficiently that carbon no longer can diffuse through or over the surface of the catalyst particles. It is also possible that the particles become that much coated with a carbon layer that they cannot absorb more and the nanotubes stop growing. The SWNTs formed are bundled together by van der Waals forces.

Laser ablation is almost similar to arc discharge, since the optimum background gas and catalyst mix is the same as in the arc discharge process. This might be due to very similar reaction conditions needed, and the reactions probably occur with the same mechanism. The condensates obtained by laser ablation are normally contaminated

with amorphous carbon particles. In the case of pure graphite electrodes, MWNTs would be synthesised, but uniform SWNTs could be synthesised if a mixture of graphite with Co, Ni, Fe or Y is used instead of pure graphite. Transmission electron microscopic (TEM) image of a bundle of SWNTs ('ropes') synthesised by laser ablation is shown in figure 1.4.[26]

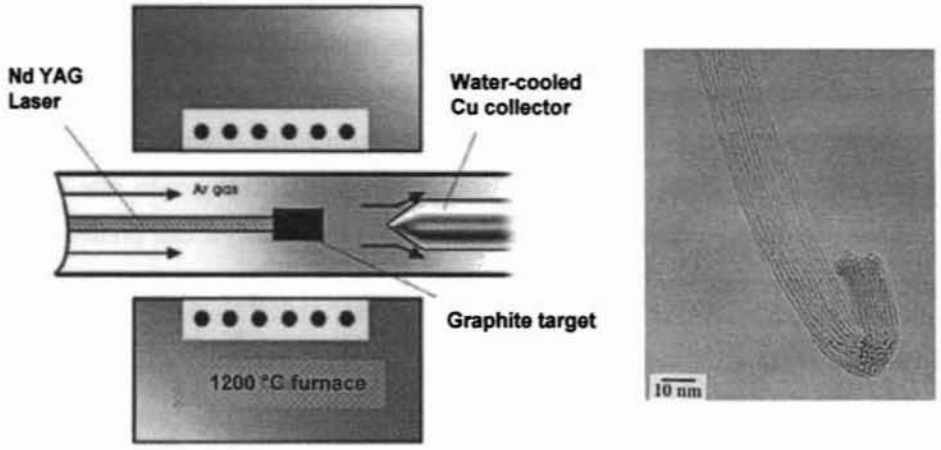

Fig. 1.4 Left: Schematic drawing of a laser ablation apparatus (from ref. 24). Right: TEM image of a bundle of SWNTs catalysed by Ni/Y (2:0.5 at wt%) mixture, produced with a continuous laser (from ref. 26)

Laser vaporisation results in a higher yield of SWNTs having better properties and a narrower size distribution than those produced by arc-discharge. In the case of a continuous laser at 1200 °C and Ni/Y catalyst (Ni/Y = 2/0.5), SWNTs with an average diameter of 1.4 nm were formed with 20-30 % yield. Because of the good quality of nanotubes produced by this method, scientists are trying to scale up laser ablation. However the results are not yet as good as for the arc discharge method, but they are still promising.

1.1.2.3 Chemical vapour deposition

Chemical vapour deposition (CVD) synthesis is achieved by putting a carbon source in the gas phase and using an energy source, such as plasma or a resistively heated coil, to transfer energy to gaseous carbon source. Commonly used gaseous carbon sources include CH_4, CO and C_2H_2. The energy is used to 'crack' the molecule into reactive atomic carbon. Then the carbon diffuses towards the substrate, which is heated and coated with a catalyst (usually a first row transition metal such as Ni, Fe or Co) where it will bind. Carbon nanotubes will be formed if the proper parameters are maintained. Excellent alignment, as well as positional control on nanometer scale, can be achieved by using CVD.[27,28] Control over the diameter, as well as the growth rate of the nanotubes can also be maintained. The appropriate metal catalyst can preferentially grow single rather than multi walled nanotubes.[29]

CVD carbon nanotube synthesis is essentially a two-step process consisting of a catalyst preparation step followed by the actual synthesis of the nanotubes. The catalyst is generally prepared by sputtering a transition metal onto a substrate and then using either chemical etching or thermal annealing to induce catalyst particle nucleation. Ammonia may be used as the etchant.[30] Thermal annealing results in cluster formation on the substrate, from which the nanotubes will grow. The temperatures for the synthesis of nanotubes by CVD are generally within the 650-900 °C ranges.[31] Typical yields of CVD are approximately 30 %. In the last decennia, different techniques for the carbon nanotubes synthesis with CVD have been developed, such as plasma enhanced CVD, thermal chemical CVD, alcohol catalytic CVD, vapour phase growth, aero gel-supported CVD and laser-assisted CVD.

1.1.2.4 CoMoCat process

In this method, SWNTs are grown by CO disproportionation at 700-950 °C. The technique is based on a unique Co-Mo catalyst formulation that inhibits the sintering of Co particles and therefore inhibits the formation of undesired forms of carbon that lower the selectivity.

During the reaction, cobalt is progressively reduced from the oxidic state to the metallic form. Simultaneously molybdenum is converted to the carbidic form (Mo_2C). Co acts as the active species in the activation of CO, while the role of Mo is possibly dual. It would stabilise Co as a well-dispersed Co^{2+}, avoiding its reduction and would act as a carbon sink to moderate the growth of carbon, inhibiting the formation of undesirable forms of carbon.[32] It was found that one of the critical conditions for an effective reactor operation is that the space velocity has to be high enough to keep the CO conversion as low as possible.

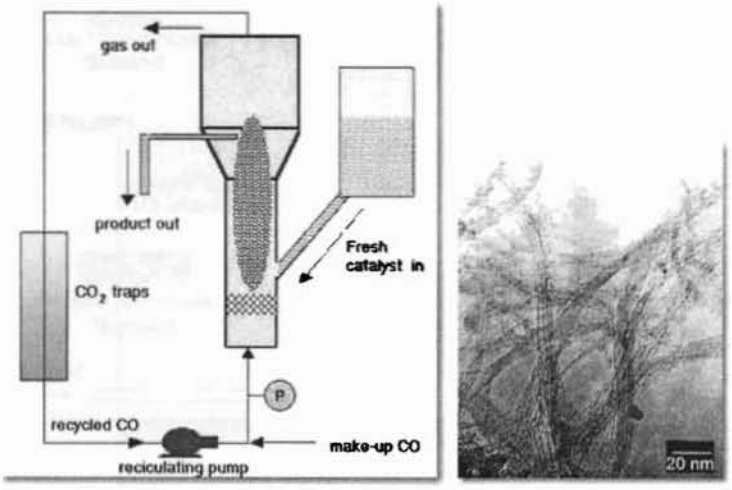

Fig. 1.5 Schematic diagram of a CoMoCat apparatus (left), TEM image of a raw product (right) (from ref. 33)

Figure 1.5 shows a fluidised bed reactor for a CoMoCat process. The most important advantage of fluidised bed reactors is that they permit continuous addition and removal of solid particles from the reactor, without stopping the operation. CoMoCat process is a method that can be scaled up without losses in SWNT quality. By varying the operation conditions, SWNTs can be produced with different diameter ranges. The CoMoCat catalyst has a high selectivity towards SWNTs, namely 80-90 %.[33]

1.1.2.5 High pressure CO disproportionation process

The high pressure CO disproportionation (HiPCO) process is a technique for catalytic production of SWNTs in a continuous-flow gas phase using CO as the carbon containing feedstock and $Fe(CO)_5$ as the iron-containing catalyst precursor. SWNTs are produced by flowing CO, mixed with a small amount of $Fe(CO)_5$ through a heated reactor. Figure 1.6 shows the layout of a CO flow-tube reactor. Size and diameter distribution of the nanotubes can be roughly selected by controlling the pressure of CO. This process is promising for the bulk production of SWNTs. Nanotubes as small as 0.7 nm in diameter, which are expected to be the smallest achievable chemically stable SWNTs, have been produced by this method.[34]

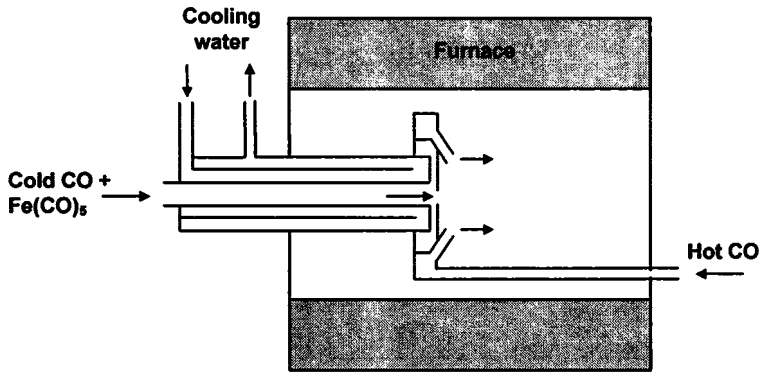

Fig. 1.6 Layout of CO flow-tube reactor

The average diameter of HiPCO SWNTs is 1.1 nm. The yield that could be achieved is approximately 70 %. The highest yields and narrowest tubes could be produced at the highest accessible temperature and pressure.[35] SWNT material with 97 % purity could be produced at rates of upto 450 mg/h.[36]

1.1.2.6 Growth mechanism

The way in which carbon nanotubes are formed is not exactly known. The growth mechanism is still a subject of controversy, and more than one mechanism might be operative during their formation.

One of the proposed mechanisms which is based on *in-situ* TEM observations consists of three steps. First, a precursor to the formation of nanotubes and fullerenes, C_2, is formed on the surface of the metal catalyst particle. From this metastable carbide particle, a rod like carbon is formed rapidly. Secondly there is a slow graphitisation of its wall (figure 1.7).[37]

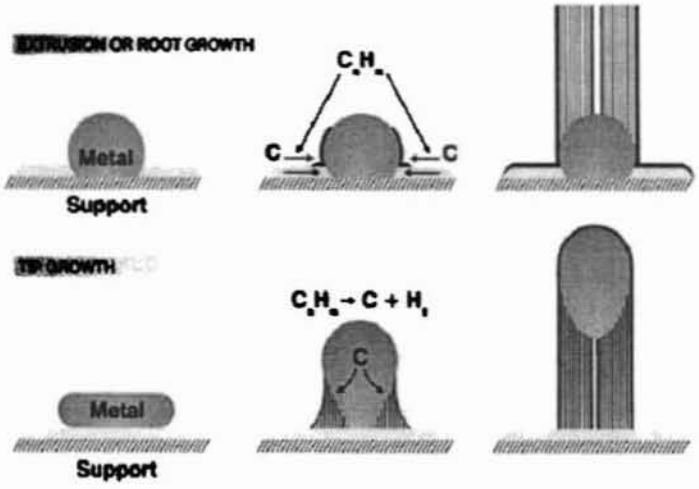

Fig. 1.7 Visualisation of a possible carbon nanotube growth mechanism (from ref. 37)

There are several other theories on the exact growth mechanism for nanotubes. One of them postulates that metal catalyst particles are floating or are supported on graphite or another substrate.[29] It presumes that the catalyst particles are spherical or pear-shaped, in which case the deposition will take place only on one half of the surface (this is the lower curvature side for the pear shaped particles). The carbon diffuses along the concentration gradient and precipitates on the opposite half, around and below the bisecting diameter. However, it does not precipitate from the apex of the hemisphere, which accounts for the hollow core that is characteristic of these structures.

For supported metals, nanotubes can form either by 'extrusion' (also known as base growth) in which they grow upwards from the metal particles that remain attached to the substrate, or the particles detach and move at the head of the growing nanotube,

labelled 'tip-growth'. Depending on the size of the catalyst particles, SWNTs or MWNTs are grown. In arc discharge, if no catalyst is present in the graphite electrode, MWNTs will be grown on the C_2 particles that are formed in the plasma.

1.1.3 Structure and properties

1.1.3.1 Structure of carbon nanotubes

It is the chemical genius of carbon that it can bond in different ways to create structures with entirely different properties. Graphite and diamond, the two bulk solid phases of pure carbon, bear testimony to this. The mystery lies in the different hybridisation that carbon atoms can assume. The four valence electrons in carbon, when shared equally (sp^3 hybridised), create isotropically strong diamond. But when only three are shared covalently between neighbours in a plane and the fourth is allowed to be delocalised among all atoms, the resulting material is graphite. The latter (sp^2) type of bonding builds a layered structure with strong in-plane bonds and weak out-of-plane bonding of the van der Waals type. Graphite, hence, is weak normal to its planes and is considered as a soft material due to its ability to slide along the planes. The story of fullerenes and nanotubes belongs to the architecture of sp^2 bonded carbon and the subtlety of a certain group of topological defects that can create unique, closed shell structures out of planar graphite sheets.[38]

Graphite is the thermodynamically stable bulk phase of carbon upto very high temperatures under normal ranges of pressure (diamond is only kinetically stable). It is now well known that this is not the case when there are only a finite number of carbon atoms. Simply speaking, this has to do with the high density of dangling bond atoms when the size of the graphite crystallites becomes small (say, nanosize). At small sizes, the structure does well energetically by closing onto itself and removing all the dangling bonds. Preliminary experiments done in the mid 1980s, which served as the precursor to the fullerene discovery, suggested that when the number of carbon atoms is smaller than a few hundred, the structures formed correspond to linear chains, rings, and closed shells.[39] The latter, called fullerenes, are closed shell all

carbon molecules with an even number of atoms (starting at C_{28}) and sp^2 bonding between adjacent atoms.

To form curved structures (such as fullerenes) from a planar fragment of hexagonal graphite lattice, certain topological defects have to be included in the structure. To produce a convex structure, positive curvature has to be introduced into the planar hexagonal graphite lattice. This is done by creating pentagons. It is a curious consequence of the Euler's principle that one needs exactly 12 pentagons to provide the topological curvature necessary to completely close the hexagonal lattice; hence, in C_{60} and all the other fullerenes (C_{2n} has (n-10) hexagons) there are many hexagons but only 12 pentagons. The rule of pentagon numbers will hold, however big the closed structure may be created out of hexagons and pentagons. One can thus imagine that a greatly elongated fullerene can be produced with exactly 12 pentagons and millions of hexagons. This would correspond to a carbon nanotube.[40]

The structure of a single walled carbon nanotube (SWNT) can be conceptualized by wrapping a one-atom-thick layer of graphite (called graphene) into a seamless cylinder and when concentric cylinders, one inside the other are present, they are referred to as multi walled carbon nanotubes (MWNTs).[41] Most SWNTs have a diameter of close to 1 nm, with a tube length that can be many thousands of times larger (figure 1.8). SWNTs with length upto orders of centimeters have been produced.

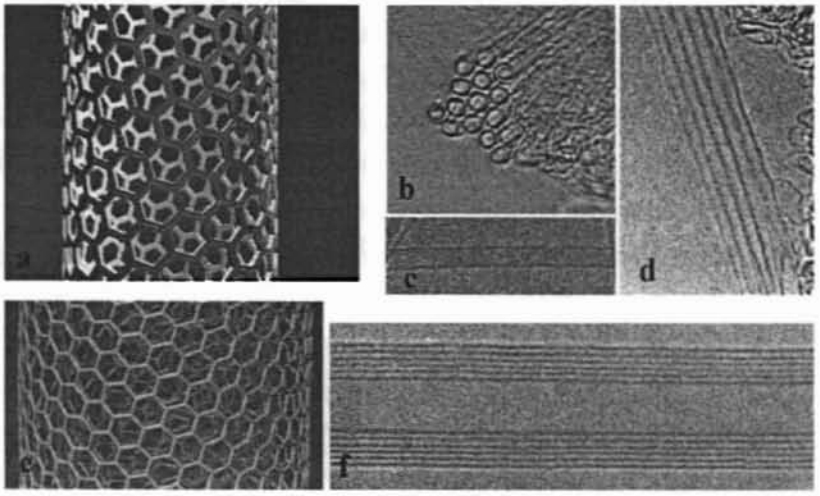

Fig. 1.8 Structure of single walled (SWNT) (a-d) and multi walled (MWNT) (e, f) carbon nanotubes (from ref. 38)

In the figure, (a) shows a schematic of an individual SWNT. (b) shows a cross-sectional view (TEM image) of a bundle of SWNTs [transverse view shown in (d)]. Each nanotube has a diameter of ~ 1.4 nm and the tube-tube distance in the bundles is 0.315 nm. (c) shows the HRTEM image of a 1.5 nm diameter SWNT. (e) is the schematic of a MWNT and (f) shows HRTEM image of an individual MWNT. The distance between layers of the tube in (f) is 0.34 nm.

The way the graphene sheet is wrapped is represented by a pair of indices (n,m) called the chiral vector. The integers n and m denote the number of unit vectors along two directions in the honeycomb crystal lattice of graphene. If m=0, the nanotubes are called 'zigzag'. If n=m, the nanotubes are called 'armchair'. Otherwise, they are called 'chiral' (figure 1.9).

The (n,m) nanotube naming scheme can be thought of as a vector (C_h) in an infinite graphene sheet that describes how to 'roll up' the graphene sheet to make the nanotube. a_1 and a_2 are unit vectors of graphene in real space.

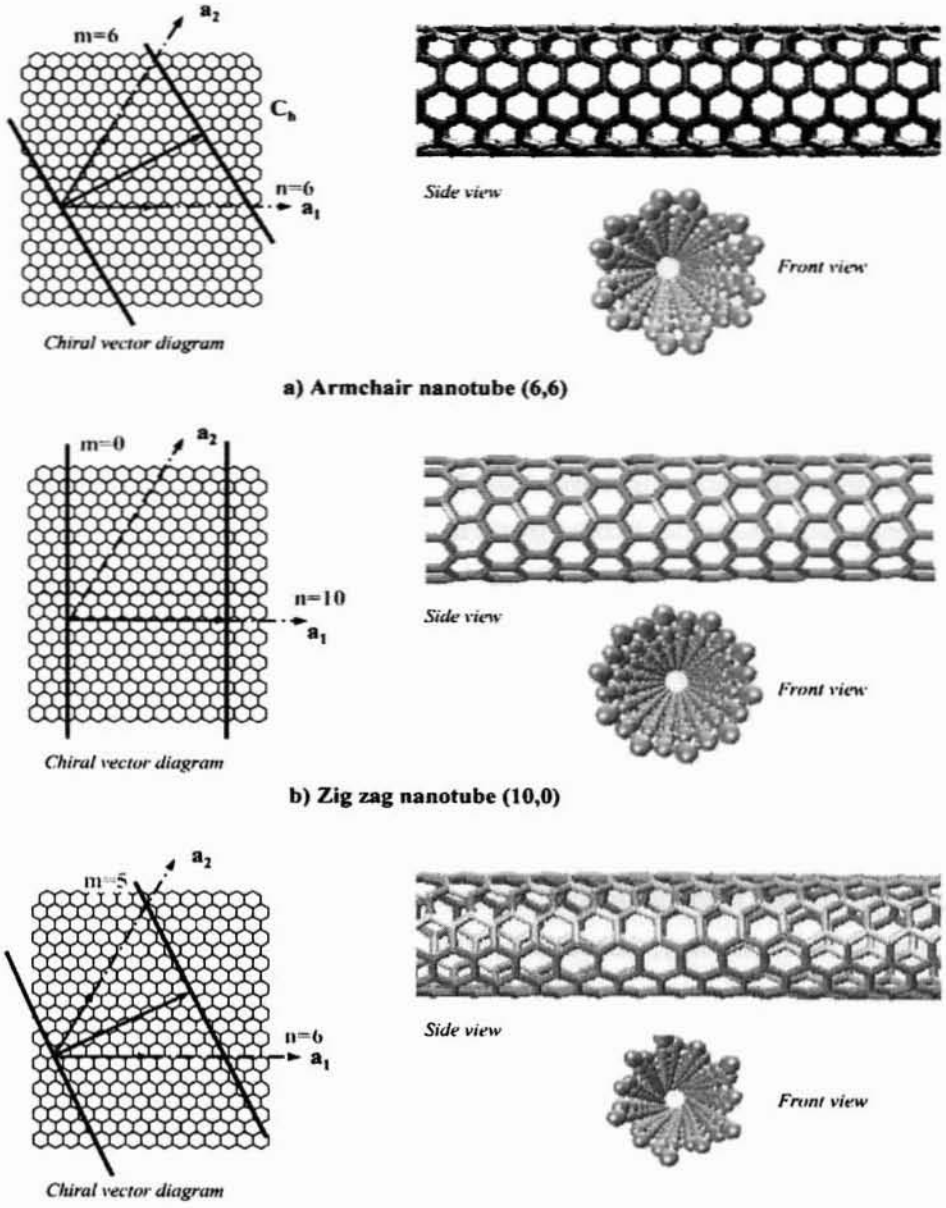

Fig. 1.9 Structure of carbon nanotubes with the (n,m) naming scheme (from ref. 61)

1.1.3.2 Mechanical, electrical and thermal properties of carbon nanotubes

Carbon nanotubes are one of the strongest materials known to man, both in terms of tensile strength and elastic modulus.[42] The strength results from the covalent sp^2 bonds formed between the individual carbon atoms. In 2000, a nanotube was tested to have a tensile strength of 63 GPa. In comparison, high-carbon steel has a tensile strength of approximately 1.2 GPa. CNTs also have very high elastic modulus, of the order of 1 TPa.[43] Since carbon nanotubes have a low density for a solid of 1.3-1.4 g/cm^3, its specific strength is the best of known materials.

Under excessive tensile strain, the tubes will undergo plastic deformation, which means the deformation is permanent. This deformation begins at strains of approximately 5 % and can increase till the maximum strain the tube undergoes before fracture by releasing strain energy. CNTs are not nearly as strong under compression. Due to their hollow structure, they tend to undergo buckling when placed under compressive, torsional or bending stress.

Multi walled carbon nanotubes, multiple concentric nanotubes precisely nested within one another, exhibit a striking telescoping property whereby an inner nanotube core may slide, almost without friction, within its outer nanotube shell thus creating an atomically perfect linear or rotational bearing. This is one of the first true examples of molecular nanotechnology, the precise positioning of atoms to create useful machines. This property has already been utilized to create the world's smallest rotational motor and a nanorheostat.

Due to the symmetry and unique electronic structure of graphene, the structure of a nanotube strongly affects its electrical properties. For a given (n,m) nanotube, if $2n + m = 3q$ (where q is an integer), then the nanotube is metallic, otherwise the nanotube is a semiconductor. Thus all armchair $(n=m)$ nanotubes are metallic, and nanotubes (5,0), (6,4), (9,1), etc. are semiconducting. In theory, metallic nanotubes can have an electrical current density more than 1,000 times stronger than metals such as silver and copper.

All nanotubes are expected to be very good thermal conductors along the tube, exhibiting a property known as 'ballistic conduction', but good insulators laterally to the tube axis.

1.1.3.3 Defects in nanotubes

As with any material, the existence of defects affects the nanotube properties. Defects can occur in the form of atomic vacancies. High levels of such defects can lower the tensile strength by upto 85 %.[44] Another well-known form of defect that occurs in carbon nanotubes is the Stone Wales defect, which creates a pentagon and heptagon pair by rearrangement of the bonds. Due to the almost one-dimensional structure of CNTs, the tensile strength of the tube is dependent on the weakest segment of it in a similar manner to a chain, where a defect in a single link diminishes the strength of the entire chain.

The nanotube's electrical properties are also affected by the presence of defects. A common result is the lowered conductivity through the defective region of the tube. Some defect formation in armchair-type tubes (which are metallic) can cause the region surrounding that defect to become semiconducting. Futhermore, single monoatomic vacancies induce magnetic properties. The thermal properties of the nanotubes are also heavily affected by defects.

1.1.4 Nanotube research

The method for producing nanotubes described by Iijima in 1991 gave relatively poor yields, making further research into their structure and properties difficult. A significant advance came in July 1992 when Thomas Ebbesen and Pulickel Ajayan made a serendipitous discovery of preparing nanotubes in gram quantities.[45] Further research made the availability of nanotubes in bulk quantities possible, which in turn gave an enormous boost to the pace of nanotube research worldwide.[46]

One area, which attracted early interest, was the idea of using carbon nanotubes as 'molecular containers'.[47] A landmark in this field was the demonstration by Ajayan

and Iijima that nanotubes could be filled with molten lead and thus be used as molds for 'nanowires'.[48] Subsequently more controlled methods for opening and filling nanotubes have been developed, enabling a wide range of materials, including biological ones, to be placed inside. The resulting opened or filled tubes might have fascinating properties, with possible applications in catalysis, or as biological sensors. Filled carbon nanoparticles may also have important applications in areas as diverse as magnetic recording and nuclear medicine.

Perhaps the largest volume of research into nanotubes has been devoted to their electronic properties. A short time after the publication of Iijima's 1991 letter in *Nature*, two other papers appeared on the electronic structure of carbon nanotubes.[49,50] Noriaki Hamada and colleagues from Iijima's laboratory in Tsukuba carried out band structure calculations on narrow tubes and demonstrated that the electronic properties are a function of both tube structure and diameter. These remarkable predictions stimulated a great deal of interest, but attempts to determine the electronic properties of nanotubes experimentally presented great difficulties. Since 1996, however, experimental measurements have been carried out on individual nanotubes, to confirm the theoretical predictions. The results have prompted speculation that nanotubes might become components of the future nanoelectronic devices.

SWNTs are the most likely candidates for miniaturizing electronics past the microelectromechanical scale that is currently the basis of modern electronics. The most basic building block of these systems is the electric wire, and SWNTs can be excellent conductors. One useful application of SWNTs is in the development of intramolecular field effect transistors (FETs).

A variety of other possible applications of nanotubes are currently of exciting interest. For example, transparent and electrically conductive films of carbon nanotubes have been developed to replace indium tin oxide (ITO) in LCDs, touch screens, and photovoltaic devices. Carbon nanotube films are substantially more mechanically robust than ITO films, making them ideal for high reliability touch screens and flexible displays. A number of groups are exploring the idea of using nanotubes as tip for

scanning probe microscopy. With their elongated shapes, pointed caps, and high stiffness, nanotubes would appear to be ideally suited for this purpose, and initial experiments in this area have produced some extremely impressive results.[51,52]

Conductive carbon nanotubes have been used for several years in brushes for commercial electric motors. They replace traditional carbon black, which are mostly impure spherical carbon particles. The nanotubes improve electrical and thermal conductivity because they stretch through the plastic matrix of the brush. This permits the carbon filler content to be reduced from 30 % down to 3.6 %, so that more matrix is present in the brush. Nanotube composite motor brushes are better-lubricated (from the matrix), cooler-running (both from better lubrication and superior thermal conductivity), less brittle (more matrix), stronger and more accurately moldable (more matrix). Since brushes are critical failure points in electric motors, and since they don't need much material, they became economical before almost any other application.

Experiments carried out using transmission electron spectroscopy and atomic force microscopy (AFM) have demonstrated that the mechanical characteristics of carbon nanotubes may be just as exceptional as their electronic properties. The strength and flexibility of carbon nanotubes make them of potential use in controlling other nanoscale structures, which suggests they will have an important role in nanotechnology engineering. As a result, there is growing interest in using nanotubes in composite materials. Overall, the volume of the nanotube research is growing at an astonishing rate, and commercial applications will surely not be far behind.[53]

1.2 Polymer-carbon nanotube nanocomposites

In recent years polymer nanocomposites have attracted great interest, both in industry and in academia, because they often exhibit remarkable improvement in materials properties when compared with virgin polymer or conventional micro and macro-composites. These improvements include high modulii, increased strength and heat resistance, decreased gas permeability and flammability, and increased biodegradability in the case of biodegradable polymers.[54-60] On the other hand, there has been considerable interest in theory and simulations addressing the preparation and

properties of these materials, and they are also considered to be unique model systems to study the structure and dynamics of polymers in confined environments.[61]

For the past one decade, carbon nanotube reinforced polymeric composite materials have spurred considerable attention in the materials research community, in part due to their potential to provide orders of magnitude increase in strength and stiffness when compared to typical fiber reinforced polymer composites. Their mechanical properties, coupled with their relatively low density, make these materials ideal candidates for weight-efficient structures and have been heavily scrutinized for the same. And for the same reason, CNTs are considered to be the ultimate reinforcement in polymeric composites. Since their documented discovery in early 1990s and the realisation of their unique physical properties, including mechanical, thermal and electrical, many investigators have endeavored to fabricate advanced CNT composites that exhibit one or more of these properties.[62-66] For example, as conductive filler in polymers, CNTs are quite effective compared to traditional carbon black microparticles, primarily due to their large aspect ratios. Similarly, CNTs possess one of the highest thermal conductivities known which suggests their use in composites for thermal management.[67]

The carbon nanotubes-polymer composites were initially reported by Ajayan *et al.*[68] They mechanically mixed purified MWNTs with epoxy resin, a most widely studied nonconjugated polymer-based composite system. Later Sandler *et al.* also reported the electrical percolation threshold at 0.0025 wt% nanotube loading and conductivity of 2 S/m at 1.0 wt% nanotubes in epoxy matrices.[69] Biercuk *et al.* have observed a monotonic increase of resistance to indentation by upto 3.5 times on adding 2 wt% SWNTs in epoxy resin.[70] Gong *et al.* also reported that using surfactants as wetting agents might improve the dispersion and thermo mechanical properties of carbon nanotubes-epoxy composites, but even with the addition of the surfactant, complete homogeneous dispersion of the nanotubes was not obtained.[71] There have also been many other reports in literature regarding the preparation and characterization of nanotube-epoxy nanocomposites.[72-77]

Composite films of polyvinyl alcohol (PVA) and nanotubes have been prepared by Shaffer *et al.*[78] Followed by casting to make films, chemically treated nanotubes were

mixed with aqueous polyvinyl alcohol solution, in order to prevent reaggregation. Each nanotube must be covered with a layer of polymer to form a stable mixture before it is able to interact with a number of other nanotubes. It was believed that 'in colloidal terms, the absorbed polymer sterically stabilizes the nanotube dispersion and protects it against bridging flocculation and depletion aggregation'. The electrical conductivities of composites showed typical percolation behavior and the presence of nanotubes stiffened the material, particularly at high temperature. However, the plausible mechanism seems to be too simple and was not confirmed directly. Zhang *et al.* also prepared PVA-SWNT composite films.[79] They observed a significant improvement in tensile strength and modulus for the composites as compared to control PVA. Cadek *et al.* found that adding 1 wt% MWNTs to polyvinyl alcohol increased the modulus and hardness by 1.8 times and 1.6 times, respectively.[80]

Poly(methyl methacrylate) (PMMA)-nanotubes composites were fabricated through an *in situ* process by Jia *et al.*[81] In the process, chemically treated nanotubes could link with PMMA, thus obstructing the growth of PMMA, producing a C-C bond between nanotubes and the PMMA. The dispersion ratio of nanotubes in the PMMA matrix is increased and the properties of the composites improved due to high interfacial strength. Stephan *et al.* also fabricated thin film of PMMA-SWNT composite by spin coating.[82] It was found that the polymer intercalated between nanotube bundles. At low concentration, the nanotubes dispersed well, thus more uniform films were prepared. A combination of solvent casting and melt mixing has also been used to fabricate SWNT-PMMA composites.[83] 'Melt mixing produced compositionally uniform films on the micrometer scale, while the films prepared by solvent casting were heterogeneous'. Mechanical properties and electrical conductivity of the aligned nanocomposite fibers were improved by melt spinning. Drawback of this method is that the melt spinning method described by the authors is too complex and time-consuming.

MWNTs have also been dispersed well in polystyrene by an ultrasonic assisted solution-evaporation method.[84] TEM investigations indicated that the nanotubes are homogeneously distributed at ~ 1 μm length scale. Only 1 wt% nanotube addition increased the polymer mechanical properties significantly.

Ago *et al.* reported that a uniform film of MWNTs and poly(p-phenylene vinylene) (PPV) was prepared by spin-coating a highly concentrated MWNT dispersion.[85] They used atomic force microscopy to confirm that PPV covers the surface of MWNTs and forms a well-mixed composite. Results suggested that MWNTs form a complex interpenetrating network with polymer chains.

The combination of carbon nanotubes with π-conjugated polymers is of interest because their π-conjugation enables the polymers to be used as an active material for light-emitting diodes (LEDs), field-effect transistors (FETs), and photovoltaic devices. Chen *et al.* reported a novel electrochemical method for the synthesis of a nanotube-polypyrrole (PPy) composite that has a high concentration of well-dispersed nanotubes.[86] High-resolution TEM revealed a remarkably uniform PPy coating on individual nanotubes, indicating that nanotubes are wetted by the continuous polymer phase. Although further mechanism was not investigated, the uniform coating on individual nanotubes promises controlled modification of the surface of nanotubes. This is 'the first example of nanotubes acting as a strong and conductive dopant in the polymerization of a conducting polymer'.

The optical polymer characteristics have been established for nanotube solubility, based on research on Poly(p-phenlyene vinylene-co-2,5-dioctoxy-m-phenylene vinylene) (PmPV) and its derivatives.[87] The combination of π-conjugation, twist allowing backbone and solubilizing side groups, resulted in a successful polymer conformation (a flat helix, with exposed backbone and outward pointing side groups-figure 1.10).

It was also suggested that the binding of conjugated polymers is the combination of electrostatic forces and van der Waals forces. It is not surprising that the forces are stronger than van der Waals binding for nonconjugated polymers, which, to some extent, may explain that nanotubes are generally dispersed better in conjugated polymers.

Fig. 1.10 Molecular model showing how conjugated polymer would helically wrap itself around a carbon nanotube

Composites of polyamide-6 and carbon nanotubes have been prepared on a co-rotating twin-screw extruder by Meincke *et al.*[88] It was shown by TEM that the nanotubes are dispersed homogeneously in the polyamide matrix (figure 1.11). The CNT-filled polyamide-6 showed an onset of electrical conductivity at filler loadings of 4-6 wt%. In agreement with rheological measurements, this onset in the conductivity is attributed to a percolation of nanotubes in the insulating polymer matrix. Tensile tests of the composites showed a significant increase of 27 % in the Young's modulus; however the elongation at break of these materials dramatically decreased due to an embrittlement of the polyamide-6 matrix. Blends of these composites and acrylonitrile-butadiene-styrene (ABS) have been prepared by extrusion. It was found that the CNTs are selectively located in the polyamide-6. These selectively filled polyamide-6/ABS blends showed a highly irregular, co-continuous morphology. Due to the confinement of the conductive filler to one blend component, these materials showed an onset in the electrical conductivity at low filler loadings (2-3 wt%). The authors explain these findings by a double percolation effect. The CNT-filled blends also showed superior mechanical properties.

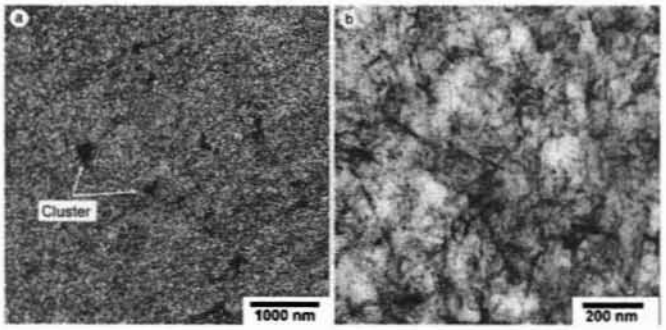

Fig. 1.11 TEM images of polyamide-6 filled with 5 wt% carbon nanotubes (a: 1000 nm scale bar, b: 200 nm scale bar) (from ref. 88)

Based on overview of literature, it is found that the interaction between pristine nanotubes and polymers is dependent on the choice of the matrix polymer and also polymer conformation, thus the molecular structure may play a critical role in the interaction. Even with 'best polymer', pristine nanotube may not form strong interfaces. It has been proposed that functionalizing nanotubes or chemical bonding might increase the interaction with polymer matrix, but it was found that some mechanical properties decrease after covalent chemical modification, and the structure of nanotubes would be destroyed partially.[89] It seems that MWNTs are more suitable for chemical treatment because their inner graphene layers can remain unreacted, thus the essential electronic structure can be retained, but less excellent properties than SWNTs and weak interaction between layers make them not attractive for a lot of applications.

After nearly a decade of research, the potential of carbon nanotubes as reinforcement for polymers has not been fully realised; the mechanical properties of atleast some of the derived composites have fallen short of predicted values. Few mechanisms about adhesion, load transfer and deformation were investigated, which make it difficult to accurately predict behaviors of nanotube-polymer composites and fabricate 'ideal' nanocomposites. Even though carbon nanotubes possess excellent mechanical characteristics, significant improvement in the composites' properties is possible only when the CNT's unique attributes exhibited at the nanoscale are transferred to

the macroscale. This essentially defines the fundamental challenge for applied CNT-polymer composites research.[90] A better understanding of the relationships between processing, interfacial optimization, and composite properties is a major goal of this area of research, which may lead to optimal reinforcement of polymer matrices with CNTs. The single largest impediment to use nanotubes as a filler phase for polymers is currently cost but as nanotube production methods continue to develop they will gradually become commercially viable fillers for multiphase materials.

1.3 Objectives of the current work

The present study has been undertaken to explore the potential of single walled carbon nanotubes (SWNTs) as reinforcement in an engineering plastic [poly(ethylene terephthalate)- PET] and a regionally important elastomer [natural rubber- NR] to widen their application spectra. The salient objectives of the current research are:

(a) To disperse SWNTs in polymer matrices of PET and NR

(b) To investigate the effect of SWNTs on the crystallization, mechanical, dynamic mechanical, rheological, thermal, dimensional and electrical conducting characteristics of PET

(c) To explore the effect of processing methods (conventional as well as sophisticated) on the materials properties

(d) To fabricate and characterize fibers from PET-SWNT nanocomposites

(e) To study the effect of SWNTs on the mechanical, electrical, thermal and ageing characteristics of NR

References

1. Ajayan PM, Schadler LS, Braun PV. Nanocomposite Science and Technology. Wiley-VCH; 2003.
2. Reich S, Thomsen C, Maultzsch J. Carbon Nanotubes: Basic Concepts and Physical Propeties. Wiley-VCH; 2004.
3. Endo M, Iijima S, Dresselhaus MS, editors. Carbon Nanotubes. Pergamon; 1996.
4. Treacy MMJ, Ebbesen TW, Gibson JM. Nature 1996;381:678.
5. Wong EW, Sheehan PE, Lieber CM. Science 1997;277:1971.
6. White CT, Todorov TN. Nature 1998;393:240.
7. Qin LC, Zhao X, Hirahara K, Miyamoto Y, Ando Y, Iijima S. Nature 2000;408:50.
8. Ding W, Eitan A, Fisher FT, Chen X, Dikin DA, Andrews R, Brinson LC, Schadler LS, Ruoff RS. Nano Letters 2003;3:1593.
9. Champion Y, Fecht HJ, editors. Nano-Architectured and Nanostructured Materials: Fabrication, Control and Properties. Wiley-VCH; 2004.
10. Fecht HJ, Werner M, editors. The Nano-Micro Interface: Bridging the Micro and Nanoworlds. Wiley-VCH; 2004.
11. Łojkowski W, Blizzard JR, editors. Interfacial Effects and Novel Properties of Nanomaterials. Scitec Publications; 2003.
12. Kelsall R, Hamley I, Geoghegan M, editors. Nanoscale Science and Technology. Wiley; 2005.
13. Schmid G, editor. Nanoparticles: From Theory to Application. Wiley-VCH; 2004.
14. Wolf EL, editor. Nanophysics and Nanotechnology: An Introduction to Modern Concepts in Nanoscience. Wiley-VCH; 2004.

15. Harris PJF. Carbon Nanotubes and Related Structures: New Materials for the Twenty First Century. Cambridge University Press; 1999.

16. Saito R, Dresselhaus G, Dresselhaus MS. Physical Properties of Carbon Nanotubes. Imperial College Press; 1998.

17. Kroto HW, Heath JR, O'Brien SC, Curl RF, Smalley RE. Nature 1985;318:162.

18. Smalley RE. Rev. Mod. Phys. 1997;69:723.

19. Krätschmer W, Lamb LD, Fostiropoulos K, Huffman DR. Nature 1990;347:354.

20. Iijima S. Nature 1991;354:56.

21. Jung SH. Appl. Phys. A- Mater. Sci. Processing 2003;76:285.

22. Gamaly EG, Ebbesen TW. Phys. Rev. B: 1995;52:2083.

23. Journet C, Bernier P. Appl. Phys. A- Mater. Sci. Processing 1998;67:1.

24. Guo T, Nikolaev P, Thess A, Colbert DT, Smalley RE. Chem. Phys. Lett. 1995;243:49.

25. Scott CD, Arepalli S, Nikolaev P, Smalley RE. Appl. Phys. A- Mater. Sci. Processing 2001;72:573.

26. Maser WK, Munoz E, Benito AM, Martinez MT, de la Fuente GF, Maniette Y, Anglaret E, Sauvajol JL. Chem. Phys. Lett. 1998;292:587.

27. Ren ZF, Huang ZP, Xu JW, Wang JH, Bush P, Siegel MP, Provencio PN. Science 1998;282:1105.

28. Ren ZF, Huang ZP, Wang DZ, Wen JG, Xu JW, Wang JH, Calvet LE, Chen J, Klemic JF, Reed MA. Appl. Phys. Lett. 1999;75:1086.

29. Sinnot SB, Andrews R, Qian D, Rao AM, Mao Z, Dickey EC, Derbyshire F. Chem. Phys. Lett. 1999;315:25.

30. Masako Y, Rie K, Takeo M, Yoshimasa O, Susumu Y, Etsuro O. Appl. Phys. Lett. 1995;67:2477.

31. Masako Y, Rie K, Yoshimasa O, Etsuro O, Susumu Y. Appl. Phys. Lett. 1997;70:1817.

32. The CoMoCAT process. http://www.ou.edu/engineering/nanotube.2003.

33. http://www.ou.edu/engineering/nanotube/NT2001Production.PDF.2003.

34. Smalley RE, Boris Y. Solid State Commun. 1998;107:597.

35. Pavel N, Michael JB, Kelley BR, Frank R, Daniel TC, Smith KA, Smalley RE. Chem. Phys. Lett. 1999;313:91.

36. Michael JB, Peter AW, Daniel TC, Smith KA, Smalley RE. J. Vacuum Sci. Technol. A: Vacuum, Surfaces, and Films 2001;19:1800.

37. Ayumu Y, Noboru K, Wataru M. J. Phys. Chem. B 2002;106:13294.

38. Ajayan PM. Chem. Rev. 1999;99:1787.

39. Stankevich IV, Nikerov MV, Bochvar DA. Russ. Chem. Rev. 1984;53:640.

40. Avouris P. Chem. Phys. 2002;281:429.

41. Ajayan PM, Zhou OZ. Topics Appl. Phys. 2001;80:391.

42. Srivastava D, Wei C. Appl. Mech. Rev. 2003;56:215.

43. Qian D. Appl. Mech. Rev. 2002;55:495.

44. Dresselhaus MS, Dresselhaus G, Eklund PC. Science of Fullerenes and Carbon Nanotubes. Academic Press; 1996.

45. Ebbesen TW, Ajayan PM. Nature 1992;358:220.

46. Baughman RH, Zakhidov AA, de Heer WA. Science 2002;297:787.

47. Kim BM, Sinha S, Bau HH. Nano Letters 2004;4:2203.

48. Ajayan PM, Iijima S. Nature 1993;361:333.

49. Saito R, Fujita M, Dresselhaus G, Dresselhaus MS. Phys. Rev. B. 1992;46:1804.

50. Hamada N, Sawada S, Oshiyama A. Phys. Rev. Lett. 1992;68:1579.

51. Dai HJ, Hafner JH, Rinzler AG, Colbert DT, Smalley RE. Nature 1996;384:147.

52. Dai H, Franklin N, Han J. Appl. Phys. Lett. 1998;73:1508.

53. Miller JC, Serrato R, Represas-Cardenas JM, Kundahl G. The Handbook of Nanotechnology: Business, Policy and Intellectual Property Law. John Wiley and Sons, Inc.; 2005.

54. Curran SA, Ajayan PM, Blau WJ, Carroll DL, Coleman JN, Dalton AB, Davey AP, Drury A, McCarthy B, Maier S, Strevens A. Adv. Mater. 1998;10:1091.

55. Dalton AB, Stephan C, Coleman JN, McCarthy B, Ajayan PM, Lefrant S, Bernier P. J. Phys. Chem. B 2000;104:10012.

56. McCarthy B, Coleman JN, Curran SA, Dalton AB, Davey AP, Konya Z, Fonseca A. J. Mater. Sci. Lett. 2000;19:2239.

57. Dalton AB, Blau WJ, Chambers G, Coleman JN, Henderson K, Lefrant S, McCarthy B. Synth. Met. 2001;121:1217.

58. Andrews R, Weisenberger MC. Current Opinion in Solid State and Materials Science 2004;8:31.

59. Lau T, Hui D. Composites: Part B 2002;33:263.

60. Lau T, Hui D. Carbon 2002;40:1597.

61. Pipes RB, Frankland SJV, Hubert P, Saether E. Compos. Sci. Technol. 2003;63:1349.

62. Ounaies Z, Park C, Wise KE, Siochi EJ, Harrison JS. Compos. Sci. Technol. 2003;63:1637.

63. Ma RZ, Wu J, Wei Q, Liang J, Wu DH. J. Mater. Sci. 1998;33:5243.

64. Weisenberger MC, Grulke EA, Jacques D, Rantell T, Andrews R. J. Nanosci. Nanotech. 2003;3.

65. Mitchell CA, Bahr JL, Arepalli S, Tour JM, Krishnamoorti R. Macromolecules 2002;35:8825.

66. Cooper CA, Ravich D, Lips D, Mayer J, Wagner HD. Compos. Sci. Technol. 2002;62:1105.

67. Kim P, Shi L, Majumdar A, McEuen PL. Phys. Rev. Lett. 2001;87:2155021.

68. Ajayan PM, Stephan O, Colliex C, Trauth D. Science 1994;265:1212.

69. Sandler JKW, Kirk JE, Kinloch IA, Shaffer MSP, Windle AH. Polymer 2003;44:5893.

70. Biercuk MJ, Llaguno MC, Radosavljevic M, Hyun JK, Johnson AT. Appl. Phys. Lett. 2002;80:2767.

71. Gong XY, Liu J, Baskaran S, Voise RD, Young JS. Chem. Mater. 2000;12:1049.

72. Xu X, Thwe MM, Shearwood C, Liao K. Appl. Phys. Lett. 2002;81:2833.

73. Gojny FH, Nastalczyk J, Roslaniec Z, Schulte K. Chem. Phys. Lett. 2003;370:820.

74. Schadler LS, Giannaris SC, Ajayan PM. Appl. Phys. Lett. 1998;73:3842.

75. Lau K, Shi S. Carbon 2002;40:2961.

76. Valentini L, Puglia D, Frulloni E, Armentano I, Kenny JM, Santucci S. Compos. Sci. Technol. 2004;64:23.

77. Wang Z, Liang Z, Wang B, Zhang C, Kramer L. Composites Part A- Appl. Sci. Manufactur. 2004;35:1225.

78. Shaffer MSP, Windle AH. Adv. Mater. 1999;11:937.

79. Zhang X, Liu T, Sreekumar TV, Kumar S, Moore VC, Hauge RH, Smalley RE. Nano Letters 2003;3:1285.

80. Cadek M, Coleman JN, Barron V, Hedicke K, Blau WJ. Appl. Phys. Lett. 2002;81:5123.

81. Jia ZJ, Wang ZY, Xu C, Liang J, Wei BQ, Wu DH, Zhu SW. Mater. Sci. Eng. 1999;A271:395.

82. Stephan C, Nguyen TP, de la Chapelle, Lamy M, Lefrant S, Journet C, Bernier P. Synth. Met. 2000;108:139.

83. Haggenmueller R, Gommans HH, Rinzler AG, Fischer JE, Winey KI. Chem. Phys. Lett. 2000;30:219.

84. Qian D, Dickey EC, Andrews R, Rantell T. Appl. Phys. Lett. 2000;76:2868.

85. Ago H, Petritsch K, Shaffer MSP, Windle AH, Friend RH. Adv. Mater. 1999;11:1281.

86. Chen GZ, Shaffer MSP, Coleby D, Dixon G, Zhou WZ, Fray DJ, Windle AH. Adv. Mater. 2000;12:522.

87. Panhuis M, Munn RW, Blau WJ. Synth. Met. 2001;121:1187.

88. Meincke O, Kaempfer D, Weickmann H, Friedrich C, Vathauer M, Warth H. Polymer 2004;45:739.

89. Garg A, Sinnott SB. Chem. Phy. Lett. 1998;295:273.

90. Thostenson ET, Chou TW. J. Phys. D. Appl. Phys. 2003;36:573.

Chapter 2

PET-SWNT nanocomposites through melt compounding

Preparation and crystallization characteristics*

Abstract

Nanocomposites of poly(ethylene terephthalate) (PET) and single walled carbon nanotubes (SWNTs) have been prepared through melt compounding. Differential scanning calorimetry studies showed that SWNTs at weight fractions as low as 0.03 % enhance the rate of crystallization in PET, as the cooling nanocomposite melt crystallizes at a temperature 10 °C higher as compared to neat PET. Isothermal crystallization studies also revealed that SWNTs significantly accelerate the crystallization process. Wide angle X-ray diffraction (WAXD) experiments showed oriented crystallization of PET induced by oriented SWNTs in a randomized PET melt, indicating the role of SWNTs as nucleating sites.

---

*K. Anoop Anand, U.S. Agarwal, Rani Joseph. ***Polymer*** ***2006; 47(11): 3976-3980.***

A part of the work described in this chapter has been presented at the *58th Annual Session of Indian Institute of Chemical Engineers (IIChE), Indian Chemical Engineers Congress-* ***CHEMCON 2005****, Dec 14-17, 2005, Indian Institute of Technology, New Delhi, India* and at the *18th* ***Kerala Science Congress****, Jan 29-31, 2006, CESS, Thiruvananthapuram, India.*

2.1 Introduction: Poly(ethylene terephthalate)

Poly(ethylene terephthalate) (PET) is one of the most extensively used thermoplastic polyesters, which has assumed a role of primacy in fibers, films, packaging and molding materials.[1] It has a high glass transition temperature (T_g) of ~ 85 °C and a high melting temperature of ~ 255 °C.[2] Owing to its excellent performance characteristics such as hardness, clarity, wear-resistance, melt mobility, spinnability, thermal and dimensional stability, resistance to chemicals etc., this commodity polymer has worldwide consumption next only to polyolefins.[3-8]

PET is a linear condensation polymer whose structure is given in figure 2.1. It is formed by the step growth polycondensation of ethylene glycol (EG) and terephthalic acid (TPA). The synthesis involves two steps. The first is the esterification of TPA with EG, forming the so-called *prepolymer,* which contains the monomer, bishydroxyethyl terephthalate (BHET) and short chain oligomers. The second reaction step is polycondensation in which a trans esterification reaction takes place in the melt phase. High viscosity PET grades for bottles or technical yarns are typically produced by further polycondensation in an additional solid-state process (SSP) under vacuum or in an inert atmosphere respectively.[9] Today, more than 70 % of the global PET production is based on TPA even though the formation of the prepolymer can also be achieved by trans esterification of dimethyl terephthalate (DMT) with EG.

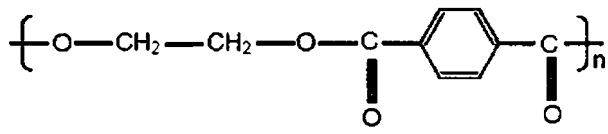

Fig. 2.1 Structure of PET

Two PET grades now dominate the global market, i.e. fiber grade PET and bottle grade PET (figure 2.2). These standard grades differ mainly in molecular weight or intrinsic viscosity [η], optical appearance and the production recipes. Fiber grade PET has a number average molecular weight (M_n) of 15,000 to 20,000 g/mol which

refers to an [η] of between 0.55 and 0.67 dL/g. The average molecular weight of bottle grade PET ranges from 24,000 to 36,000 g/mol, which refers to an [η] of 0.75 to 1.00 dL/g. Other PET grades are manufactured for packaging films, as well as for the production of video and audio tapes, which are often standard grades with an intrinsic viscosity of 0.64 dL/g.

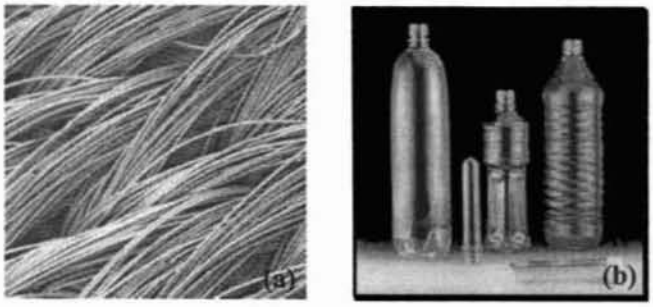

Fig. 2.2 (a) Micrograph of woven polyester-fiber cloth (b) PET bottles

As compared to poly(butylene terephthalate) (PBT), the slower crystallization of PET, however, limits its usage in engineering applications which require fast crystallization for low cycle time for injection molding etc. Enhancement in crystallization rate of PET is generally achieved through the addition of minerals such as talc or organic acid salts such as sodium benzoate. Other nucleating agents that have been mentioned in the literature include metal oxides and hydrides, residual catalysts, thermotropic liquid crystalline polymers and diamide segments.[10-19]

Several researchers have reported the use of nanoparticles, such as organically modified nanoclays as crystallization promoters for a variety of polymers.[20,21] For example, Suoboda *et al.* reported that organically modified nanoclays are acting as effective nucleating agents for the crystallization of polypropylene.[22] Choi *et al.* also observed that organoclays are acting as nucleating agents for the crystallization of poly(hydroxy butyrate-co-hydroxy valerate).[23] These studies have prompted the evaluation of nanoclays for crystallization enhancement in PET also. For example, Ke *et al.* have studied the crystallization, properties and crystal and nanoscale morphology of PET-clay nanocomposites.[24] They observed that the nanocomposites

had three times greater crystallization rate than that of pure PET at clay concentrations as low as 0.5 wt%. Liu *et al.* have studied the crystallization characteristics of PET-nanosilica nanocomposites.[25] They observed that the nanosilica particles enhanced the rate of melt crystallization in PET while not affecting the processing characteristics. Qu *et al.* prepared PET-$BaSO_4$ nanocomposites through *in situ* polymerisation.[26] They observed that nanosized $BaSO_4$ particles also act as nucleating agents for PET crystallization. The crystallization temperature of PET was increased by ~ 12 °C with $BaSO_4$ at a concentration of 0.5 wt%. A detailed list of nucleating agents used for PET is given in section 2.1.2.1.

2.1.1 Crystallization: Theory

2.1.1.1 Crystallization from a quiescent melt

In most thermoplastic polymer processing methods, a polymer mass is first taken to an elevated temperature, at which the viscosity is low enough for the material to be formed into a shape. When the required shape has been formed, the polymeric mass is cooled to a temperature at which its shape is retained. Examples of such processing are fiber spinning, injection molding, blow molding, compression molding etc. If the polymer is crystallizable, the material is taken above the melting point in the first step, and then crystallized in the second step. Thus for the crystallizable polymers, crystallization from the melt pervades polymer processing.

The process of crystallization consists of *nucleation* and *growth*. Growth of crystalline polymers has been extensively investigated, with well-established predictive theories available for several polymers.[27-29] It takes place with the formation of lamellae radiating outwards from the nucleus by chain folding normal to the direction of growth as shown in figure 2.3.

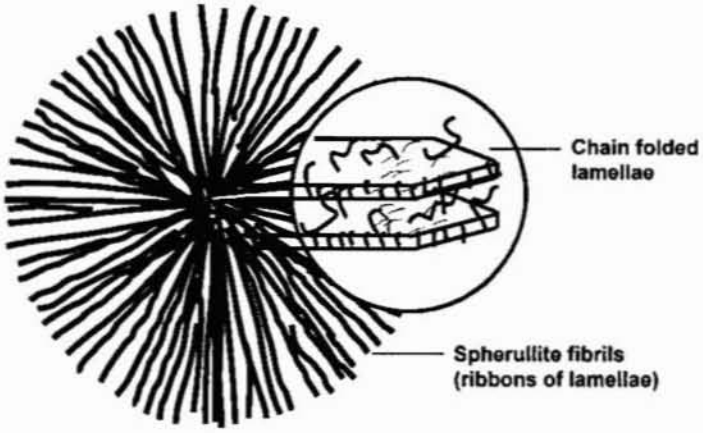

Fig. 2.3 Illustration of spherullite growth

In contrast, only little is known about nucleation of crystalline polymers.[30-32] Nevertheless, nucleation is of great importance in determining crystalline morphology. The number and distribution of crystal nucleus can profoundly influence the product performance. Indeed, in many cases where there is a deliberate attempt to control the properties of a given polymer by manipulating its morphology; it has been achieved via the use of nucleating agents. At present, it is somewhat a mystery as to the mechanisms of these nucleating agents. As a result, searching for effective nucleating agents is more or less an empirical process.

2.1.1.2 Theory of nucleation

Nucleation is usually described in terms of the free energy balance between the creation of a new crystal and new surface(s) associated with the crystal. Forming a nucleus smaller than a critical size causes an initial increase in the free energy due to the need to create surface(s) and therefore, is not thermodynamically favorable. As the nuclei grow larger, the free energy reaches a maximum and becomes negative afterwards, leaving a stable nucleus. From Hoffman's nucleation theory, the rate of nucleation (I), i.e. the formation of stable nucleus, is expressed by the following equation:[33]

$$I = Io\,\beta \exp(-\Delta\Phi^{*}/kT) \tag{2.1}$$

where Io is a proportionality constant, $\Delta\Phi^{*}$ is the free energy barrier for the formation of critical nucleus, k is Boltzmann's constant, T is temperature and β has the following formula:

$$\beta = \beta o\ kT/h \exp[-U^{*}/R(T-T_{\infty})] \tag{2.2}$$

Here, βo is a proportionality constant, U^{*} is the activation energy for transporting polymer chain segments from the melt to a growing crystal front, and T_{∞} is the temperature at which such a transport is ceased, usually (T_g-30), although $T_{\infty} = T_g$ has been proposed for crystalline polymers.[34,35] For *homogeneous* nucleation, where nucleation starts in a pure polymer melt with no help from extrinsic entities,

$$\Delta\Phi^{*} = 32\,\sigma^{2}\,\sigma e / \Delta F^{2} \tag{2.3}$$

where ΔF is (volume) free energy driven force for transformation (i.e. crystallization), and σ and σe stand for surface energies for lateral and chain-folding surfaces of a growing crystalline lamella, respectively. In practice, however, unless under very special conditions, it is rare to observe homogeneous nucleation for crystalline polymers. Whenever there is a foreign surface present in the polymer melt, it can affect the free energy balance for nucleation, usually, so as to increase nucleation rate and prevent homogeneous nucleation. The significant effect of a surface is to modify the surface energy term in equation (2.3) into the following form:

$$\Delta\Phi^{*} = 16\,\sigma\,\sigma e\,\Delta\sigma / \Delta F^{2} \tag{2.4}$$

where $\Delta\sigma = \sigma + \sigma os - \sigma s$, in which σos is the interfacial energy between the foreign surface and the polymer melt, and σs is the interfacial energy between the foreign surface and the polymer crystal.

The same dependence of nucleation rate upon undercooling appears in both equations (2.3) and (2.4) for homogeneous and heterogeneous nucleation. For *heterogeneous* nucleation, however, due to a much reduced surface energy (i.e. small $\Delta\sigma$ in equation (2.4)), nucleation rate can increase by several orders of magnitude. Therefore, the effect of homogeneous nucleation can be totally smeared by heterogeneous nucleation and becomes inaccessible experimentally.

So far in the above discussion, it has been assumed that heterogeneous nucleation is achieved via foreign surfaces, and the presence of these high-energy surfaces can favorably affect the free energy balance for nucleation. The following mechanisms can be proposed to explain the effect of a surface in reducing $\Delta\Phi^*$:

1) epitaxial arrangements of polymer chains on a crystalline surface, assuming certain crystallographic match and misfit, which lowers the surface energy for the forth-forming nucleus
2) absorption of polymer chains onto a surface, due to polar interaction and/or topological effect, which causes a reduction of melt entropy and results in an increase in equilibrium melting temperature and apparent undercooling as well
3) a slight closer packing of polymer chains in the vicinity of a foreign surface, which eases the transport of polymer chain segments during crystallization

Obviously, more than one mechanism can be effective simultaneously. The above nucleation theory is based on the formation of crystal nucleus, and it can be referred as *crystal nucleation*. A process of *molecular nucleation* has been proposed and distinguished from crystal nucleation.[36] Crystal nucleation is mainly concerned with the formation of new crystals or new crystal layers, and it is irrespective of the effect of non-crystallized polymer chains. On the other hand, molecular nucleation emphasizes the reptation process, which establishes the first part of a polymer chain in the crystal phase, and it is a process that spans the whole nucleation and growth stages of crystallization. According to this theory, for flexible polymers, nucleation is dominated by crystal nucleation; for rigid polymers, however, nucleation is dominated by

molecular nucleation. The difference in nucleation mechanism explains why flexible and rigid polymers are very different both in crystallization kinetics and morphology.

Nucleation of crystalline polymers was also discussed from a standpoint of *phase separation* in a homogeneous melt.[37] According to this theory, crystallization starts with a preceding un-mixing event in the melt, whereby segments that can be stretched and incorporated into a growing crystalline lamella are separated from others that are prohibited from nucleation - including entanglements, chain ends, and other perturbations such as branching and conformational defects. This phase separation eventually leads to crystalline and amorphous phases as seen for crystalline polymers. Indeed, such an un-mixing phenomenon has been detected for cold crystallization of PET and poly(ether ether ketone) (PEEK) and melt crystallization of polypropylene (PP) and poly(butylene terephthalate) (PBT) by time-resolved X-ray scattering experiments.[38-41]

2.1.2 Nucleating agents for PET

Using nucleating agents to increase the crystallization rate of PET has been well documented. However, the understanding of nucleation mechanism is not yet complete. It has been agreed that these nucleating agents can reduce the surface energy required for nucleation and therefore promote nucleation process, and this can be referred as a physical (surface) nucleation mechanism. On the other hand, it has been demonstrated that certain strong nucleating agents are based on a chemical nucleation mechanism, i.e. these nucleating agents react with polymer chains and result in ionic chain-ends serving as real nucleating agents. Furthermore, homogeneous nucleation can be promoted by incorporation of rigid segments in polymer backbone via co-polymerization. Given in the section 2.1.2.1 is a partial list of nucleating agents utilized for PET.

2.1.2.1 A list of nucleating agents for PET[#]

Inorganic compounds

- ✓ chalk, gypsum, clay, mica, talc
- ✓ cadmium red, cobalt yellow, chromium oxide, phthalocyanine
- ✓ titanium oxide, magnesium oxide, antimony trioxide
- ✓ phosphates, carbonates, sulphates, fluorides, nitrides of B and Na
- ✓ hydrides of Al, Cu, Ni, In, Ba, Co, La

Organic compounds

- ✓ salts of monocarboxylic or polycarboxylic acids
- ✓ alkali metal salts of ethylene terephthalate oligomers and benzonic acids
- ✓ amine carboxylate, diphenylamine, tetrachloroethane, nitromethane, toluene, benzophenone, tetralin, aromatic alcohols, amines
- ✓ alkali aralkylsulphonates, epoxides

Residual catalysts

- ✓ catalysis remnants in transesterification (derivatives of Ca, Mn, Mg, Zn, Sn, etc.) and in polycondensation (derivatives of Sb, Ti, Ge, etc.)
- ✓ catalysis deactivators (phosphorous derivatives)

Polymers

- ✓ polyolefins (PE, PP), fluoropolymers (PTFE), copolymers of ethylene, unsaturated carboxylic esters, styrene derivatives, conjugated dienes, ionomers
- ✓ blending with faster crystallizing polymers (PBT) and LCPs
- ✓ incorporation of rigid chain segments by copolymerization

[#]Based on Gachter-Muller, *Plastics Additives*, Chapt. 17, Hanser Publishers, 1992.

2.1.2.2 Carbon nanotubes as nucleating agents

Carbon nanotubes, the long thin cylinders of carbon, have been evaluated in recent years as additives to polymers for imparting several properties such as mechanical reinforcement, electrical and thermal conductivity, as well as faster crystallization.[42,43] For example, Probst *et al.* found that carbon nanotubes nucleate crystallization of polyvinyl alcohol (PVA) at concentrations as low as 0.1 wt%.[44] The crystallization behaviour of polypropylene (PP) in the presence of single walled carbon nanotubes (SWNTs) has been reported by Grady *et al.* and Bhattacharyya *et al.*[45,46] Valentini *et al.* observed that, SWNTs when melt blended with PP at a concentration of 5 wt% increased the crystallization temperature of the matrix polymer by ~ 13 °C.[47] Assouline *et al.* also reported about the nucleation ability of multi walled carbon nanotubes (MWNTs) in polypropylene composites.[48] Nogales *et al.* found that SWNTs did not influence the crystal structure of PBT, but they did not evaluate the influence on crystallization rate.[49] The effect of MWNTs on the non-isothermal crystallization of ethylene-vinyl acetate copolymer (EVA) was investigated by Li *et al.*[50] They observed that the onset and maximum crystallization temperatures for the MWNT-EVA (10 wt%) composite were, respectively, about 10 and 5 °C higher than those for the neat EVA, indicating nucleation ability of MWNTs in EVA. Kim *et al.* also have studied the unique nucleation of melt compounded nanocomposites of MWNTs and poly(ethylene 2,6-naphthalate) (PEN) during non-isothermal crystallization.[51] They observed that MWNTs act as effective nucleating agents for PEN crystallization, the effect of which was more predominant at low concentrations.

So far there has been no report in literature that addresses the effect of carbon nanotubes on the rate of PET crystallization. This is investigated here through differential scanning calorimetry in transient and isothermal modes, carried out on nanocomposite samples of PET, melt compounded with SWNTs at concentrations of 0-3 wt%. Wide angle X-ray diffraction (WAXD) is used to demonstrate the orientation of crystallizing PET chains along SWNTs.

2.2 Experimental

2.2.1 Materials

2.2.1.1 Poly(ethylene terephthalate), PET

Poly(ethylene terephthalate) (PET) pellets (characteristic cylindrical diameter ~ 2.5 mm, length ~ 3 mm) were obtained from Acordis Research (Arnhem, the Netherlands). The intrinsic viscosity, [η] of the polymer was determined to be 0.98 dL/g in 1/1 mixture of phenol and 1,1,2,2-tetrachloroethane at 30 ± 0.1 °C.

2.2.1.2 Single walled carbon nanotubes, SWNTs

Single walled carbon nanotubes (SWNTs) were purchased from CarboLex Inc. (Lexington, U.S.A). They were prepared by arc discharge method and the average diameter of an individual tube was 1.4 nm and length in the range of 2-5 μm. A scanning electron micrograph of the SWNT sample used in the present study is given in figure 2.4.

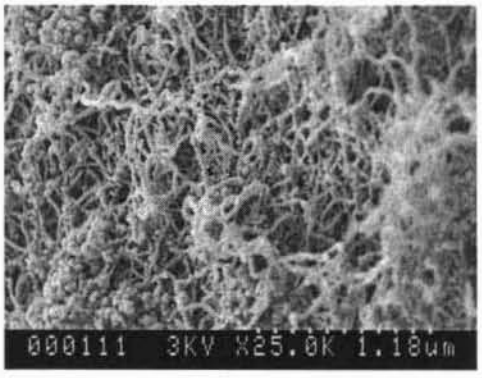

Fig. 2.4 SEM image of SWNTs

The purity of the sample was > 70 %. Impurities include residual catalysts (Ni, Y), which are usually encapsulated in carbon shells. Some amorphous carbon may also be found on the outer surfaces of the tubes. A typical TGA trace of the SWNT sample indicating its thermal stability is given in figure 2.5.

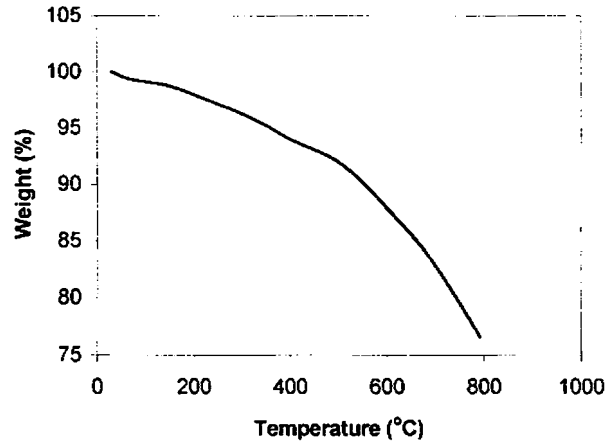

Fig. 2.5 Typical TGA trace of SWNTs (@ 20 °C/min from ambient to 800 °C in nitrogen atmosphere)

The as-prepared grade sample of SWNTs was a mixed one, containing both semi conducting and metallic tubes with chiral angles distributed between 0 and 30°. The thermal conductivity of disordered samples of SWNTs was -35 W/mK at room temperature and for the highly aligned samples it could be 200 W/mK, within an order of magnitude of the room temperature thermal conductivity of highly crystalline graphite. (It is most possible that an individual SWNT will have significantly higher thermal conductivity than the bulk samples.)

2.2.1.3 Solvents

Phenol (99+ %) and 1,1,2,2-tetrachloroethane (99+ %, TCE) were supplied by Aldrich. 1/1 mixture of these two was prepared and was dried using regenerated sodium based molecular sieves (bead size ~ 2 mm, pore size ~ 0.4 nm, Merck Ltd.) before using for intrinsic viscosity measurements.

2.2.2 Preparation of the nanocomposites: Melt compounding

A simple melt compounding route was adopted for the preparation of PET-SWNT nanocomposites. The polymer along with SWNTs was vacuum dried at 150 °C for

atleast 12 h to avoid moisture induced degradation phenomena. The melt compounding was performed using a laboratory scale (60 cm^3) Thermo Haake Polylab system operating with counter rotating screws at 40 rpm for 4 min at 270 °C (figure 2.6). The polymer and the nanotubes have been charged to the mixing chamber together. A mixing time of 4 min was fixed since the torque stabilized to constant values during this time. The stabilization of torque may be related to the attainment of a stable structure. Nanocomposites at different concentrations (0.0-3.0 wt%) of SWNTs were prepared.

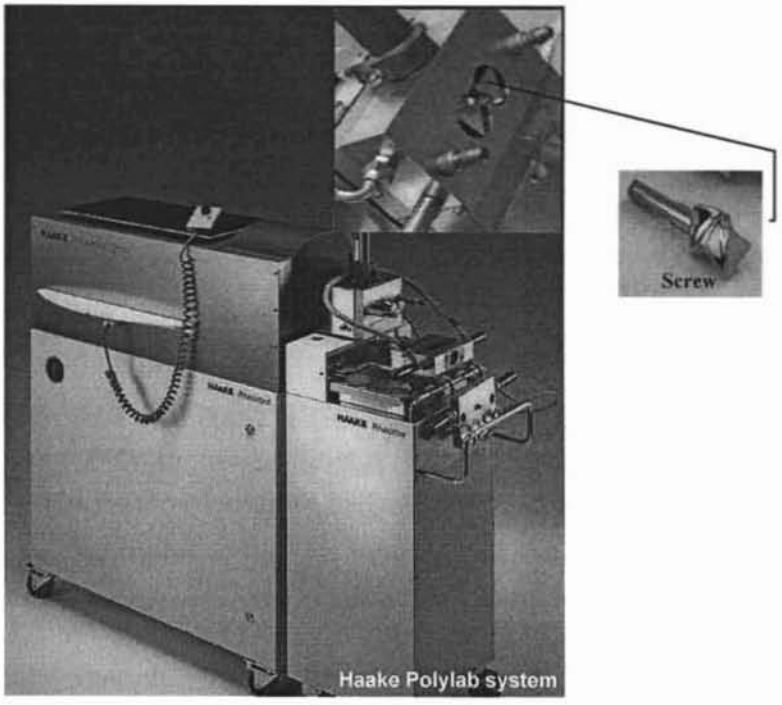

Fig. 2.6 Thermo Haake Polylab system (Shown in the inset is the mixing chamber and the screw/rotor)

2.2.3 Intrinsic viscosity measurements

To monitor the extent of molecular weight depletion during melt processing, so as to maintain relatively identical molecular weight for the entire composite samples under evaluation, intrinsic viscosity measurements have been carried out.

Relative viscosities (η_{rel}) of (c = 0.5 g/dL) solutions of PET or PET-SWNT samples in 1/1 mixture of phenol and 1,1,2,2-tetrachloroethane were determined using a Schott-Gerate viscometer (GmbH D 6238 Type CT 42) at a constant temperature of 30 ± 0.1 °C. The solutions were prepared by dissolving the samples at ~ 70 °C in the solvent, which is predried with molecular sieves. They were filtered prior to the measurements so that the presence of small amounts of undispersed components from SWNTs in the nanocomposite samples did not affect the measurements.

The intrinsic viscosity, [η] values were calculated using a single point determination method according to the relation:[52]

$$[\eta] = (1/c)\,[2\,(\eta_{rel}-1)-2\ln(\eta_{rel})]^{1/2} \qquad (2.5)$$

Intrinsic viscosity may be related to the number average molecular weight, M_n using Mark-Houwink relationship:

$$[\eta] = KM_n^a \qquad (2.6)$$

where K and a are coefficients, the values of which have been reported by several workers for the measurements in the same solvent mixture.[53-55] Indeed, in the present case comparison is made with the [η] values.

2.2.4 Differential scanning calorimetry (DSC)

Differential scanning calorimetry (DSC Q-100, TA Instruments) was employed to study the effect of SWNTs on the crystallization characteristics of nanocomposites. Indium was used for temperature and enthalpy calibration (T_m = 156.63 °C, ΔH_m = 28.47 J/g). All the samples were dried prior to the measurements and analyses were carried out in nitrogen atmosphere using standard aluminum pans. Calorimetric measurements were done while the samples (4-5 mg) were exposed to the following temperature scans: heating at a rate of 20 °C/min to 310 °C, holding for 10 min to erase thermal history effects and then cooling to 50 °C at a rate of

20 °C/min during which the peak of crystallization exotherm was taken as the crystallization temperature, T_c. The heat of fusion (ΔH_m) and the heat of crystallization (ΔH_c) were determined from the areas of the melting and crystallization peaks respectively.

For analysis of the isothermal crystallization characteristics, the samples were subsequently reheated to 310 °C at a rate of 20 °C/min, held at 310 °C for 2 min, and then cooled rapidly (60 °C/min) to the desired temperature for isothermal crystallization (210 °C, 215 °C, 220 °C or 225 °C) and kept at each temperature for 4 min isothermally.

2.2.5 Optical microscopy/ Hot stage experiments

To study the SWNT-induced oriented crystallization in PET-SWNT nanocomposites, melt compounded samples of neat PET and PET-SWNT 1 wt% composite have been compression molded into 0.5 mm thick, 4 mm wide strips, and stretched these (L_x/L_x^0 =) 4 times while heating in contact with a stainless steel plate at 150 °C. The strips were then positioned on glass slides with their ends glued to the glass slides to resist future macroscopic deformation (shrinkage). They were then heated to melt using a Linkam hot stage (THMSE 600) at a rate of 20 °C/min to 300 °C. The polymer melting was monitored using an optical microscope (Zeiss LM Axioplan) under cross polars. Subsequent cooling was carried out on the hot stage at a rate of 10 °C/min to observe polymer crystallization.

2.2.6 Wide angle X-ray diffraction (WAXD)

The wide-angle X-ray diffraction (WAXD) experiments were carried out with a Rigaku X-ray generator, using Ni filtered Cu K_α radiation (λ = 0.154056 nm) at 40 kV and 30 mA. The sample-to-film distance was 70 mm. The films were exposed for 3 h to the X-ray beam from a pinhole collimator with a diameter of 0.4 mm. Photographs were taken using a flat film camera.

2.3 Results and discussion

Considering the known strong dependence of the PET crystallization rate on its molecular weight, an evaluation of the effect of SWNTs on PET crystallization requires comparison at similar molecular weights. For this purpose, virgin PET was also subjected to melt compounding under identical conditions as that for the PET-SWNT nanocomposite preparation and hereafter called the 0 wt% (SWNT concentration) or neat PET sample.

Figure 2.7 shows the torque data measured during mixing at 270 °C in Haake Polylab system. From the figure it is evident that the torque values stabilize in < 4 min indicating that the mixing is homogeneous. It is also notable that the addition of carbon nanotubes does not appreciably affect the peak torque or steady state torque.[56] The position of the maximum peak torque is dependent on the loading time, which in the present case remains unaffected, as the experiments have been done more or less identical.

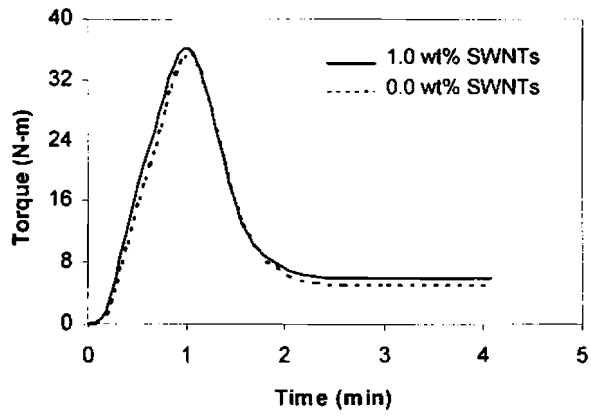

Fig. 2.7 Torque Vs. time curves for neat PET and PET-SWNT 1 wt% nanocomposite measured at 270 °C from Haake Polylab system

Figure 2.8 shows the digital photographs of the melt compounded neat PET and PET-SWNT 1.0 wt% nanocomposite sample after grinding them using a cryogrinder (Lloyd Instruments Ltd.). Colour uniformity is observed in each sample.

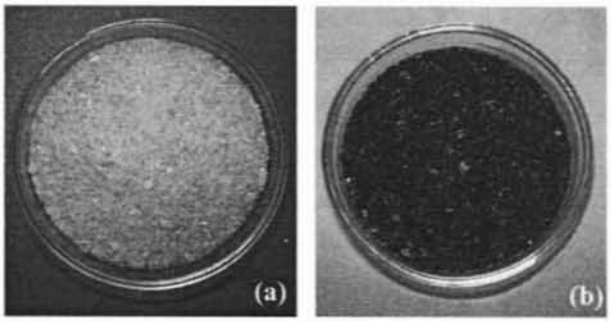

Fig. 2.8 Digital photographs of melt compounded (a) neat PET and (b) 1.0 wt% PET-SWNT nanocomposite

2.3.1 Monitoring molecular weight depletion

Even though PET is included in the group of hydrophobic polymers in regard to the small amount of water that it can absorb under saturated conditions, it can also be considered as a hygroscopic thermoplastic, which absorbs moisture from its environment at a relatively rapid rate.[57-60] The traces of moisture absorbed will cause hydrolytic degradation of the polymer during melt compounding at elevated temperatures, which will substantially reduce its molecular weight. The reaction responsible for this reduction in molecular weight is shown in scheme 2.1.

The decline in molecular weight of PET as a result of thermal/ hydrolytic/ oxidative degradation during melt processing is monitored by intrinsic viscosity, [η] measurements. It is observed that the [η] of PET drops from 0.98 dL/g to 0.88 dL/g during melt compounding (table 2.1). The reported [η] values in table 2.1 are the average of atleast five concordant measurements. Since all the samples have comparable [η] (or molecular weight) after processing under identical conditions, it is inferred that the possible dependence of the crystallization measurements on the molecular weights of the samples has been eliminated.

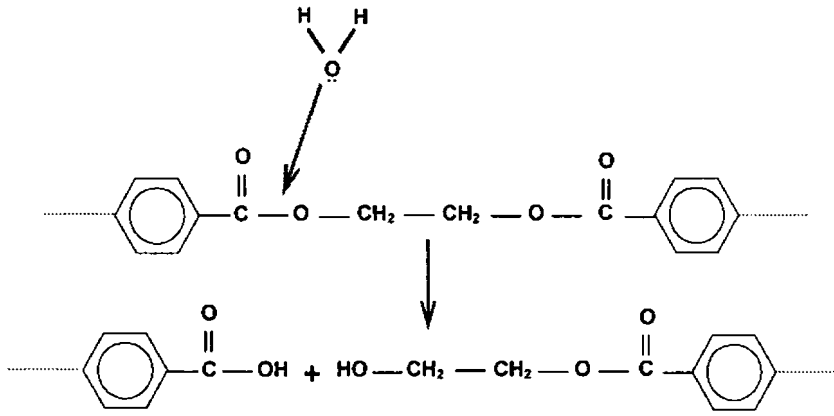

Scheme 2.1 Reaction responsible for the reduction in molecular weight of PET during melt processing

Table 2.1

Intrinsic viscosities of melt compounded PET-SWNT nanocomposite samples (0.5 g/dL solutions in 1/1 phenol/TCE at 30 ± 0.1 °C)

Concn. of SWNTs (wt%)	[η] (dL/g)
0.0	0.884
0.03	0.878
0.1	0.881
0.3	0.875
1.0	0.883
3.0	0.879

2.3.2 Crystallization characteristics

Differential scanning calorimetry (DSC) is one of the most widely accepted techniques of thermal analysis for studying the crystallization characteristics of polymers and their composites. The materials, as they undergo temperature changes, will undergo changes

in chemical and physical properties, which are detected by transducers, which convert the changes into electrical signals that are collected and analyzed to give thermograms. In DSC, the crystallization characteristics are studied from the heat flows associated with the corresponding transitions as a function of temperature.

The effect of SWNTs on the crystallization characteristics of melt compounded PET-SWNT nanocomposite samples was analyzed first with non-isothermal DSC experiments. The crystallization temperatures (T_c), the apparent melting temperatures (T_m) and the corresponding enthalpies (ΔH_c and ΔH_m) for all the samples are reported in table 2.2.

Table 2.2

DSC-determined thermal characteristics of PET-SWNT nanocomposite samples

Concn. of SWNTs (wt%)	T_c (°C)	ΔH_c (J/g)	T_m (°C)	ΔH_m (J/g)
0.0	199.92	38.16	253.03	37.51
0.03	209.92	37.46	251.73	37.80
0.1	211.51	36.59	252.54	36.19
0.3	212.41	37.58	253.51	37.32
1.0	214.33	37.25	251.08	37.67
3.0	219.08	36.82	252.54	38.79

Figure 2.9 shows the DSC cooling scans of PET-SWNT nanocomposite samples. During cooling from the melt, the SWNT containing samples show crystallization exotherms earlier than neat PET, as also seen from the corresponding T_c values indicated in table 2.2. It is found that the nanocomposite sample containing SWNTs at a concentration as low as 0.03 wt% crystallizes 10 °C earlier than neat PET, indicating that SWNTs are acting as nucleating agents for PET crystallization.

The T_c values continue to increase with increasing SWNT concentration, but at a slower rate, as with the further 100 fold increase in SWNT concentration from 0.03 to 3.0 wt%, the additional T_c increase is only about 10 °C. In other words, there is a saturation of the nucleant effect at low SWNT concentrations, resulting in diminishing dependence on the increasing SWNT induced nucleation, possibly because of the large surface area and good dispersion of SWNTs.

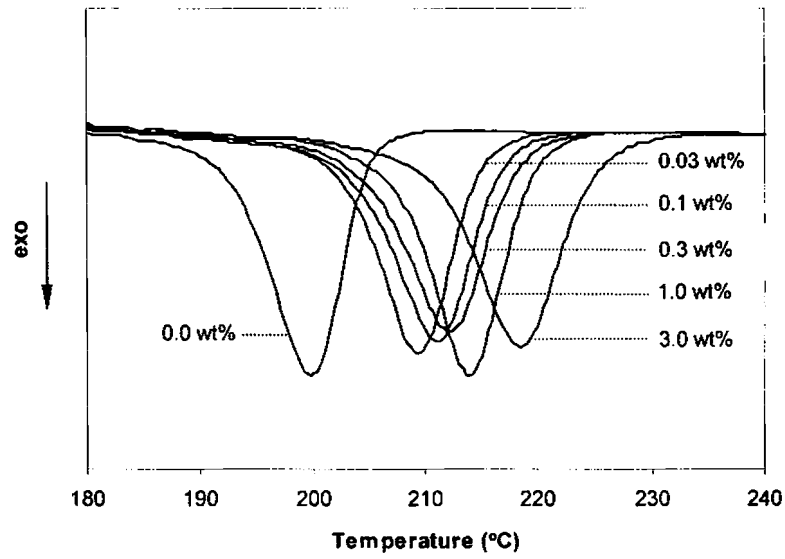

Fig. 2.9 DSC cooling scans (20 °C/min from 310 °C melt) of PET-SWNT nanocomposite samples

The non-linear dependence of the SWNT content on its nucleant effect of crystallization of the matrix polymer has also been reported by Valentini *et al.* and Probst *et al.*[47,44] Figure 2.10 indicates the non-isothermal crystallization curves of PP and PP-SWNT nanocomposites showing this behaviour. The authors describe the observed reduction in the ΔH_c values as a result of the proportional reduction of PP concentration in the composites.

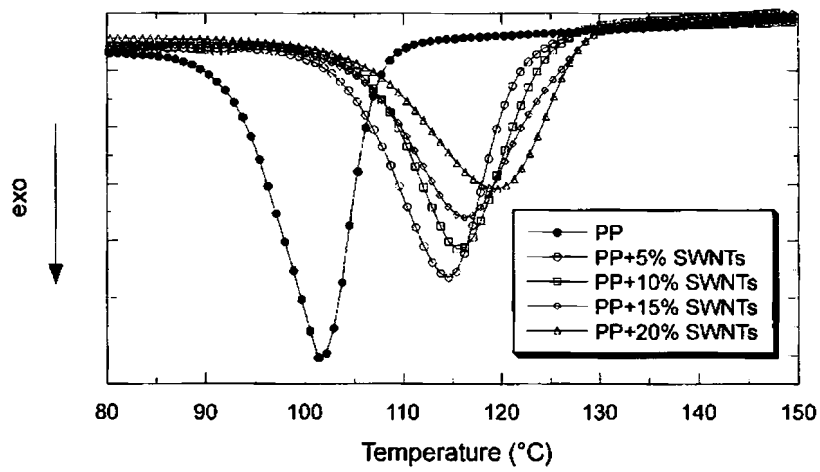

Fig. 2.10 DSC cooling scans of PP and PP-SWNT nanocomposites[#]

In programmed cooling, the crystallization temperature and the degree of supercooling ($\Delta T = T_m - T_c$) may be a measurement of the crystallizability; i.e. smaller the ΔT, higher the crystallizability.[26] The ΔT values of the PET-SWNT nanocomposites given in table 2.3 are smaller by ~ 11 to 20 °C than that of neat PET. This reveals that the crystallizability of the nanocomposites is greater than that of neat PET.

Table 2.3

ΔT values of PET-SWNT nanocomposite samples

Concn. of SWNTs (wt%)	ΔT (°C)
0.0	53.11
0.03	41.81
0.1	41.03
0.3	41.10
1.0	36.75
3.0	33.46

[#]Reproduced from: Valentini L. *et al.* Compos. Sci. Technol. 2003;63:1149.

The melting temperature (T_m), defined as the ratio between the heat of melting (ΔH_m) and the entropy of melting (ΔS_m) is also determined from DSC. It is known that ΔH_m is dependent on cohesion and intermolecular forces, whereas ΔS_m depends on parameters such as regularity of arrangements and flexibility of polymer chains. In the present case, the melting temperature and enthalpies of PET stay unaffected by melt compounded SWNTs.

2.3.3 Isothermal crystallization

Figure 2.11 shows the typical isothermal crystallization curves of the PET-SWNT nanocomposite samples at four temperatures (210, 215, 220 and 225 °C). The time corresponding to the maximum in the heat flow rate (exotherm) is taken as peak time of crystallization (t_{peak}). Such peaks are seen at each of the four isothermal crystallization temperatures for the 0.03 and 0.3 wt% SWNT containing nanocomposites, with the earlier or faster crystallization (smaller t_{peak}) corresponding to lower temperature of isothermal crystallization as compared to neat PET.

For the case of neat PET, no peak is seen at the highest temperature of 225 °C because crystallization is very slow and would require longer time than the 4 minutes employed in the DSC program. On the other hand, for the nanocomposite samples with 1.0 and 3.0 wt% SWNTs, the rate of crystallization is so fast near the lowest temperatures that most of the crystallization occurs already during the cooling scan (60 °C/min) employed to reach the temperatures (210 or 215 °C). This results in absence of exothermic peaks in the heat flow curves at those temperatures.

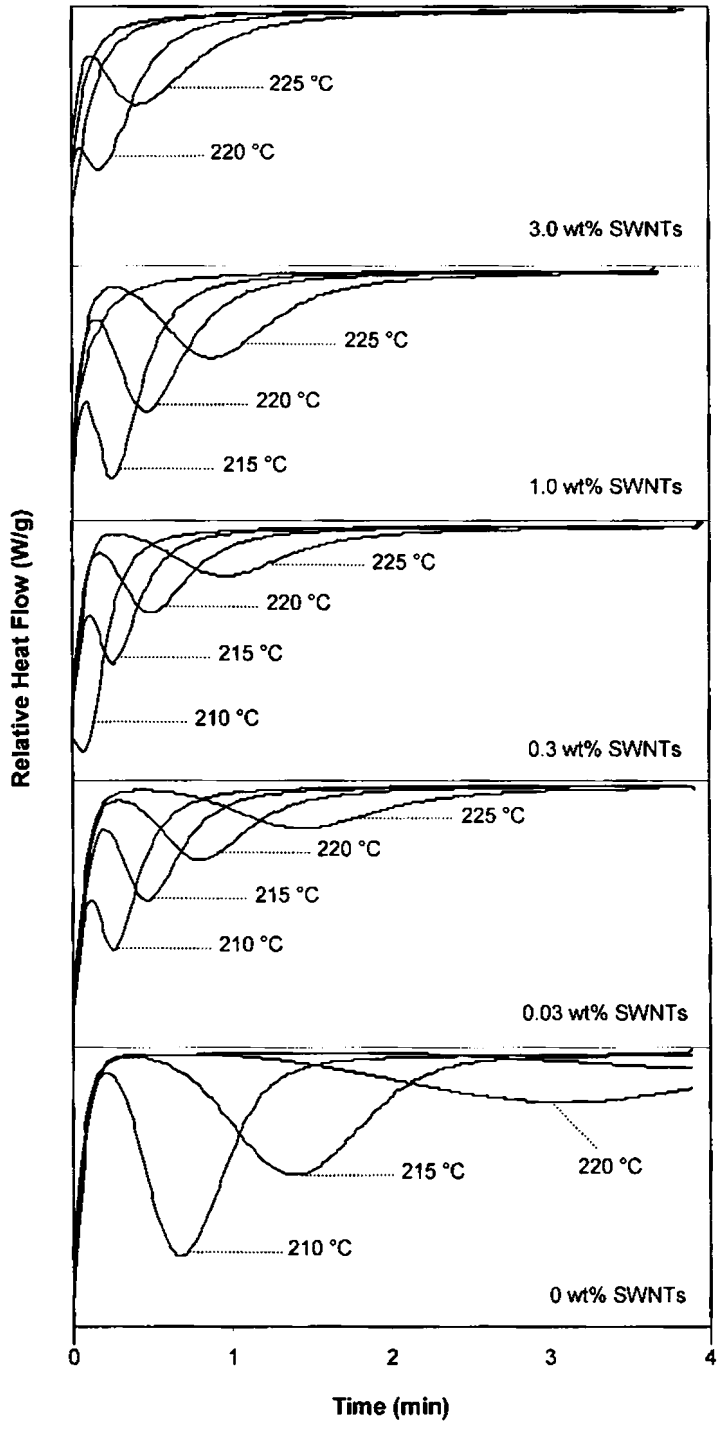

Fig. 2.11 Heat flow during isothermal crystallization of PET-SWNT nanocomposites

The peak times of crystallization at each of the temperatures for all the PET-SWNT nanocomposite samples are plotted against the isothermal crystallization temperature (figure 2.12). It is noticeable that the t_{peak} values for the nanocomposite samples reduce to less than 50 % as compared to neat PET due to the presence of SWNTs at concentrations as low as 0.03 wt%. With the increasing SWNT concentration there is further increase in the crystallization rate (as indicated by the decrease in t_{peak}), demonstrating the role of SWNTs in enhancing the rate of crystallization.

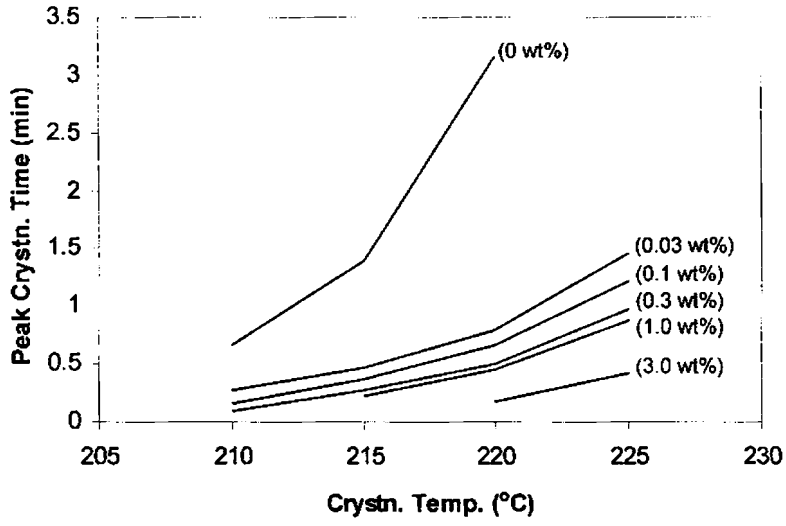

Fig. 2.12 Effect of SWNT concentration on the peak crystallization time of the nanocomposites at different isothermal crystallization temperatures

2.3.4 SWNT- induced aligned crystallization

Wide-angle X-ray diffraction (WAXD) experiments provide opportunity to simultaneously analyse the crystalline structure, the extent of crystallization, as well as the crystalline orientation. According to this method, the sample is scanned in a wide angle X-ray goniometer and when the X-rays are directed into the solid, they will scatter in predictable patterns based upon the internal structure of the solid. It is seen that the diffraction from an unoriented film is cylindrically symmetrical about the incident beam, whereas that from a drawn film is highly dependent on the azimuthal

angle of diffraction. This can be understood in that the diffraction can be regarded as a kind of reflection of crystal planes. Cylindrically symmetrical diffraction corresponds to random orientation of such planes, whereas diffraction at specific orientation angles corresponds to the orientation of crystals at particular angles. These, combined with the rigid rod like nature (large aspect ratio) of SWNTs resulting in their easy orientation and difficult relaxation in highly viscous melts, offers an interesting possibility of directly verifying the role of SWNTs as nucleating sites for crystallization of the matrix polymer using WAXD. Macroscopic orientation of SWNTs in relaxed PET was created by first stretching the solid nanocomposite sample under mechanical stress to orient both SWNTs and the matrix polymer, followed by orientational relaxation of the matrix polymer alone.[61]

The compression molded (0.5 mm thick, 4 mm wide) films of neat PET and PET-SWNT 1 wt% sample have been stretched (L_x/L_x^0 =) 4 times while heating in contact with a stainless steel plate at 150 °C (scheme 2.2).

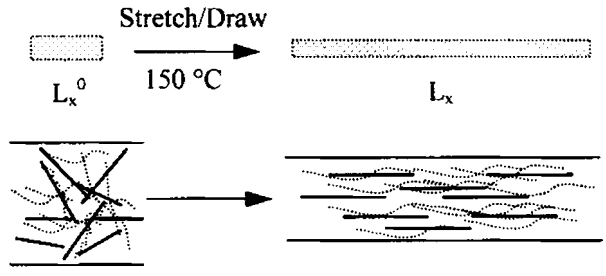

Scheme 2.2 Stretching of the compression molded nanocomposite film to achieve orientation of SWNTs and polymer chains. '_____' represents SWNTs and '.....' represents polymer chains

Figures 2.13 (a) and 2.14 (c) show the oriented PET crystal structure in the drawn PET-SWNT nanocomposite and neat PET samples respectively. It is expected that, in the case of the nanocomposite sample, orientation of the PET molecules be accompanied by the orientation of the rigid rod like SWNTs embedded therein.

The strips were then positioned on glass slides with their ends glued to the glass slides to resist future macroscopic deformation (shrinkage). Subsequent heating at 20 °C/min to 300 °C on a hot stage allowed microscopic visualization of the polymer melting under cross polars. During melting, it is to be expected that the polymer molecules lose their orientation and randomize, while the SWNTs may retain their orientation since their disorientation would demand the difficult rotation of the entire long rod like structure entangled within the polymer matrix.[62] Subsequent cooling at a slow rate of 10 °C/min on the microscope hot stage allowed observation of PET crystallization.

WAXD patterns of the resulting PET-SWNT 1 wt% nanocomposite and neat PET samples, shown in figures 2.13 (b) and 2.14 (d) respectively, indicate that the crystalline orientation is random in the neat PET case, as expected, whereas, the PET-SWNT sample shows oriented crystallization along the original stretching direction.

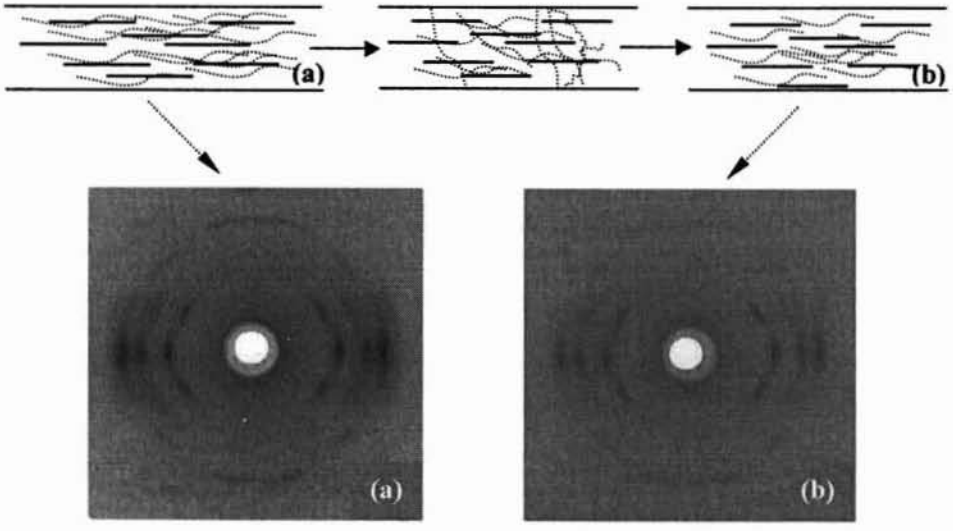

Fig. 2.13 WAXD patterns of (a): PET-SWNT 1 wt% nanocomposite film after drawing, (b): PET-SWNT 1 wt% nanocomposite drawn film after melting and subsequent slow cooling at constant length. The drawing direction was vertical. Top of the figure is a schematic representation of melting of the stretched nanocomposite film and its subsequent cooling.

This PET crystalline orientation in the composite emerging from the randomly unoriented quiescent melt is inferred to be a result of the oriented SWNTs therein, which are being responsible as nucleating sites for the reorientation of the crystallizing PET molecules.

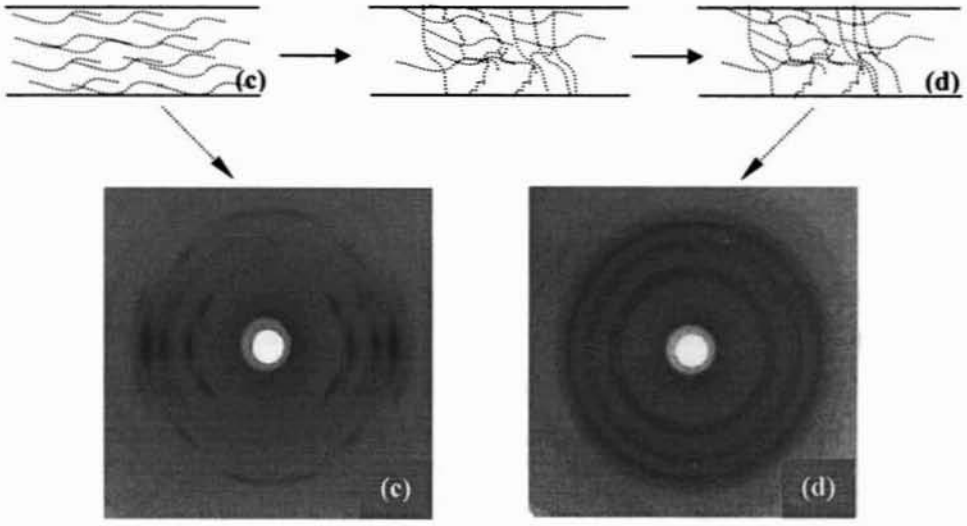

Fig. 2.14 WAXD patterns of (c): neat PET film after drawing, (d): neat PET drawn film after melting and subsequent slow cooling at constant length. The drawing direction was vertical. Top of the figure is a schematic representation of melting of the stretched PET film and its subsequent cooling.

2.3.5 SWNT-induced crystallization: A comparison with conventional nucleating agents

In order to compare the effectiveness of carbon nanotubes as nucleating agents over its traditional counterparts, poly(ethylene terephthalate) was compounded with sodium benzoate and talc at two concentrations viz., 0.1 and 1.0 wt%, under identical conditions as that for the PET-SWNT nanocomposite preparation. The crystallization temperatures (T_c) as determined from DSC are reported in table 2.4.

Table 2.4

DSC-determined T_c values for PET-sodium benzoate and PET-talc composites

Concentration of the nucleating agent (wt%)	Crystallization temperature, T_c (°C)	
	Sodium benzoate	Talc
0.0	199.9	199.9
0.1	208.4	205.2
1.0	211.8	207.4

The increase in the crystallization temperature for the composites with traditional nucleating agents is found to be much lower as compared to that with SWNTs. Table 2.5 presents a comparison of the increase in the T_c values of PET with SWNTs, sodium benzoate and talc at two different concentrations. These results indicate that SWNTs are excellent candidates as nucleating agents when compared to the conventional nucleating agents used for PET.

Table 2.5

Comparison of the T_c rise of PET with different nucleating agents

Nucleating agent	Increase in T_c (°C)	
	0.1 wt%	1.0 wt%
SWNTs	11.6	14.4
Sodium benzoate	8.5	11.9
Talc	5.3	7.5

2.4 Conclusions

PET-SWNT nanocomposites have been prepared through a simple melt compounding route. Melt compounded SWNTs have been shown to act as effective nucleating agents for PET crystallization. The SWNTs at a concentration as low as 300 ppm enhanced the crystallization temperature during melt cooling by 10 °C, and reduced the melt's isothermal crystallization time by more than 50 %. WAXD experiments indicated oriented crystallization of PET during cooling from randomized melts containing oriented SWNTs, supporting the hypothesis that SWNTs induce crystallization of PET chains along the SWNTs. A comparison of the nucleation ability of the nanotubes with their traditional counterparts also revealed that SWNTs are potentially very attractive candidates as nucleating agents.

References

1. Paul DR, Barlow JW, Keskkula H. In: Mark HF, Bikales NM, Overberger ChG, Menges G, editors. Encyclopedia of Polymer Science and Engineering. vol. 12. Wiley; 1989.
2. Fakirov S, editor. Handbook of Thermoplastic Polyesters. Wiley-VCH; 2002.
3. Scheirs J, Long TE, editors. Modern Polyesters. Wiley; 2003.
4. http://www.polysurfacesbookstore.com/pages/3775.html.
5. Hwang SH, Paeng SW, Kim JY, Huh W. Polym. Bull. 2003;49:329.
6. Ravindranath K, Mashelkar RA. Chem. Eng. Sci. 1986;41:2197.
7. Wang D, Zhu J, Yao Q, Wilkie CA. Chem. Mater. 2002;14:3837.
8. Lebaron PC, Wang Z, Pinnavaia TJ. Appl. Clay Sci. 1999;12:11.
9. Ullmann's Encyclopaedia of Industrial Chemistry. Wiley-VCH; 1996.
10. Van Bennekom ACM, Gaymans RJ. Polymer 1997;38:657.
11. Bouma K, de Wit G, Lohmeijer JHGM, Gaymans RJ. Polymer 2000;41:3965.

12. Agarwal US, de Wit G, Lemstra PJ. Polymer 2002;43:5709.

13. Joseph EG, Wilkes GL. Prepar. Am. Chem. Soc. Div. Polym. Chem. 1983;24:304.

14. Sukhadia AM, Done D, Baird DG. J. Polym. Eng. Sci. 1990;30:519.

15. Bhattacharya SK, Tendokar A, Misra A. Mol. Cryst. Liq. Cryst. 1987;153:501.

16. Sharma SK, Tendokar A, Misra A. Mol. Cryst. Liq. Cryst. 1988;157:597.

17. Zhu P, Ma D. Euro. Polym. J. 2000;36:2471.

18. Reinsch VE, Rebenfeld L. J. Appl. Polym. Sci. 1994;52:649.

19. Saujanya C, Imay Y, Tateyama H. Polym. Bull. 2002;49:69.

20. Ou CF. J. Appl. Polym. Sci. 2003;89:3315.

21. Ou CF. J. Polym. Sci. Part B: Polym. Phys. 2003;41:2902.

22. Suoboda P, Zeng C, Wang H, Lee LJ, Tomasko DL. J. Appl. Polym. Sci. 2002;85:1562.

23. Choi WM, Kim TW, Park OO, Chang YK, Lee JW. J. Appl. Polym. Sci. 2003;90:525.

24. Ke Y, Long C, Qi Z. J. Appl. Polym. Sci. 1999;71:1139.

25. Liu W, Tian X, Cui P, Li Y, Zheng K, Yang Y. J. Appl. Polym. Sci. 2004;91:1229.

26. Qu MH, Wang YZ, Wang C, Ge XG, Wang DY, Zhou Q. Euro. Polym. J. 2005;41:2569.

27. Wunderlich B. Macromolecular Physics, Vol. I. Academic Press; 1973.

28. Bassett DC. Principles of Polymer Morphology. Cambridge University Press; 1980.

29. Phillips PJ. Rep. Prog. Phys. 1990;53:549.

30. Price FP. General Electric Research Report. No. 61-RL-2730.

31. Binsbergen FL. Progress in Solid State Chemistry. Vol. 8; 1973.

32. Mercier JP. Polym. Eng. Sci. 1990;30:270.

33. Jr. Lauritzen JI, Hoffman JD. Res. Natl. Bur. Stand. (US), 1960;66A:73.

34. Hoffman JD, Davis GT, Lauritzen JI. Treatise on Solid State Chemistry, Vol. 3; 1976.

35. Maffezzoli A, Kenny JM, Nicolais LN. J. Mater. Sci. 1993;28:4994.

36. Wunderlich B, Aspy M. J. Polym. Sci. Part B: Polym. Phys. 1974;12:255.

37. Strobl GR. The Physics of Polymers. Springer-Verlag; 1996.

38. Imai M, Mori K, Mizukami T, Kaji K, Kanaya T. Polymer 1992;33:4457.

39. Ezquerra A, Lopez-Cabarcos E, Hsiao BS, Balta-Calleja FJ. Phys. Rev. 1996;54:989.

40. Terrill NJ, Fairclough PA, Towns-Andrews E, Komanschek BU, Young RJ, Ryan A. Polymer 1998;39:2381.

41. Liu Y. Macromol. Mater. Eng. 2001;286:611.

42. Iijima S. Nature 1991;56:354.

43. Ajayan PM. Chem. Rev. 1999;99:1787.

44. Probst O, Moore EM, Resasco DE, Grady BP. Polymer 2004;45:4437.

45. Grady BP, Pompeo F, Shambaugh RL, Resasco DE. J. Phys. Chem. 2002;B-106:5852.

46. Bhattacharyya AR, Sreekumar TV, Liu T, Kumar S, Ericson LM, Hauge RH, Smalley RE. Polymer 2003;44:2373.

47. Valentini L, Biagiotti J, Kenny JM, Santucci S. J. Appl. Polym. Sci. 2003;87:708.

48. Assouline E, Lustiger A, Barber AH, Cooper CA, Klein E, Wachtel E, Wagner HD. J. Polym. Sci. Part B: Polym. Phys. 2003;41:520.

49. Nogales A, Broza G, Roslaniec Z, Schulte K, Sics I, Hsiao BS, Sanz A, Garcia-Gutierrez MC, Rueda DR, Domingo C, Ezquerra TA. Macromolecules 2004;37:7669.

50. Li SN, Li ZM, Yang MB, Hu ZQ, Xu XB, Huang R. Mater. Lett. 2004;58:3967.

51. Kim JY, Park HS, Kim SH. Polymer 2006;47:1379.

52. Solomon OF, Ciuta IZ. J. Appl. Polym. Sci. 1962;6:683.

53. Parashar MK, Gupta RP, Jain A, Agarwal US. J. Appl. Polym. Sci. 1998;67:1589.

54. Ma Y, Agarwal US, Sikkema DJ, Lemstra PJ. Polymer 2003;44:4085.

55. Koepp HM, Werner H. Macromol. Chem. 1959;32:79.

56. Shofner ML, Rodriguez-Macias FJ, Viadyanathan R, Barrera EV. Composites Part A. Appl. Sci. Manufactur. 2003;34:1207.

57. Fukada M, Kawai H. Polymer 1990;31:295.

58. Jabarin SA, Lofgren EA. Polym. Eng. Sci. 1983;26:620.

59. Dargent E, Denis G, Caron C, Saiter JM, Grenet J. J. Appl. Polym. Sci. 2000;77:1056.

60. Torres N, Robin JJ, Boutevin B. Euro. Polym. J. 2000;36:2075.

61. Jin L, Bower C, Zhou O. Appl. Phy. Lett. 1998;73:1197.

62. Doi M, Edwards SF. The Theory of Polymer Dynamics. Oxford University Press; 1986.

Chapter 3

PET-SWNT nanocomposites

Reinforcement and electrical properties*

Abstract

Melt compounded nanocomposites of PET and SWNTs have been compression molded. With increasing concentration of SWNTs, the mechanical and dynamic mechanical properties improved, corresponding to an effective reinforcement. Melt rheological characterization indicated the effective entanglements provided by SWNTs in the melt state as well. Thermogravimetric analysis and thermal expansion studies suggested no significant influence of SWNTs on the thermal and dimensional stability of PET. Electrical conductivity measurements on the composite films pointed out that melt compounded SWNTs can result in electrical percolation albeit at concentrations exceeding 2 wt%.

---

*K. Anoop Anand, U.S. Agarwal, Rani Joseph. ***Journal of Applied Polymer Science 2006 (in press)***.

A part of the work described in this chapter has been presented at the *International Conference on Nanoscience and Technology- **ICONSAT 2006**, March 16-18, 2006, India Habitat Center, New Delhi, India* and at the *17th AGM of Materials Research Society of India, **AGM-MRSI**, Feb 13-15, 2006, University of Lucknow, India.*

3.1 Introduction: Carbon nanotubes as reinforcement in polymers

The mechanical behavior of carbon nanotubes is exciting since they are seen as the 'ultimate' carbon fibers ever made. For the same reason, they hold promise as a possible reinforcing phase in composite materials of a new kind.[1-4] The traditional carbon fibers have about *fifty times* the specific strength (strength/density) of steel and are excellent load-bearing reinforcements in composites.[5] Nanotubes should then be ideal candidates for structural applications for high strength, light weight, high performance composite materials; for a series of products ranging from expensive tennis rackets to spacecraft and aircraft body parts. For example, NASA has recently invested large amount of money in developing carbon nanotube-based composites for applications such as futuristic Mars mission.[6]

3.1.1 Reinforcement of poly(ethylene terephthalate)

Statistical reports indicate a great potential for poly(ethylene terephthalate) in non-fiber applications, which mainly include its applications to bottles, films and engineering purposes.[7-9] These non-fiber applications stimulate research on the development of PET. Patents and papers concerning PET or overall polyesters are numerous, in which some cover a variety of fields including blends and/or composites of PET, which provide enormous improvements in its properties e.g. thermal and mechanical properties.[10,11] In most studied cases, however, the phase separation resulting from the difference in the surface tension force between the filler and the polymer matrix is usually obvious which has produced an obstacle on the ultimate dispersion and adhesion of the particles to the polymer matrix.

Nanoparticles are often used to directly blend with polymer resins and have achieved some successful results.[12] The direct blending method cannot avoid the particle-clustering tendency and hence the advantages of such systems have been limited. But these limitations, to a certain extent, have been overcome by using solvent assisted methods along with ultrasound treatments etc. or *in-situ* polymerization. For example, Ke *et al.* have studied the crystallization, properties and crystal and nanoscale morphology of PET-clay nanocomposites.[13] They reported that 'intercalation followed

by *in-situ* polymerisation' resulted in good dispersion of clay platelets in the polymer matrix and enormously improved the properties of PET.

For the past one decade, carbon nanotubes have been widely employed to reinforce a large number of polymers, so also thermoplastics. This chapter presents the results of investigations on the effect of melt compounded single walled carbon nanotubes (SWNTs) on the mechanical, dynamic mechanical, thermo mechanical, rheological, thermal, and electrical conducting characteristics of poly(ethylene terephthalate).

3.2 Experimental

3.2.1 Sample preparation: Compression molding

PET-SWNT nanocomposites were prepared by melt compounding (section 2.2.1 and 2.2.2 of this thesis). These samples were compression molded at 270 °C for 4 min in an electrically heated hydraulic press. They were quenched from the melt to avoid excessive degradation during the otherwise slow cooling, and then annealed at 150 °C for 1 h before using for further characterization.

3.2.2 Mechanical properties

Mechanical properties of the compression-molded samples of PET-SWNT nanocomposites were studied using a Universal testing machine (UTM, Shimadzu, model-AG1) with a load cell of 10 kN capacity. The specimens used were rectangular strips of dimensions 30 × 5 × 0.5 mm. The gauge length between the jaws at the start of each test was adjusted to 20 mm and the measurements were carried out at a cross-head speed of 1 mm/min. Average of atleast six sample measurements were taken to represent each data point.

3.2.3 Scanning electron microscopy (SEM)

Scanning electron micrographs of the cryofractured surfaces of the samples have been recorded using a Philips Scanning electron microscope (XL 30, ESEM-FEG).

The fractured surfaces have been sputtered with gold before they were observed in SEM. The acceleration voltage used for image acquisition was 20 kV.

3.2.4 Dynamic mechanical analysis (DMA)

Dynamic mechanical analyser (DMA Q-800, TA Instruments) was used to study the effect of SWNTs on the viscoelastic properties of PET. Rectangular shaped specimens of dimensions 20 × 4 × 0.5 mm were exposed to a series of increasing isothermal temperatures from room temperature to 200 °C at a temperature increment rate of 2.5 °C and an isothermal soak time of 5.0 min. At each temperature the material was deformed at a constant amplitude of 10.0 μm over a frequency of 1 Hz. The dynamic storage modulus, loss modulus and tan δ (loss modulus/storage modulus) were measured.

3.2.5 Melt rheology

Rheological measurements were performed using an Advanced Rheometric Expansion System (ARES) oscillatory rheometer (Rheometric Scientific). Plate-plate geometry with a plate diameter of 25 mm was employed. Prior to the experiment, the samples were vacuum dried at 150 °C for atleast 2 h in order to limit hydrolytic degradation during the measurement at 280 °C. Solid samples of diameter 25 mm and thickness 1 mm were placed between the preheated plates and were allowed to equilibrate for approximately 10 min before each frequency sweep run.

Oscillatory strain (γ (t)) of the form,

$$\gamma(t) = \gamma_0 \sin(\omega t) \tag{3.1}$$

where γ_0 is the strain amplitude, ω is the frequency and t is the time, was applied.[14-16]

The resulting time-dependent linear shear stress ($\sigma(t)$) is interpreted as,

$$\sigma(t) = \gamma_0 [G' \sin(\omega t) + G'' \cos(\omega t)] \tag{3.2}$$

where G' and G" are the storage and loss modulus, respectively.

The complex viscosity (η^*) defined as in (3.3) was also determined.

$$\eta^* = 1/\omega\ [(G')^2 + (G'')^2]^{1/2} \tag{3.3}$$

Data were recorded in a frequency range of 0.1-100 rad/sec. All measurements in this study were linear (i.e. G' and G" are independent of γ_0). The strain region in which the material can be regarded as linear viscoelastic was determined by amplitude sweep measurements and it was in the order of 10 %. The measurements were conducted in nitrogen atmosphere in order to minimize thermo-oxidative degradation.

3.2.6 Thermogravimetric analysis (TGA)

Thermogravimetric analyser (TGA Q-50, TA Instruments) was used to study the effect of SWNTs on the thermal stability of PET. Approximately 5 mg of the samples were heated at a rate of 20 °C/min from ambient to 700 °C. The chamber was continuously swept with nitrogen at a rate of 90 mL/min.

3.2.7 Coefficient of thermal expansion (CTE)

The coefficient of thermal expansion (CTE) of the samples in different temperature ranges was measured using a Thermo mechanical analyser (TMA, TA Instruments). The samples were cut into cubic specimens (4 × 4 × 4 mm) by milling and then annealed at 150 °C for 1 h before the test to eliminate the influence of thermal history.

3.2.8 Electrical conductivity

The D.C. electrical conductivity of the nanocomposite samples (rectangular strips of dimensions, 40 × 15 × 0.5 mm) was measured using a Keithley Nanovoltmeter (model 2182) in dry air at ambient temperature. A standard four-probe electrode configuration was used for the measurements.

3.3 Results and discussion

Even though melt compounding is one of the most viable and commercially versatile routes for the preparation of plastics based nanocomposites, this method has limitations in completely dispersing the ingredients in the matrix. This fact is predominant in the case of SWNTs because of the strong tube-tube interactions leading to their clustering in highly viscous polymer melts. Figure 3.1 represents the transmission mode optical micrograph of a thin compression-molded nanocomposite film with 3.0 wt% SWNTs. The black particles indicate the amorphous/undispersed components from SWNTs.

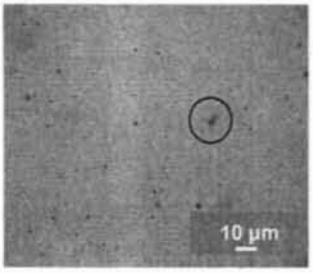

Fig. 3.1 Optical micrograph of 3 wt% PET-SWNT nanocomposite film

3.3.1 Molecular weight depletion during melt processing

Considering the sensitivity of properties of PET to molecular weight, an evaluation of the effect of SWNTs on PET properties requires comparison at similar molecular weights. For this purpose, virgin PET was also subjected to melt compounding and compression molding processes under identical conditions as that for the PET-SWNT nanocomposite preparation.

The decline in molecular weight of PET as a result of thermal/ hydrolytic/ oxidative degradation during melt processing was monitored by intrinsic viscosity, [η] measurements (section 2.2.3). It is observed that the [η] of PET drops from 0.98 dL/g to 0.88 dL/g during melt compounding and to 0.79 dL/g during compression molding. As shown in table 3.1, the nanocomposite samples also have comparable [η] after the processing steps. The reported [η] values are the average of atleast five concordant measurements. Since all the samples have comparable [η] (or molecular weight) after

processing under identical conditions, it is inferred that the possible dependence of property measurement studies on the molecular weights of the samples has been eliminated.

Table 3.1

Intrinsic viscosities of compression molded samples of neat PET and PET-SWNT nanocomposites (0.5 g/dL solutions in 1/1 phenol/TCE at 30 ± 0.1 °C)

Concn. of SWNTs (wt%)	[η] (dL/g)
0.0	0.794
0.03	0.796
0.1	0.793
0.3	0.798
1.0	0.783
3.0	0.790

3.3.2 Strength, modulus and elongation

The ability of a material to resist breaking under tensile stress is one of the most important and widely measured properties of plastics used in structural applications. The force per unit area required to break a material in such a manner is called the *tensile strength*. The *tensile modulus* is the ratio of stress to elastic strain in tension. A high tensile modulus means that the material is rigid i.e. more stress is required to produce a given amount of strain.

The *elongation at break* or *ultimate elongation* of a plastic is the percentage increase in length that occurs before it breaks under tension. Ultimate elongation values of several hundred percent are common for elastomers and for film/packaging polyolefins. Rigid plastics, especially fiber reinforced ones, often exhibit values around 5 %. The combination of high tensile strength and high elongation leads to materials of high toughness.

Tensile tests were performed on flat tensile bars cut from the compression molded PET-SWNT nanocomposite films. The results in figure 3.2 show the expected increase in the tensile strength and modulus of PET with increasing concentration of SWNTs. For example, incorporation of SWNTs at a level of 1 wt% increases the strength by about 25 % and modulus by over 50 %.

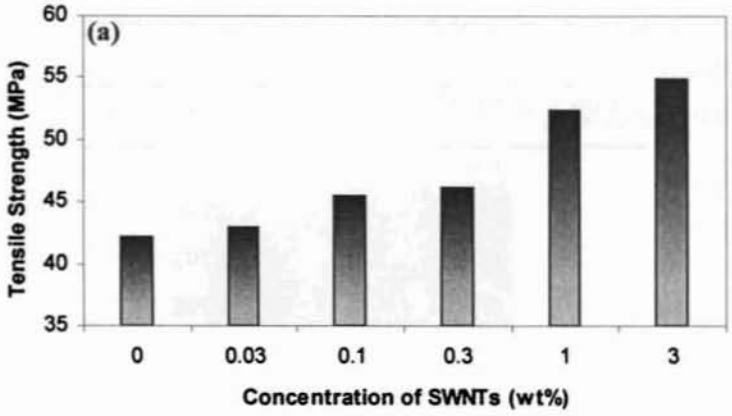

Fig. 3.2 (a) Effect of SWNT concentration on the tensile strength of PET

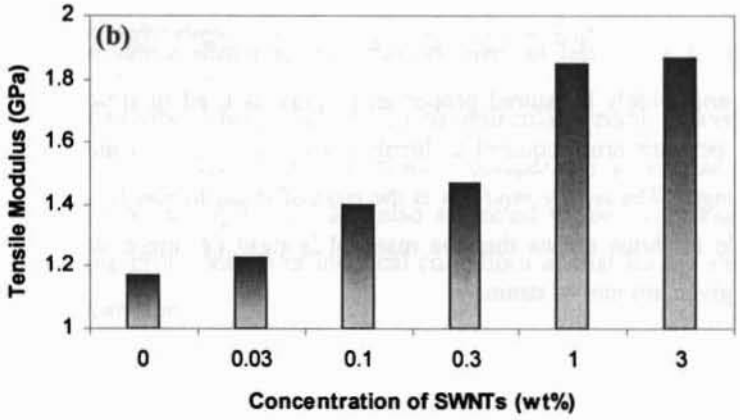

Fig. 3.2 (b) Effect of SWNT concentration on the tensile modulus of PET

These results are almost in agreement with a report by Qian and his colleagues, which says that the addition of 1 wt% nanotubes into polystyrene matrix results in 25 % increase in tensile strength and 36-42 % increase in modulus.[17]

The elongation at break is found to be decreasing with the increasing loading of SWNTs, indicating that the nanocomposites become brittle (figure 3.2 (c)). These results demonstrate that even a small fraction of SWNTs provide effective reinforcement to the PET matrix. Zhang *et al.* also reported that carbon nanotubes in polyamide matrix improved the polymer mechanical properties enormously.[18]

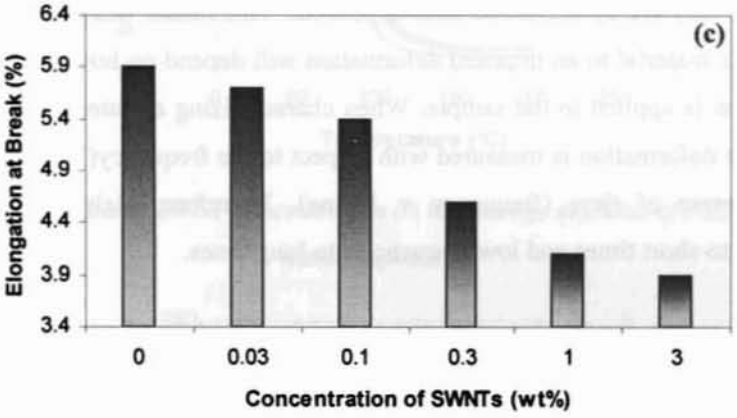

Fig. 3.2 (c) Effect of SWNT concentration on the elongation of PET

The morphology of the samples has been investigated using scanning electron microscopy. The SEM photographs of the cryofractured surfaces of neat PET and 1 wt% SWNT containing nanocomposite are shown in figure 3.3. No significant variation in morphology is observed at this magnification level.

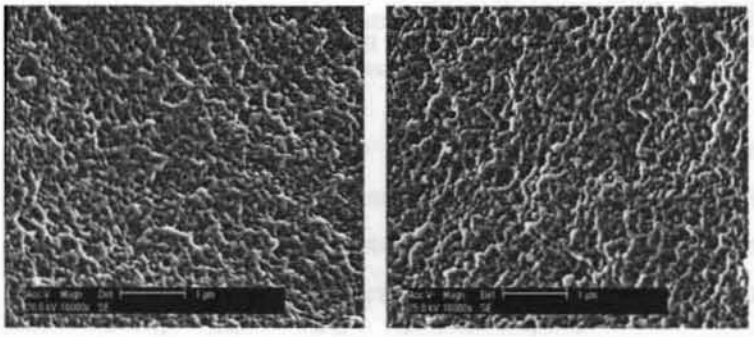

Fig. 3.3 Scanning electron micrographs of cryogenically fractured surfaces of neat PET (left) and (1 wt%) PET-SWNT nanocomposite (right)

3.3.3 Temperature dependence of the solid's viscoelastic characteristics

In dynamic mechanical analysis (DMA), the viscoelastic properties of a material are characterized by applying a sinusoidal deformation to the material at a single or at multiple frequencies, and monitoring the response of the material. Since polymers are viscoelastic materials, i.e. they simultaneously exhibit solid-like and liquid-like properties, they are by definition time-dependent. This means that the response of a viscoelastic material to an imposed deformation will depend on how fast or slow the deformation is applied to the sample. When characterizing a material by DMA, the time of the deformation is measured with respect to the frequency(ies), as frequency is the inverse of time (frequency = 1/time). Therefore, high frequencies are analogous to short times and low frequencies to long times.

The DMA results for the dynamic storage and loss modulii of neat PET and PET-SWNT nanocomposite samples as a function of temperature at 1 Hz are shown in figure 3.4. Following a slow decrease of the storage modulii with temperature in the glassy state, a rapid decrease in the modulii is observed corresponding to the glass-rubber transition (figure 3.4 (a)). The storage modulii of the nanocomposite samples below glass transition increase substantially with the SWNT concentration due to the stiffening effect of nanotubes, and indicating efficient stress transfer between the polymer matrix and SWNTs. The loss modulus values also increase substantially with the nanotube loading (figure 3.4 (b)). The reinforcing effect of SWNTs in the nanocomposite systems can be attributed to their specific interactions and the formation of a rigid percolating nanotube network within the thermoplastic polymer matrix.

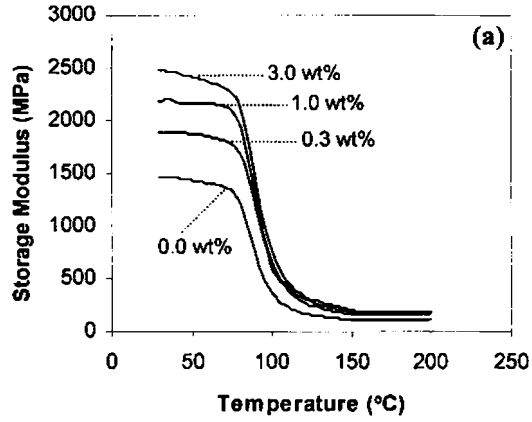

Fig. 3.4 (a) Effect of SWNT concentration on the storage modulus of PET-SWNT nanocomposites

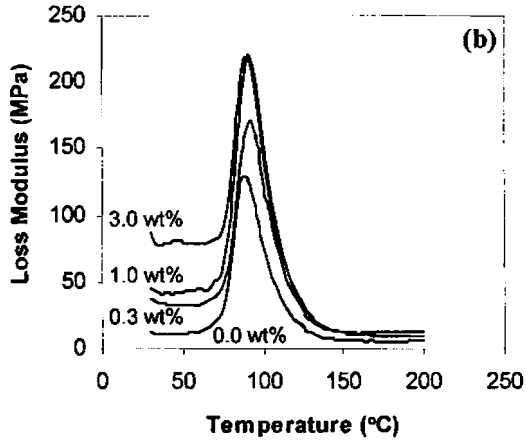

Fig. 3.4 (b) Effect of SWNT concentration on the loss modulus of PET-SWNT nanocomposites

DMA is most widely used to measure the glass transition temperature (T_g) of polymers.[19] Glass transition occurs when a hard, solid material or component undergoes its transformation to a soft rubbery phase. It represents the lower end use temperature since the material cannot be processed once its temperature drops below T_g. Factors increasing the stiffness of the polymeric molecular segments will tend to increase T_g. Glass transition is a kinetic transition; molecular relaxation that involves cooperative segmental motion, whose rate is strongly influenced by the frequency

(rate) and temperature of testing. In the present case, the frequency is 1 Hz and temperature range is from ambient to 200 °C. It has already been reported that carbon nanotubes may affect the glass transition temperature of the matrix polymer.[20] For example, with 1 wt% well-dispersed SWNTs, the glass transition temperature of PMMA is reported to be increased by 40 °C.[21] Ogasawara *et al.* also observed that the T_g of polyimide matrix increased with the incorporation of multi walled carbon nanotubes.[22] On the other hand, there have also been reports in literature indicating no effect of CNTs on the T_g of polymers.

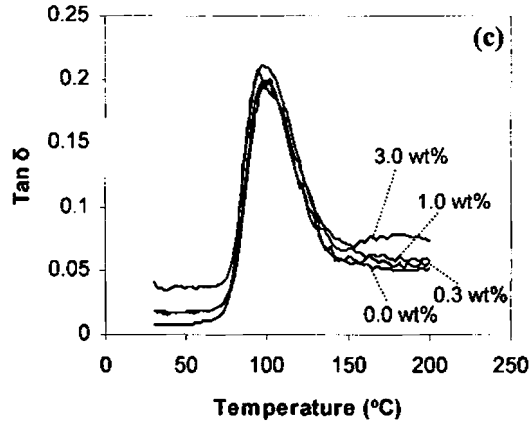

Fig. 3.4 (c) Effect of SWNT concentration on the tan δ of PET-SWNT nanocomposites

Though the storage modulus values are enhanced by SWNTs, the tan δ (tan δ = loss modulus/storage modulus) curves in figure 3.4 (c) indicate that the SWNTs at concentrations of upto 3.0 wt% have no significant influence on the glass transition temperature of PET. The effect of SWNTs on the glass transition temperature of thermoplastic polymers is not well understood, as both the increase and lack of dependence have been reported.[23,24]

3.3.4 Viscoelastic characteristics of the melts

The processability of polymers and their composite materials has been a great concern to the polymer processing industry, which is very closely related to their rheological properties in the molten state.[25] In the case of a composite system, these properties are

very sensitive to the dispersion state of the filler and to a lesser extent, to the interactions between the filler and the polymer.[26-28] Because the rheological properties of the filled polymer systems are responsive to the structure, particle size, geometry, and the surface characteristics of the fillers, rheological measurements are commonly used to describe the dispersion of the filler in polymer matrices.[29,30]

The dynamic spectra representing the linear viscoelastic properties of PET-SWNT nanocomposites at different concentrations of SWNTs are shown in figure 3.5.

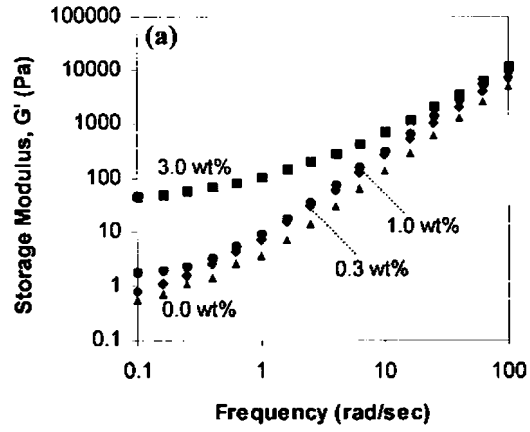

Fig. 3.5 (a) Effect of SWNT concentration on the storage modulus of PET-SWNT nanocomposites

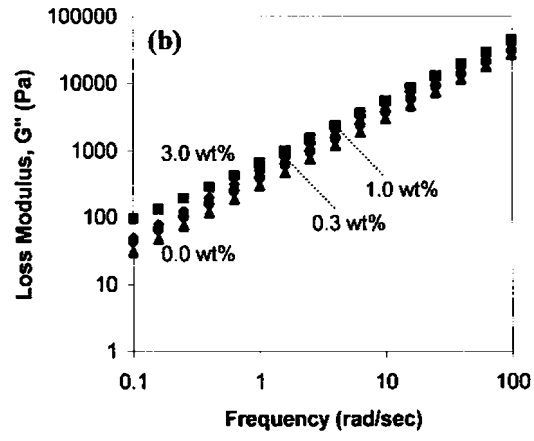

Fig. 3.5 (b) Effect of SWNT concentration on the loss modulus of PET-SWNT nanocomposites

It is noticed that, with increasing SWNT loading, the storage (G') and loss (G") modulii increase at all frequencies (figure 3.5 (a) and (b)). In particular, G' at low frequencies increases 100 fold on incorporation of 3.0 wt% SWNTs. These results indicate that melt compounded SWNTs are effectively entangled in the melt state also.

Figure 3.5 (c) illustrates the frequency dependence of complex viscosity (η^*) of the PET-SWNT nanocomposites. It is noticed that neat PET as well as the samples with low SWNT content display the expected Newtonian behaviour at low frequencies, and shear thinning behaviour at higher frequencies. However, the 3.0 wt% SWNT sample shows a marked enhancement in the complex viscosity and strong shear thinning behaviour even at the lowest frequency examined.

These results are in agreement with those reported by Li *et al.* who observed the decrease of shear viscosity of PET composites with MWNTs.[31] Pötschke *et al.* also observed shear thinning even at low frequencies for polycarbonate nanocomposites with carbon nanotube concentration exceeding 2.0 wt%.[32]

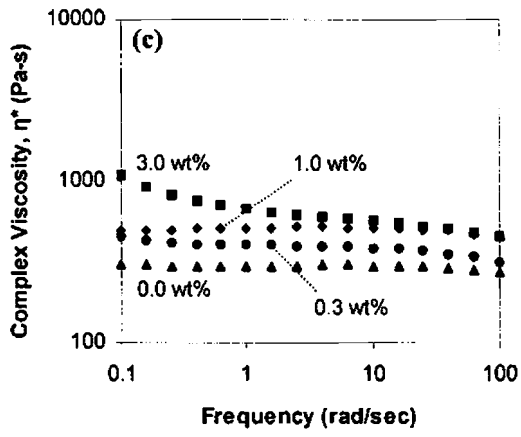

Fig. 3.5 (c) Effect of SWNT concentration on the complex viscosity (T = 280 °C, strain = 10 %) of PET-SWNT nanocomposites

Figure 3.5 (d) indicates the torque curves of the nanocomposites. As expected, the torque required in the case of nanocomposite samples is slightly higher as compared to neat PET at all frequencies.

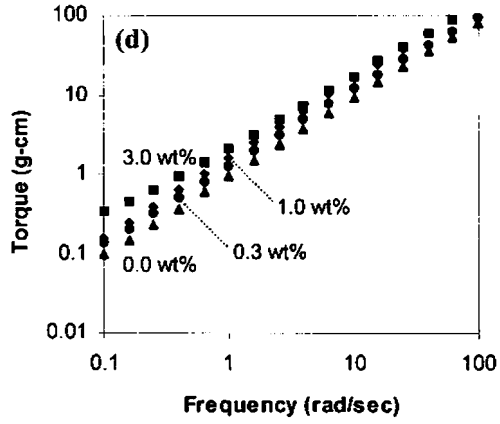

Fig. 3.5 (d) Effect of SWNT concentration on the torque values of PET-SWNT nanocomposites

In a particularly impressive report by Hu *et al.*, they have mentioned the dynamic rheological characteristics of PET-MWNT nanocomposites.[33] It was observed that the viscosity of neat PET is almost independent of frequency, and the nanocomposite at MWNT loading of 0.5 wt% showed a weak shear thinning behavior, whereas the nanocomposites with higher MWNT loadings exhibited strong shear thinning behavior and the viscosities were orders of magnitude higher than that of neat PET at low frequency. However Shin *et al.* reported that the addition of MWNTs to PET led to an increase in complex viscosity but the viscosity did not depend on the nanotube content upto 1.0 wt%.[34]

3.3.5 Thermal stability

Thermal stability of high polymers is of prime importance in fabrication processes. Knowledge gained from studies of polymer degradation may lead to more useful and stable products. Thermal degradation of PET is a major problem at temperatures above the melting point and inevitably occurs in polymer melts during synthesis and processing. Study of thermal degradation can be best complimented or corroborated by such techniques as thermogravimetric analysis (TGA) which measures the weight loss as a function of temperature, or derivative TGA (DTG).

There are several reports in literature regarding the enhancement of thermal stability of polymers with nanofillers. For e.g. Yang *et al.* have observed that nanosized silica improved the thermal stability of poly(methyl methacrylate).[35,36] Qu *et al.* have shown that the composites of PET with $BaSO_4$ nanoparticles possessed higher thermal stability than neat PET.[37] Some researchers have reported the enhancement of thermal stability of polymers with carbon nanotubes also.[38,39] Kashiwagi *et al.* have studied the thermal degradation and flammability properties of PP-MWNT nanocomposites.[40,41] They observed that the thermal stability of the matrix polymer (in nitrogen atmosphere) enhanced with carbon nanotubes. On the other hand, unpurified SWNTs have also been reported as enhancing the thermal degradation of polyamides.[42]

There are many reports in literature mentioning the effect of various metal catalysts influencing the thermal degradation of PET.[43,44] Since unpurified SWNT sample has residual catalysts such as Ni, thermal degradation studies of PET-SWNT nanocomposites are of prime importance. In this section, the temperature dependence of weight loss characteristics of melt compounded PET-SWNT nanocomposites has been examined.

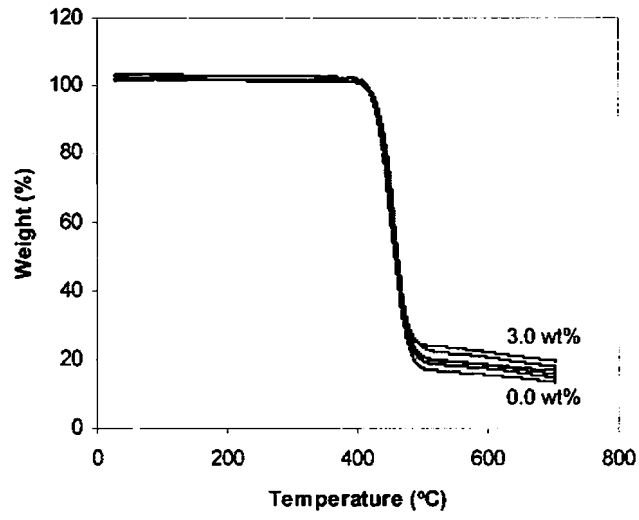

Fig. 3.6 Temperature dependence of the weight loss characteristics (TGA) of PET-SWNT nanocomposite samples

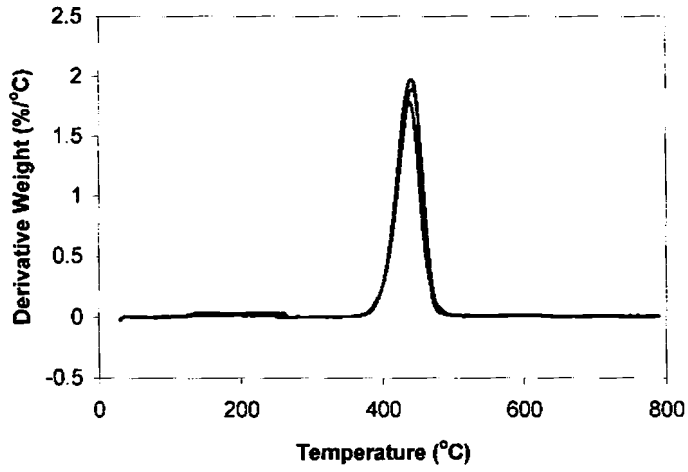

Fig. 3.7 Typical DTG traces for neat PET and PET-SWNT nanocomposites (1.0 and 3.0 wt%)

The TGA plots of nanocomposites in figure 3.6 indicate that the decomposition of all samples starts at around 420 °C irrespective of the SWNT concentrations and thus the thermal stability of PET is inferred to be unaffected by the presence of SWNTs upto a concentration of 3.0 wt%. Figure 3.7 indicates typical derivative thermogravimetric (DTG) curves for neat PET and PET-SWNT nanocomposites with two selected compositions.

3.3.6 Dimensional stability

One of the major issues for polymers in engineering applications is to reduce the coefficient of thermal expansion (CTE) to achieve dimensional stability more comparable with metals. The traditional concept to lower the thermal expansion coefficient of polymers is by adding a second component, such as an inorganic filler, with relatively low thermal expansion coefficient and suppressing the expansion by simple mechanical restraints.[45-47]

Numerous studies have examined how filler shape, size, concentration and its dispersion influence the thermal expansion of polymer composites.[48-54] However, since the filled polymer composites often suffer from poor toughness, bad appearance and

difficulty in processing, the reduction in the thermal expansion coefficient by this approach remains with significant limitations in practical applications. Using fillers of nanoscale dimensions may eliminate some of these limitations. For example, Liang *et al.* have prepared poly(etherimide)-montmorillonite nanocomposites by melt intercalation.[55] They observed that the coefficient of thermal expansion of the matrix polymer significantly reduced with clay concentrations beyond 10 wt%. However the data shown in table 3.2 indicate that melt compounding of SWNTs at a level of upto 3 wt% is unable to influence the CTE of PET.

Table 3.2

Coefficient of thermal expansion (CTE) for PET-SWNT nanocomposites at different temperature ranges

Concn. of SWNTs (wt%)	Coefficient of thermal expansion ($/°C \times 10^{-5}$)		
	$^{-}$20 – 80 °C	0 – 80 °C	20 – 80 °C
0.0	6.3	6.4	6.4
0.03	6.5	6.6	6.7
0.1	6.4	6.5	6.5
0.3	6.5	6.6	6.6
1.0	6.8	6.9	7.0
3.0	6.1	6.2	6.3

3.3.7 Electrical conductivity

Insulating polymers can be imparted electrical conducting properties by dispersion of electrically conducting particles that may form a percolative path of conducting network through the sample at concentrations exceeding certain minimum value called the percolation threshold. This approach reduces the manufacturing and maintenance costs of components as compared with those previously coated with an antistatic paint. The technology is also relevant to other applications where static electrical dissipation is needed such as computer housings or exterior automotive parts.

Though carbon black is traditionally used as a conductive filler, the small diameter and large aspect ratio of SWNTs (helps creating extensive networks that facilitate electron transport) has enabled achievement of very low percolation threshold concentrations, presumably depending on the quality of their dispersion. Earlier literature reports have revealed the percolation threshold for electrical conductivity at fairly high concentrations of nanotubes. For example, Bin *et al.* prepared MWNT/high-density polyethylene nanocomposites by gelation/crystallization from solutions, and revealed that the percolation occurred between 5 and 15 wt%.[56] Meincke *et al.* also found that CNT-filled polyamide-6 showed an onset of electrical conductivity at nanotube loadings of 4-6 wt%.[57]

Later, researchers have reported percolation threshold concentrations at around 1-2 wt% (or even less) of the nanotubes in polymer matrices. Kharchenko *et al.* prepared polypropylene-MWNT nanocomposites by melt blending, and displayed that the percolation threshold was at concentrations ranging from 0.25 to 1 wt%.[58] Du *et al.* used coagulation method to produce SWNT-poly(methyl methacrylate) nanocomposites and disclosed percolation threshold between 0.2 and 2 wt%.[59,60] Ounaies *et al.* reported that the conductivity of pristine polyimide was increased from an order of magnitude of 10^{-18} S cm^{-1} to 10^{-8} S cm^{-1} at nanotube concentrations between 0.02 and 0.1 vol%.[61]

Coleman *et al.* observed that the physical doping with carbon nanotubes in a conjugated polymer matrix such as poly(p-phenylene vinylene-co-2,5-dioctoxy-m-phenylene vinylene) (PmPV), could increase the conductivity of the matrix polymer by ten orders of magnitude.[62] Regev *et al.* also have observed that SWNTs increased the conductivity of polystyrene by ten orders of magnitude at very low percolation threshold concentrations.[63] Indeed, there are several other reports in literature regarding the CNT-induced electrical conductivity in a variety of insulating polymer matrices.[64]

The room temperature D.C. electrical conductivity results of the PET-SWNT nanocomposite samples are shown in figure 3.8. Neat PET is an excellent insulating material and has a conductivity value of the order of 10^{-17} S cm^{-1}.[33] It is evident from

figure 3.8, that SWNTs are effective in imparting electrical conductivity to the PET matrix and the conductivity reaches percolation, a value of the order of 10^{-6} S cm^{-1} at concentrations exceeding 2.0 wt%. It is also well known that the percolation threshold is sensitive to the polymer matrix in which the nanotubes are dispersed and the processing methods.[65] This effect is due to the role of enhanced interfacial properties found for the nanocomposites.

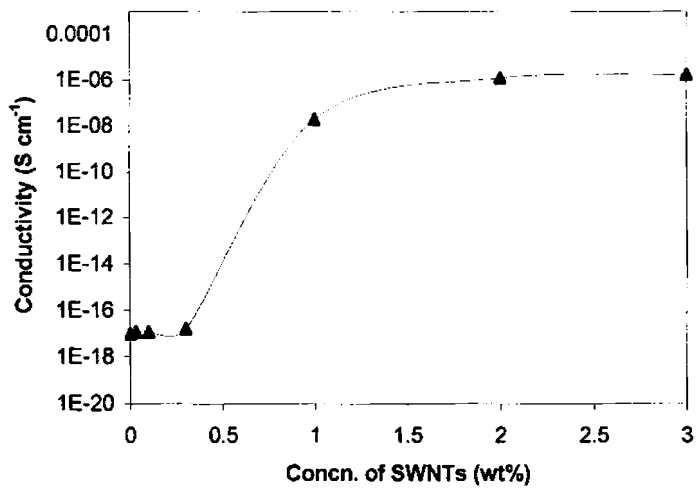

Fig. 3.8 Electrical conductivity of PET-SWNT nanocomposites

3.3.8 The challenge

Application of carbon nanotubes as reinforcement in composite materials is dependent on the efficient dispersion of nanotubes in the matrix. The characterization of such dispersion is limited by the lack of available tools to visualize the quality of the matrix-carbon interaction. Optical techniques are typically used for characterizing the dispersion but lack the ability to visualize single bundles of nanotubes. Electron microscopy studies are hampered by a lack of contrast between the polymer and the carbon nanotubes. Advanced imaging techniques are required to visualize either the nanotubes themselves or the effect; the nanotubes have on the surrounding matrix. Electron microscopy studies and detailed characterizations of the composites are presented elsewhere.[66,67] Some researchers from NASA have also reported the use of

magnetic force microscopy (MFM) as a promising technique for characterizing the dispersion of the nanotubes in a high performance polymer matrix.[68]

3.4 Conclusions

PET-SWNT nanocomposites have been prepared by melt compounding followed by compression molding. The improved mechanical properties and dynamic mechanical analysis of the nanocomposites revealed that a small concentration of SWNTs can substantially reinforce PET. The glass transition temperature, however, was not significantly affected by the SWNT concentration of upto 3.0 wt%. Thermogravimetric analysis and thermal expansion studies indicated that carbon nanotubes did not affect the thermal and dimensional stability of PET. The dynamic rheological characteristics indicated that carbon nanotubes are effectively entangled in the melt state as well. Similarly, SWNTs at concentrations ≥ 2.0 wt% were found to impart electrical conductivity to the insulating PET matrix.

References

1. Despres JF, Daguerre E, Lafdi K. Carbon 1995;33:87.
2. Iijima S, Brabec C, Maiti A, Bernholc J. J. Chem. Phys. 1996;104:2089.
3. Wong EW, Sheehan PE, Lieber CM. Science 1997;277:1971.
4. Chopra NG, Benedict L, Crespi V, Cohen M, Louie S, Zettl A. Nature 1995;377:135.
5. Dresselhaus MS, Dresselhaus G, Sugihara K, Spain IL, Goldberg HA. Graphite Fibers and Filaments. Springer; 1988.
6. Dresselhaus MS, Dresslhous G, Avouris P. Carbon Nanotubes: Synthesis, Structure, Properties and Applications. Springer; 2001.
7. Fakirov S, editor. Handbook of Thermoplastic Polyesters. Wiley-VCH; 2002.
8. Valentini L, Biagiotti J, Kenny JM, Manchado MAL. J. Appl. Polym. Sci. 2003;89:2657.

9. Scheirs J, Long TE, editors. Modern Polyesters. Wiley; 2003.

10. Sittig M. Polyester Fiber Manufacture. New Jersey; 1971.

11. Abu-Isa IA, Jaynes CB, O Gara JF. J. Appl. Polym. Sci. 1996;59:1957.

12. Ou YC, Yang F, Zhuang Y. Acta Polym. Sin. 1997;2:199.

13. Ke Y, Long C, Qi Z. J. Appl. Polym. Sci. 1999;71:1139.

14. Brydson JA. Flow Properties of Polymer Melts. George Godwin Ltd.; 1981.

15. Cogswell FN. Polymer Melt Rheology: A Guide to Industrial Practice. George Godwin Ltd.; 1981.

16. Goel V, Chatterjee T, Bombalski L, Yurekli K, Matyjasaewski K, Krishnamoorti R. J. Polym. Sci. Part B: Polym. Phys. 2006;44:2014.

17. Qian D, Dickey EC, Andrews R, Rantell T. Appl. Phys. Lett. 2000;76:2868.

18. Zhang WD, Shen L, Phang IY, Liu T. Macromolecules 2004.

19. Turi EA, editor. Thermal Characterization of Polymeric Materials. Academic Press; 1981.

20. Jin Z, Pramoda KP, Xu G, Goh SH. Chem. Phys. Lett. 2001;337:43.

21. Velasco-Santos C, Martínez-Hernández AL, Fisher FT, Ruoff R, Castaño VM. Chem. Mater. 2003;15:4470.

22. Ogasawara T, Ishida Y, Ishikawa T, Yokota R. Composites Part A. Appl. Sci. Manufactur. 2004;35:67.

23. Pham JQ, Mitchell CA, Bahr JL, Tour JM, Krishnamoorty R, Green PF. J. Polym. Sci. Part B: Polym. Phys. 2003;41:3339.

24. Shaffer MSP, Windle AH. Adv. Mater. 1999;11:937.

25. Han CD, editor. Rheology in Polymer Processing. Academic Press; 1976.

26. Ren J, Krishnamoorti R. Macromolecules 2003;36:4443.

27. Krishnamoorti R, Giannelis EP. Macromolecules 1997;30:4097.

28. Krishnamoorti R, Ren JX, Silva AS. J. Chem. Phys. 2001;114:4968.

29. Salaniwal S, Kumar SK, Douglas JF. Phys. Rev. Lett. 2002;89:258301.

30. Solomon MJ, Almusallam AS, Seefeldt KF, Somwangthanaroj A, Varadan P. Macromolecules 2001;34:1864.

31. Li Z, Luo G , Wei F, Huang Y. Compos. Sci. Technol. 2006;66:1022.

32. Pötschke P, Bhattachryya AR, Janke A. Polymer 2003;44:8061.

33. Hu G, Zhao C, Zhang S, Yang M , Wang Z. Polymer 2006;47:480.

34. Shin DH, Yoon KH, Kwon OH, Min BG, Ik Hwang C. J. Appl. Polym. Sci. 2006;99:900.

35. Yang F, Nelson GL. J. Appl. Polym. Sci. 2004;91:3844.

36. Yang S, Castilleja JR, Barrera EV, Lozanoa K. Polymer Degradation and Stability 2004;83:383.

37. Qu MH, Wang YZ, Wang C, Ge XG, Wang DY, Zhou Q. Euro. Polym. J. 2005;41:2569.

38. Pötschke P, Fornes TD, Paul DR. Polymer 2002;43:3247.

39. Ou CF. J. Appl. Polym. Sci. 2003;89:3315.

40. Kashiwagi T, Grulke E, Hilding J, Harris R, Awad W, Douglas J. Macromol. Rapid Commun. 2002;23:761.

41. Kashiwagi T, Grulke E, Hilding J, Groth K, Harris R, Butler K, Shields J, Kharchenko S, Douglas J. Polymer 2004;45:4227.

42. Siochi EJ, Working DC, Park C, Lillehei PT, Rouse JH, Topping CC, Bhattacharyya AR, Kumar S. Composites: Part B 2004;35:439.

43. Zimmermann H, Leibnitz E. Faserforschung Textiltechnik 1965;16:282.

44. Schaaf E, Zimmermann H. Faserforschung Textiltechnik 1974;25:434.

45. Yoon PJ, Fornes TD, Paul DR. Polymer 2002;43:6727.

46. Feltham SJ, Yates B. J. Mater. Sci. 1982;7:2309.

47. Holliday L, Robinson J. J. Mater. Sci. 1973;8:301.

48. Chow TS, Wilson JC. J. Polym. Sci. Part B: Polym. Phys. 1978;16:956.

49. Engberg K, Ekblad M, Werner PE, Gedde UW. Polym. Eng. Sci. 1994;34:1340.

50. Nandan B, Lal D, Pandey KN, Alam S, Kandpal LD, Mathur GN. J. Polym. Mater. 2001;18:355.

51. Kaji M, Nakahara K, Ogami K, Endo T. J. Appl. Polym. Sci. 2000;75:528.

52. Yakushin VA, Stirna UK, Zhmud NP. Mech. Compos. Mater. 1999;35:351.

53. Usuki A, Kojima Y, Kawasumi M, Okada A, Fukushima Y, Kurauchi T, Kamigaito O. J. Mater. Res. 1993;8:1179.

54. Ashton JF, Halpin JC, Petit PH. Structure property relationship for composite materials. Primer composite materials analysis. Lancaster: Technomic; 1969.

55. Liang ZM, Yin J. J. Appl. Polym. Sci. 2003;90:1857.

56. Bin Y, Kitanaka M, Zhu D, Matsuo M. Macromolecules 2003;36:6213.

57. Meincke O, Kaempfer D, Weickmann H, Friedrich C, Vathauer M, Warth H. Polymer 2004;45:739.

58. Kharchenko SB, Douglas JF, Obrzut J, Grulke EA, Migler KB. Nat. Mater. 2004;3:564.

59. Du F, Fisher JE, Winey KI. J. Polym. Sci. Part B: Polym. Phys. 2003;41:3333.

60. Du F, Scogna RC, Zhou W, Brand S, Fischer JE, Winey KI. Macromolecules 2004;37:9048.

61. Ounaies Z, Park C, Wise KE, Siochi EJ, Harrison JS. Compos. Sci. Technol. 2003;63:1637.

62. Coleman JN, Curran S, Dalton AB, Davey AP, McCarthy B, Blau W, Barklie RC. Synth. Met. 1999;102:1174.

63. Regev O, Elkati PNB, Loos J, Koning CE. Adv. Mater. 2004;16:248.

64. Kymakis E, Alexandou I, Amaratunga GAJ. Synth. Met. 2002;127:59.

65. Miyasaka K, Watanabe K, Jojima E, Aida H, Sumita M. J. Mater. Sci. 1982;17:1610.

66. Yao N, Wang ZL, editors. Handbook of Microscopy for Nanotechnology. Kluwer Academic Publishers; 2005.

67. Park C, Ounaies Z, Watson K, Crooks R, Connell J, Lowther SE, Siochi EJ, Harrison JS, ST. Clair TL. Chem. Phys. Lett. 2002;364:303.

68. Lillehei PT, Park C, Rouse JH, Siochi EJ. NASA/CR-2002-212137, ICASE Report No. 2002-48.

Chapter 4

Nanocomposites through ultrasound assisted dissolution-evaporation*

Abstract

PET based nanocomposites have been prepared with SWNTs through ultrasound assisted dissolution-evaporation. DSC studies showed that SWNTs nucleate crystallization in PET at weight fractions as low as 0.3 %, as the nanocomposite melt crystallized during cooling at a temperature 24 °C higher than neat PET of identical molecular weight. Mechanical and dynamic mechanical properties of the nanocomposites improved as compared to neat PET indicating the effective reinforcement provided by nanotubes in the polymer matrix. Electrical conductivity measurements showed that SWNTs at concentrations exceeding 1 wt% in the PET matrix result in electrical percolation. Comparing with properties of PET-SWNT nanocomposites prepared by melt compounding, it was obvious that ultrasound assisted dissolution-evaporation method enables more effective dispersion of SWNTs in the polymer matrix.

---

*K. Anoop Anand, U.S. Agarwal, Rani Joseph. ***European Polymer Journal*** ***2006 (in press)***. A part of the work described in this chapter has been presented at the *National Conference on Frontiers in Polymer Science and Technology,* ***POLYMER 2006,*** *Feb 10-12, 2006, Indian Association for the Cultivation of Science, Kolkata, India.*

4.1 Introduction

Researchers all over the world have been trying to attain good dispersion of carbon nanotubes in polymer matrices and many attempts have resulted positive. One of the most viable and commercially versatile routes for a product development in the case of plastics based nanocomposites is melt compounding.[1] Even though this route has several advantages (e.g. no excessive solvents etc.), it has certain limitations, which will end up with poor dispersion of ingredients in the matrix, and in some cases, degradation of the matrix polymer etc. Hence people have tried *in-situ* polymerisation, ultrasound assisted dissolution-evaporation etc. for attaining better dispersion of the nano particles in matrices, the former being a better method but is not feasible in all cases, for, the monomer solution should be capable of dispersing nanoparticles.[2,3] There are several reports in literature, which mention the latter method as an effective route for the preparation of nanocomposites with carbon nanotubes. For example, Shaffer and Windle prepared polyvinyl alcohol based nanocomposites with a wide range of nanotube loadings through solution evaporation method.[4] Bower *et al.* fabricated poly(hydroxyamino ether) nanocomposites with carbon nanotubes by solution casting and studied their deformation behavior.[5] They estimated the increase in the onset buckling strain and fracture strain of the nanocomposites to be 5 % and > 18 % respectively. Hu *et al.* also have employed ultrasonication route for dispersing multi walled carbon nanotubes (MWNTs) in dichlorobenzene-phenol mixed solvent, followed by mixing with PET.[6]

In most studied nanotube-polymer composites, the polymer is also used as the nanotube dispersing agent. Polymers are appealing candidates to host the complexation of SWNTs since, given an appropriate structure, they can wrap themselves around SWNTs. Indeed, such cases have been reported in literature.[7-9] Therefore the polymer is optimised to exfoliate or atleast to disperse the nanotube bundles, but ofcourse, not to tune the properties of the nanocomposites.[10] As a consequence, most reported nanotube based composites consist either of polymers that have been specially synthesised to disperse nanotubes or alternatively the nanotubes are functionalised to enhance the interaction with the polymer.[11-13] The former method introduces a serious

limitation on the spectrum of target polymer matrices, while the latter is reported to impair some of the properties (e.g. conductivity) of the bare nanotubes. More over, the ability of the polymer to disperse and exfoliate nanotubes is not necessarily coupled with the optimised properties of the target matrix. In some cases, the dispersant is able to disperse but not to exfoliate the SWNTs.

In this part of the work, an ultrasound assisted dissolution-evaporation method is employed for the preparation of PET-SWNT nanocomposites. The crystallization characteristics, mechanical and dynamic mechanical properties, thermal stability as well as electrical conductivity of these composites have been examined.

4.2 Experimental

4.2.1 Materials

PET pellets (characteristic cylindrical diameter ~ 2.5 mm, length ~ 3 mm, [η] = 0.98 dL/g in 1/1 phenol/TCE at 30 ± 0.1 °C) were obtained from Acordis Research (Arnhem, the Netherlands) (section 2.2.1.1 and 2.2.3 of this thesis). SWNTs were purchased from CarboLex Inc. (Lexington, U.S.A) (section 2.2.1.2). 1,1,1,3,3,3-Hexafluro-2-propanol (99+ %, HFIP) was obtained from Lancaster and chloroform (99+ %) was purchased from Aldrich.

4.2.2 Preparation of the nanocomposites

PET pellets were powdered and dried at 150 °C for atleast 12 h under vacuum. HFIP was added in the weight ratio, HFIP:PET = 4:1, and allowed to stand for 2 h. Chloroform was then added in the weight ratio, chloroform:HFIP = 5:1, and mechanically shaken for a few hours to dissolve the PET. Desired amount of pre-dried SWNTs was then added and the suspension (~ 25 mL) was sonicated for 15 min using a mechanical probe sonicator (13 mm, VibraCell Processor VC 750, operating at 40 % of the maximum power 750 W- figure 4.1). The solutions were then cast onto glass petri dishes and allowed to dry slowly at room temperature to get thin films. These films were annealed at 150 °C for 1 h and were used for subsequent characterization.

Fig. 4.1 Ultrasonic processor (VibraCell, VC 750)

4.2.3 Principles of ultrasonication

The ultrasonic power supply converts 50/60 Hz line voltage to high frequency electrical energy. This high frequency electrical energy is transmitted to a piezoelectric transducer within a converter, where it is changed to mechanical vibrations. The vibrations from the converter are intensified by a probe, creating pressure waves in the liquid. This action forms millions of microscopic bubbles (cavities), which expand during the negative pressure excursion, and implode violently during the positive excursion. This phenomenon, referred to as cavitation, creates millions of shock waves in the liquid, as well as elevated pressures and temperatures at the implosion sites. Although the cavitational collapses last for a few microseconds, and the amount of energy released by each individual bubble is minute, the cumulative effect causes extremely high levels of energy to be released into the liquid. This will result in the disruption of the interaction forces between the particles thereby achieving dispersion of the suspended particles in the solvent.

Ultrasonic processing will typically cause the temperature of the sample to increase, especially with small volumes. Since high temperatures inhibit cavitation, the sample temperature is kept as low as possible. This is accomplished by immersing the sample container in an ice-salt-water bath. Before each application, the sonicator tip is placed in the solvent and energized the power supply for a few seconds to remove any residual substances.

4.2.4 Characterization

Differential scanning calorimetry (DSC Q-100, TA Instruments) was employed to study the effect of SWNTs on the crystallization characteristics of nanocomposites. Experimental procedure of analysis is given in section 2.2.4. Density measurements have been done using a density gradient column with a solvent system of carbon tetrachloride and ethanol. Mechanical properties of the PET-SWNT nanocomposite films were studied using a Shimadzu Universal testing machine (model-AG1) with a load cell of 10 kN capacity (section 3.2.2). The specimens used were rectangular strips of dimensions 30 × 5 × 0.2 mm. The gauge length between the jaws at the start of each test was adjusted to 20 mm and the measurements were carried out at a cross-head speed of 1 mm/min. Average of atleast six sample measurements were taken to represent each data point. Dynamic mechanical analyser (DMA Q-800, TA Instruments) was used to study the effect of SWNTs on the viscoelastic properties of PET (section 3.2.4). Thermogravimetric analyser (TGA Q-50, TA Instruments) was used to study the effect of SWNTs on the thermal stability of PET (section 3.2.6). The D.C. electrical conductivity of the nanocomposite films (rectangular strips of dimensions 40 × 15 × 0.2 mm) was measured using a Keithley Nanovoltmeter (model 2182) in dry air at ambient temperature (section 3.2.8).

4.3 Results and discussion

SWNTs have been dispersed by ultrasonication of its suspension in the mixed solvent HFIP-chloroform (1:5) containing dissolved PET (~ 8 wt%). Figure 4.2(a) shows that the solution containing SWNTs (1 wt%) remained stable for atleast 6 weeks. On the other hand, SWNTs have been ultrasonicated in the mixed solvent but without dissolved PET and it was observed that the nanotubes settle immediately after ultrasonication. This indicates that the polymer PET provides as an effective surfactant for SWNTs in this solvent.

Ultrasonication can result in chain scission and decrease in molecular weight of the polymers, depending on the solvent, polymer molecular weight and the ultrasound

intensity. However, there was no considerable change in the intrinsic viscosity of the PET recovered after ultrasonication of its solution, which indicates that under the conditions employed for this study, ultrasonication doesn't severely degrade PET.

PET-SWNT composite films of thickness ~ 0.2 mm were prepared by solution casting. Figure 4.2(b) compares the appearance of these films corresponding to three different concentrations of SWNTs. Colour uniformity is observed in each sample.

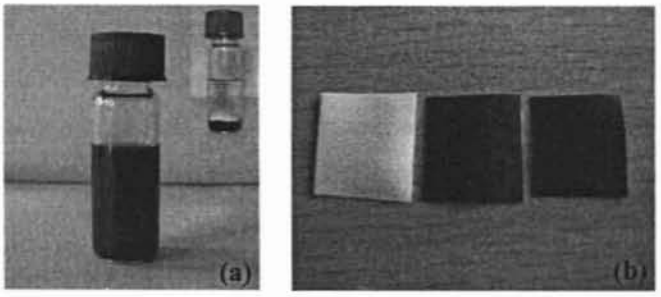

Fig. 4.2(a) Vial containing 1 wt% well dispersed SWNTs in PET solution which remained stable even after 6 weeks of its preparation. Shown in the inset is a vial containing the mixed solvent (containing no PET) with nanotubes that settled immediately on ending sonication. (b) Digital photographs of PET-SWNT nanocomposite films with 0, 1 and 3 wt% SWNT fractions. Each sample is approximately 1 cm in length and breadth.

4.3.1 Crystallization characteristics

4.3.1.1 Non-isothermal DSC analysis

The effect of SWNTs on the crystallization characteristics of PET was analysed first with non-isothermal DSC experiments.

Figure 4.3 shows the DSC cooling scans of neat PET and SWNT containing nanocomposite samples. The peak crystallization temperatures (T_c) during the cooling scans, peak melting temperatures (T_m) during the heating scans, as well as the associated

enthalpies are summarized in table 4.1. During cooling from the melt, the SWNT containing samples showed crystallization exotherms at higher T_c than the neat polymer.

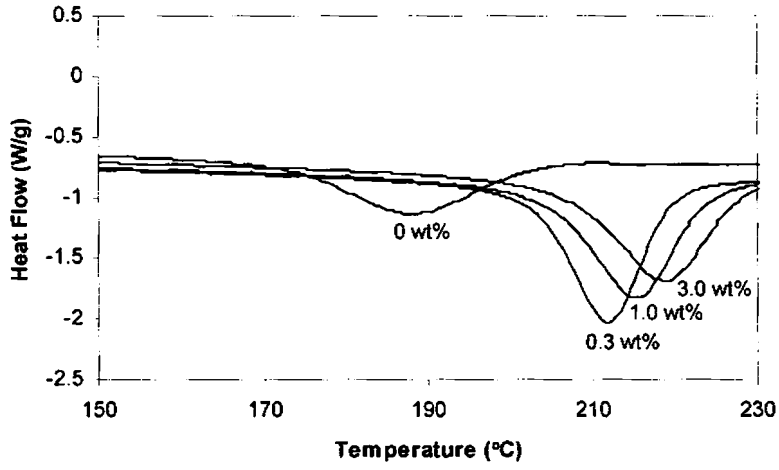

Fig. 4.3 DSC cooling scans of neat PET and PET-SWNT nanocomposite samples (20 °C/min from 310 °C melt)

Table 4.1

DSC-determined thermal parameters for neat PET and PET-SWNT nanocomposite samples ([η] ~ 0.98 dL/g) prepared by ultrasound assisted dissolution-evaporation

Concn. of SWNTs (wt %)	T_c (°C)	ΔH_c (J/g)	T_m (°C)	ΔH_m (J/g)	ΔT (°C)
0.0	187.8	23.1	254.8	32.2	67.0
0.3	212.1	42.0	252.8	35.4	40.7
1.0	215.2	39.5	252.4	36.8	37.2
3.0	219.0	42.0	253.5	39.2	34.5

According to the results obtained, crystallization temperature of PET increases by 24 °C with SWNTs at a concentration as low as 0.3 wt%. The T_c values continue to increase with increasing SWNT concentration indicating that SWNTs act as effective nucleating agents for PET crystallization. However, the rate of rise of T_c decreases with increase in SWNT concentration beyond 0.3 wt%, indicating possible saturation

of the nucleation efficiency at low SWNT concentrations. This is possibly related to the large surface area and good dispersion of SWNTs.[14,15] The melting temperature of the polymer is not significantly affected by carbon nanotubes.

In programmed cooling, the degree of supercooling ($\Delta T = T_m - T_c$) is considered as a measure of the crystallizability; i.e. smaller the ΔT, higher the crystallizability.[16] The ΔT values of PET-SWNT nanocomposites given in table 4.1 are smaller by ~ 26 to 32 °C than that of neat PET. This reveals that the crystallizability of the nanocomposites is greater than that of neat PET. Comparison of this data with the ΔT values of the nanocomposites prepared through melt compounding (table 2.3) reveals that the solution evaporation method enables to achieve more crystallizability.

4.3.1.2 Isothermal crystallization characteristics

Isothermal crystallization of neat PET and its nanocomposites are studied at four different temperatures viz., 210, 215, 220 and 225 °C (section 2.2.4). After reaching the desired isothermal crystallization temperature quickly from melt (60 °C/min), the time lapsed until the maximum in the heat flow rate, which is proportional to the crystallization rate, is taken as peak time of crystallization (t_{peak}). The peak time of crystallization, t_{peak}, at each of the isothermal temperatures for the neat polymer and the nanocomposite samples is noted and plotted against the isothermal crystallization temperature (figure 4.4).

The smaller t_{peak} values for the SWNT containing samples as compared with neat PET indicate that SWNTs enhance the rate of crystallization. For the case of neat PET, no crystallization is observed at the highest temperature of 225 °C because the crystallization is very slow and would require longer time than the four minutes employed in the DSC programme. On the other hand, for the sample containing 3.0 wt% SWNTs, the rate of crystallization is so fast that most of the crystallization occurs already during the cooling scan (60 °C/min) employed to reach the desired isothermal crystallization temperatures. This results in absence of exothermic peaks in the heat flow curves at all the isothermal temperatures in the case of this sample.

G8999

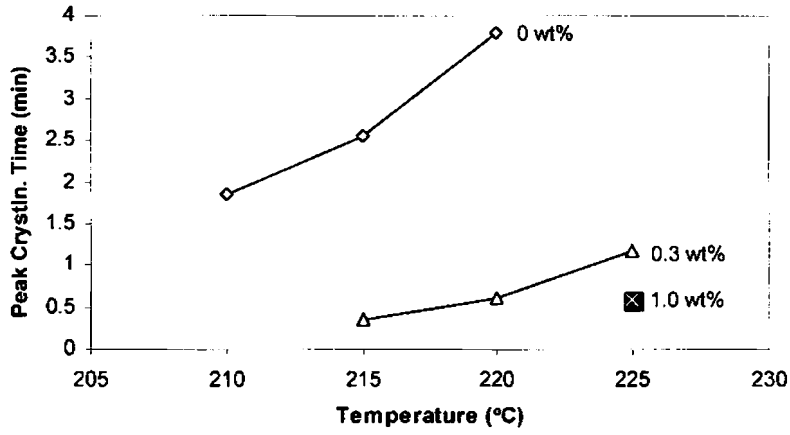

Fig. 4.4 Effect of SWNTs on the peak crystallization time of PET at different temperatures

A comparison of the present results (samples prepared through ultrasound assisted solubilization route) is made here with the results of the melt compounding route (section 2.3.2). The [η] values of PET dropped from 0.98 dL/g to ~ 0.88 dL/g after melt compounding (table 2.1 from section 2.3.1) whereas there is no change in the [η] value of PET recovered after sonication of its solution. A comparison of the T_c rise as a result of the SWNT-induced nucleation in PET-SWNT nanocomposite samples prepared via solution route and melt route is given in table 4.2.

Table 4.2

Comparison of the T_c rise as a result of the SWNT-induced nucleation in PET-SWNT nanocomposites prepared via solution route and melt route

Concn. of SWNTs (wt%)	Increase in T_c (°C)	
	Solution route	Melt route
[0.0]	[187.8]	[199.9]
0.3	24.3	12.5
1.0	27.4	14.4
3.0	31.2	19.2

UNIVERSITY LIBRARY
Cochin - 682 022
COCHIN UNIVERSITY OF SCIENCE AND TECHNOLOGY

The increase in the T_c values is found to be much higher for the composite samples prepared via the solution route, indicating a possible improved dispersion of SWNTs by this method.

4.3.2 Mechanical properties

Tensile tests were performed on flat 30 × 5 × 0.2 mm samples cut from the solvent cast films. The overall effect of SWNTs on the mechanical properties of PET is given in table 4.3. The results indicate that upon incorporation of only 1.0 wt% SWNTs to the PET matrix, the tensile strength of PET increases by 27 %. As the concentration of nanotubes increases, tensile strength increases. The modulus also increases with increasing filler loading; ~ 60 % rise is observed with 1.0 wt% nanotubes.

Table 4.3

Mechanical properties of neat PET and PET-SWNT nanocomposite samples

Concn. of SWNTs (wt%)	Density (g/cm^3)	Tensile strength (MPa)	Tensile modulus (GPa)	Elongation (%)
0.0	1.4301	27.6	1.56	5.21
1.0	1.4316	35.2	2.52	4.98
3.0	1.4368	37.2	2.54	4.34

These results demonstrate that a small fraction of SWNTs substantially enhances the mechanical strength of the polymer or in other words, SWNTs provide effective reinforcement to the PET matrix. The better mechanical performance of the nanocomposites as compared with neat PET can be attributed to the homogeneous dispersion of SWNTs in the PET matrix as well as the strong matrix-nanotube interfacial interactions enabling effective stress transfer between the matrix and filler.

4.3.3 Temperature dependence of the solid's viscoelastic characteristics

The DMA results for the dynamic storage and loss modulii of neat PET and PET-SWNT nanocomposite samples, prepared through the ultrasound assisted dissolution-

evaporation method, as a function of temperature at 1 Hz are shown in figure 4.5. The storage modulii of the nanocomposite samples below glass transition increase substantially with the SWNT concentration due to the stiffening effect of nanotubes, and indicating efficient stress transfer between the polymer matrix and SWNTs (figure 4.5 (a)).

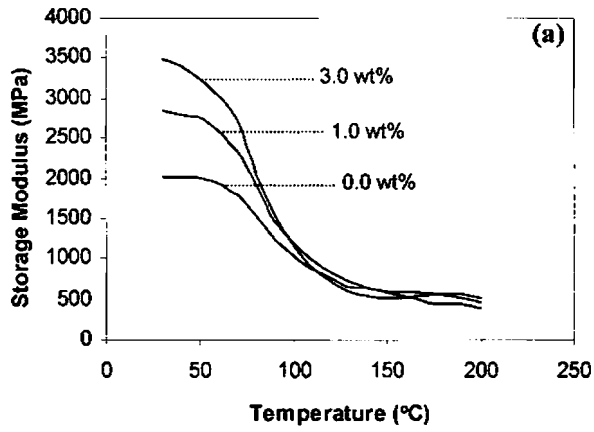

Fig. 4.5 (a) Effect of SWNT concentration on the storage modulus of PET-SWNT nanocomposites

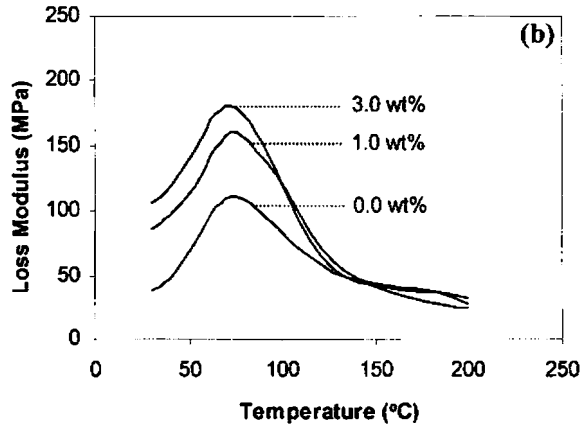

Fig. 4.5 (b) Effect of SWNT concentration on the loss modulus of PET-SWNT nanocomposites

The loss modulus values also increase considerably with nanotube loading (figure 4.5 (b)). The reinforcing effect of SWNTs in the nanocomposite systems can be attributed to their specific interactions and the formation of a rigid percolating nanotube network within the thermoplastic polyester matrix.

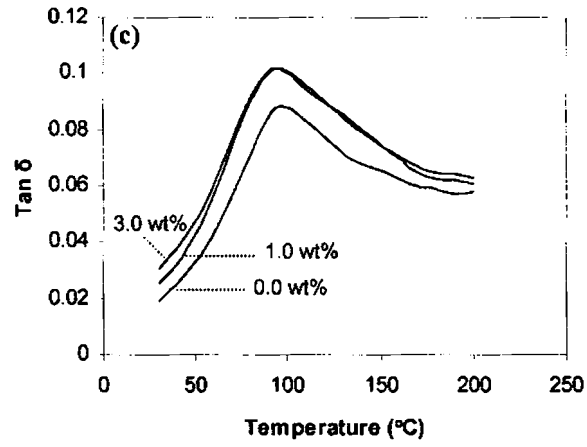

Fig. 4.5 (c) Effect of SWNT concentration on the tan δ of PET-SWNT nanocomposites

Though the modulus values are enhanced by SWNTs, the tan δ (tan δ = loss modulus/ storage modulus) curves in figure 4.5 (c) indicate that SWNTs when incorporated through the solution route at concentrations of upto 3.0 wt% have no significant influence on the glass transition temperature of PET.

4.3.4 Thermal stability

Melt compounded carbon nanotubes have already been shown to provide almost no effect on the thermal stability of PET (section 3.3.5). Same is the trend in the case of dissolution-evaporation method. The TGA plots of nanocomposite samples in figure 4.6 indicate that decomposition of all samples starts nearly at the same temperature range irrespective of the SWNT concentrations and thus the thermal stability of PET is inferred to be unaffected by the presence of SWNTs.

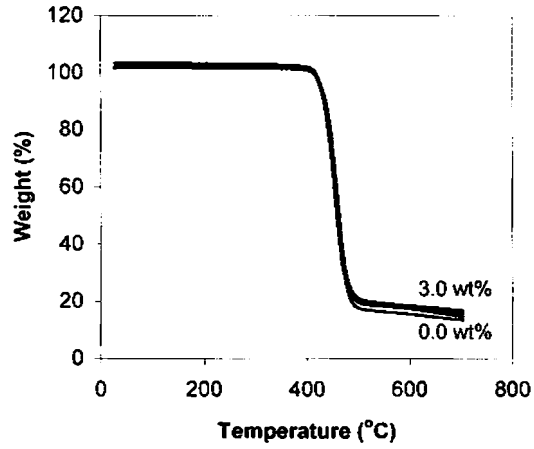

Fig. 4.6 TGA traces of PET-SWNT nanocomposites

4.3.5 Electrical conductivity

Thin electrically conductive films are one possible application of PET-SWNT nanocomposites. The room temperature D.C. electrical conductivity values of the nanocomposite samples are given in table 4.4.

Table 4.4

Electrical conductivity of neat PET and nanocomposite films at room temperature

Concn. of SWNTs (wt %)	Conductivity (S cm^{-1})
0.0	1.51×10^{-17}
0.3	1.69×10^{-8}
1.0	1.12×10^{-6}
3.0	2.63×10^{-6}

The conductivity of neat PET film is of the order of 10^{-17} S cm^{-1}.[6] At loading levels exceeding 0.3 wt%, the conductivity level surpasses the antistatic criterion of thin films (1×10^{-8} S cm^{-1}) and reaches percolation at a concentration of 1 wt%. Previous results have shown that the melt compounded SWNTs can impart conductivity to the PET

matrix of the order of 10^{-6} S cm^{-1} only at concentrations exceeding 2 wt%. Comparison with results of table 4.4 suggests a possibly improved SWNT dispersion during the dissolution-evaporation route employed here.

4.4 Conclusions

Single walled carbon nanotubes dispersed in PET through ultrasound assisted dissolution-evaporation route have been shown to act as effective nucleating agents for PET crystallization. The enhancement in the crystallization temperature of PET on dispersion of SWNTs at a weight fraction as low as 0.3 % was roughly 24 °C. Analysis of the mechanical and dynamic mechanical properties revealed that small fractions of SWNTs can substantially reinforce PET. As expected, SWNTs could also impart electrical conductivity to the PET matrix, which otherwise is an insulator. Apparently, the solution route employed here provided better dispersion of SWNTs as compared to the melt-compounding route presented in the previous chapters.

References

1. Pötschke P, Bhattacharyya AR. Polymer Preprints 2003;44:760.
2. Park C, Ounaies Z, Watson KA, Crooks RE, Jr. Smith J, Lowther SE, Connell JW, Siochi EJ, Harrison JS, St.Clair TL. Chem. Phys. Lett. 2002;364:303.
3. Ke Y, Long C, Qi Z. J. Appl. Polym. Sci. 1999;71:1139.
4. Shaffer MSP, Windle AH. Adv. Mater. 1999;11:937.
5. Bower C, Rosen R, Jin L, Han J, Zhou O. Appl. Phys. Lett. 1999;74:3317.
6. Hu G, Zhao C, Zhang S, Yang M, Wang Z. Polymer 2006;47:480.
7. Star A, Stoddart JF, Steuerman D, Diehl M, Boukai A, Wong EW, Yang X, Chung SW, Choi H, Heath JR. Angew. Chem. Int. Ed. 2001;40:1721.
8. Yudasaka M, Zhang M, Jabs C, Iijima S. Appl. Phys. A 2000;71:449.
9. Stephan C, Nguyen TP, de La Chapelle L, Lefrant S, Journet C, Bernier P. Synth. Met. 2000;108:139.
10. Panhuis M, Munn RW, Blau WJ. Synth. Met. 2001;121:1187.
11. Sandler J, Shaffer MSP, Prasse T, Bauhofer W, Schulte K, Windle AH. Polymer 1999;40:5967.
12. McCarthy B, Coleman JN, Czerw R, Dalton AB, Panhuis M, Drury A, Bernier P, Nagy JB, Lahr B, Byrne HJ, Carroll DL, Blau WJ. J. Phys. Chem. B 2002;106:2210.
13. Stevens JL, Huang Ay, Peng H, Chiang IW, Khabashesku VN, Margrave JL. Nano Letters 2003;3:331.
14. Probst O, Moore EM, Resasco DE, Grady BP. Polymer 2004;45:4437.
15. Valentini L, Biagiotti J, Kenny JM, Santucci S. J. Appl. Polym. Sci. 2003;87:708.
16. Qu MH, Wang YZ, Wang C, Ge XG, Wang DY, Zhou Q. Euro. Polym. J. 2005;41:2569.

Chapter 5

PET-SWNT nanocomposite fibers through melt spinning

Abstract

PET-SWNT nanocomposite fibers have been prepared through melt spinning and drawing. The mechanical properties indicated that SWNTs provide significant reinforcement to PET fibers. For example, the tenacity and initial modulus of the composite fiber with 2.0 wt% SWNTs were, respectively, 2.5 times and 5 times higher as compared to those of the pristine PET fiber prepared under identical conditions. When the draw ratio was increased, tenacity and modulus of the fibers increased, indicating that drawing induced orientation of the polymer molecules and SWNTs. Thermal stability of the fibers was not significantly affected by the presence of SWNTs at low concentrations.

5.1 Introduction

Today, polyester fibers are used in a wide variety of applications ranging from textiles to automobiles. They are known for their high resilience, resistance to wrinkling, high durability, dimensional stability, and resistance to chemical and environmental attack. Poly(ethylene terephthalate) fiber accounts for over 97 percent of all polyester fibers manufactured today. Only small amounts of other types of polyester fibers are presently or have been produced commercially, of which the larger volume materials include poly(1,4-cyclohexane dimethylene terephthalate) (PCDT), poly(butylene terephthalate) (PBT), and poly(trimethylene terephthalate) (PTT).

The idea of spinning polyester fibers dates back to the original W.H. Carothers (DuPont) patents and papers from the 1930s.[1] However, the use of polyester fibers did not become commercially feasible until the 1950s when J.R. Whinfield and J.T. Dickson of Calico Printers made poly(ethylene terephthalate) from terephthalic acid.

Although several types of fiber spinning methods are commercially used, essentially polyester fibers are produced by melt spinning.[2,3] Melt spinning is the least complex spinning method; it simply involves forcing a polymer melt through a spinneret and into air to cause the polymer to solidify. It does not involve the problems associated with the use of solvents and is therefore the preferred method provided that the polymer gives a stable melt. The homogenized and filtered melt is extruded through the spinneret and can solidify anywhere from a few centimeters from the spinneret plate to as far away as several meters.

Polyester fibers have been categorized on the basis of degree of orientation introduced into the fiber during the melt spinning process. These categories are Low, Medium or Partial, High, and Fully oriented fiber. Low oriented polyester fiber is used to make staple products. Of the oriented fiber categories, partially oriented yarn (POY) is by far the most common material in commercial production. POY has gained sudden popularity since its introduction in the early 1980s, and now accounts

for the majority of the polyester filament category. Highly oriented yarn (HOY) is spun at 4,000-6,500 m/min, whereas fully oriented yarn (FOY) is spun at greater than 6,500 m/min. The last of these categories is still developing, as these spinning rates have proven challenging to achieve in commercial operations.

In 1950s, PET fiber spinning typically occurred at speeds of 1,200 m/min followed by a drawing stage where the fibers were stretched to three to five times their initial length. Drawing fine-tunes the fiber properties by increasing orientation, crystallinity, and strength. Higher fiber spinning speeds increase orientation and crystallinity prior to drawing. In poly(ethylene terephthalate), interaction between the aromatic π-electron systems of the benzene rings and the carbonyl groups result in dipole-dipole interactions (chapter 2, figure 2.1). This interaction affects the alignment of the polymer molecules themselves in fibers.

PET fibers are highly crystalline; crystallinity can be altered and controlled through various processing techniques. The strength of PET fiber is a result of molecular orientation and crystallinity introduced during fiber spinning or during subsequent drawing, texturizing, and heat treating. A fiber contains crystalline areas in which the polymer units are neatly folded and stacked, and amorphous regions in which the molecules are less ordered. Tie molecules link the various regions together. It is this non-rigid structure that allows the fibers to be stretched and their properties to be tuned by post-spinning processing. The more crystalline a fiber structure becomes, the less stretchable it will be. In PET fibers, the phenylene groups provide rigidity, whereas the methylene groups provide flexibility.

Fiber spinning and drawing were conventionally two separate steps. After the fibers were spun, they were transported and drawn or stretched in a second step. Typically, the two step process yielded fibers that have high strength but low dimensional stability. The development of high speed winders led to coupled spin/draw processes being introduced in the late 1960s. In the coupled process, after the filaments are adequately cooled, they are directly stretched by moving them over heated or unheated rollers moving at different speeds. This forces the polymer molecules to

align or orient themselves along the longitudinal axis of the fiber. Spun fibers can be stretched by more than 200 percent. The actual stretch given to the fiber is generally expressed in terms of draw ratio. The draw ratio measures the fiber take-up velocity compared to the extrusion velocity. Fibers spun at higher speed will have greater pre-orientation and will need less drawing.

5.1.1 State-of-art research in nanocomposite fibers

Scientists all over the world have made several attempts in the past to modify the performance characteristics of polymer fibers; mostly PET fibers.[4-10] Carbon nanotubes have recently been reported as imparting several properties to polymer fibers.[11-14] For example, multi walled carbon nanotubes have been incorporated to nylon 6 and PET fibers by Xushan *et al.*[15] They observed that, when adding 0.03 wt% MWNTs into nylon 6 fiber, the strength of the nylon fiber enhanced by 33.3 %. Its modulus was also enhanced by 74.4 %. Adding 0.1 wt% MWNTs into PET fiber made the latter fairly conducting. The breaking strength of this conducting PET fiber showed almost no decrease and initial modulus was slightly enhanced in comparison with pure PET fiber.

Poly(p-phenylene benzobisoxazole) (PBO) based nanocomposite fibers with SWNTs have been prepared by Kumar *et al.*[16] They reported that the fibers containing 10 wt% SWNTs exhibited 50 % higher tensile strength as compared to the control PBO fiber. Sandler *et al.* also observed that carbon nanotubes act as effective reinforcements in melt spun polyamide-12 fibers.[17]

Sreekumar *et al.* have prepared polyacrylonitrile-SWNT nanocomposite fibers through solution spinning.[18] The spun nanocomposite fibers containing 10 wt% SWNTs exhibited a 100 % increase in tensile modulus at room temperature, and it increased by an order of magnitude at 150 °C. They also observed a significant reduction in thermal shrinkage as well as polymer solubility and the glass transition temperature was increased by 40 °C as compared with control PAN fiber.

Crystallization and orientation studies in PP-SWNT nanocomposite fibers have been studied by Bhattacharyya *et al.*[19] Using WAXD and Raman spectroscopy, the authors established that SWNTs have higher orientation than PP in drawn PP-SWNT nanocomposite fibers. This report also claims that even with a limited dispersion, SWNTs could act as nucleating agents for PP crystallization. PP fiber modulus has also been reported as increased by 50 % with the addition of 5 wt% carbon nanofibers.[20] It is anticipated that the shear forces during melt spinning can induce alignment of SWNTs in the fiber axis direction to impart significant reinforcement to the polymer matrix. Indeed, several other groups have demonstrated improvement in properties of polystyrene, PMMA, etc. as a result of melt/wet spinning various amounts of SWNTs with the polymer matrix.[21-23] In a recent publication, Néri *et al.* have described a surfactant free wet spinning method for the production of composite carbon nanotube fibers.[24]

Ma *et al.* have prepared poly(ethylene terephthalate) based composite fibers reinforced with various grades of carbon nano fibers (CNFs, 5 wt%).[25] They reported that the tensile modulii of the composite fibers were marginally higher than that of the pristine PET fiber. On the other hand, tensile strength of the composite fibers was either comparable to or lower than the control fiber.

Siochi *et al.* have prepared fibers from melt-processed nanocomposites of polyimide with SWNTs.[26] They demonstrated that, the fibers containing upto 1 wt% SWNTs, in which the nanotube alignment in the fiber direction was induced by shear forces during melt extrusion and fiber drawing, exhibited significantly higher tensile modulii and yield stress relative to unoriented nanocomposite films having the same SWNT concentration.

In this part of the work, nanocomposite fibers were melt spun from melt compounded PET-SWNT nanocomposites and were subsequently drawn at 100 °C. Effect of fiber formation conditions on the development of their mechanical properties has been studied.

5.2 Experimental

5.2.1 Melt spinning and drawing

Melt compounded nanocomposites (section 2.2.2 of this thesis) of PET and SWNTs were ground using a cryo-grinder (Lloyd instruments Ltd.). The ground samples were dried at 150 °C under vacuum for atleast 24 h. They were spun into fibers using a small scale spinning machine manufactured by Bradford University Research Ltd., UK, using a single hole spinneret (figure 5.1). The conditions of spinning were as follows:

Spinneret	: Single hole, dia = 1 mm, length = 7 mm
Cylinder temperature	: 265 (± 0.5) °C
Piston speed	: 3 (± 0.02) mm/min
Winding speed	: 70 (± 0.2) m/min
Filament type	: mono filament

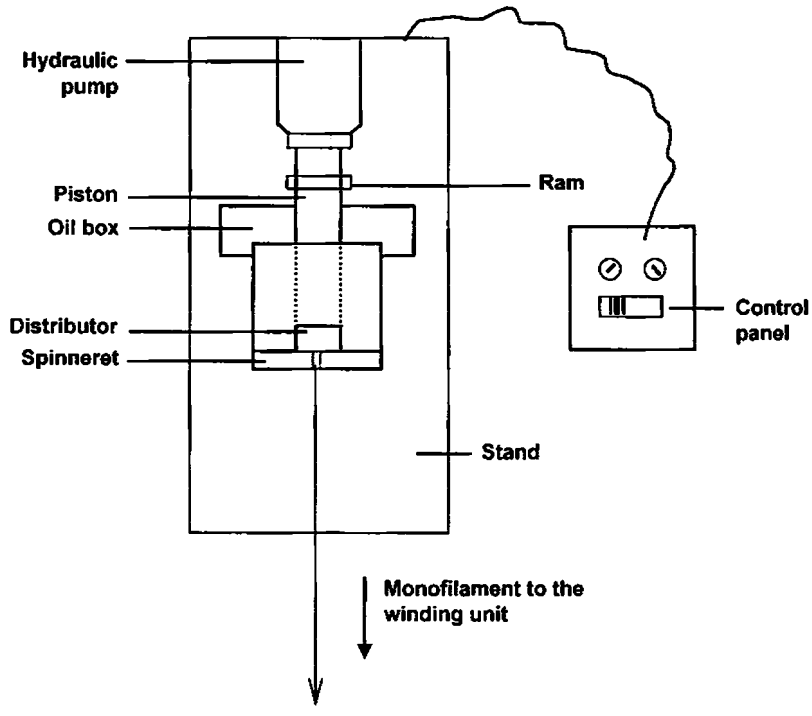

Fig. 5.1 Schematic drawing of the laboratory scale melt spinning machine

The spun fibers were subsequently drawn using a laboratory single zone drawing machine, a schematic representation of which is given in figure 5.2. PET fibers are typically drawn above 80 °C; additional heat is necessary because it provides the fiber molecules with the mobility to rearrange. The specifications and conditions of drawing were as follows:

Speed of the feed roller	: 4 rpm
Outer diameter of the rollers	: 11.2 cm
Speed of the take up roller	: variable
Length of the heating plate	: 20.5 cm
Heater temperature	: 100 ± 0.5 °C

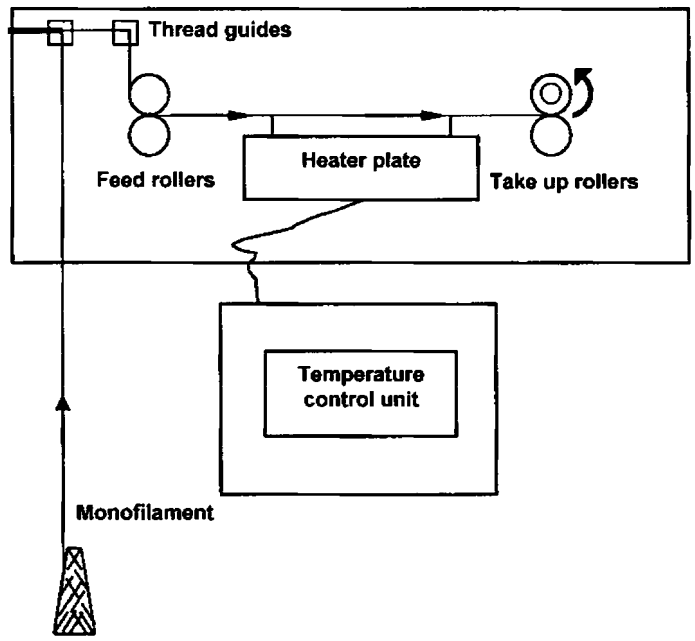

Fig. 5.2 Schematic representation of the fiber drawing set-up

5.2.2 Mechanical properties of the fibers

Mechanical properties of the PET-SWNT nanocomposite fibers were determined using a Favimat Fiber Testing machine (Textechno-textile testing technology) with a load cell of 1,200 cN capacity. The distance between the jaws at the start of the test was 20 mm and the test speed was 20 mm/min. The pretension was set at 0.50 cN/tex and the test temperature was maintained at 25 ± 1 °C. Atleast 30 measurements were taken to represent each data point.

5.2.3 Thermal analysis

Thermogravimetric analysis (section 3.2.6) was used to determine the effect of carbon nanotubes on the thermal stability of PET fibers.

5.3 Results and discussion

Figure 5.3 is a photograph of PET-SWNT nanocomposite fiber prepared by us through melt spinning followed by drawing.

Fig. 5.3 Picture of PET-SWNT nanocomposite (1.0 wt%) fiber

5.3.1 Mechanical properties

Mechanical properties of the drawn PET-SWNT nanocomposite fibers (draw ratio = 4) are given in figure 5.4. It is evident that the presence of SWNTs substantially reinforces the fiber. For example, the tenacity of the composite fiber with 2.0 wt% SWNTs is roughly 2.5 times higher the tenacity of pristine PET fiber (figure 5.4 (a)). The modulus at 2 % elongation is about five times higher as compared to that of the pristine PET fiber (figure 5.4 (b)). However, the elongation of the fibers is drastically reduced by the presence of SWNTs (figure 5.4 (c)). The increase in the true stress at break of the fibers is given in figure 5.4 (d) and it indicates that, with 2.0 wt% SWNTs the value is higher by around 30 % in relation to pristine PET fiber.

These results reveal that SWNTs offer substantial level of reinforcement to PET fibers. The improved mechanical properties of the nanocomposite fibers can be attributed to the effective matrix-filler interaction enabling load transfer from the polymer matrix to the SWNTs.

Typical force-elongation diagrams of PET-SWNT nanocomposite fibers are compared with that of the pristine PET fiber in figure 5.5.

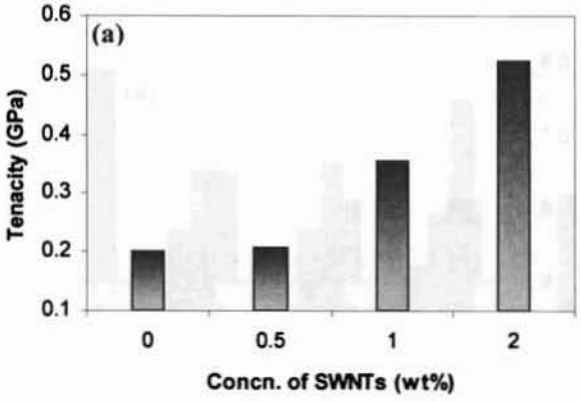

Fig. 5.4(a) Effect of SWNT concentration on the tenacity of PET fiber

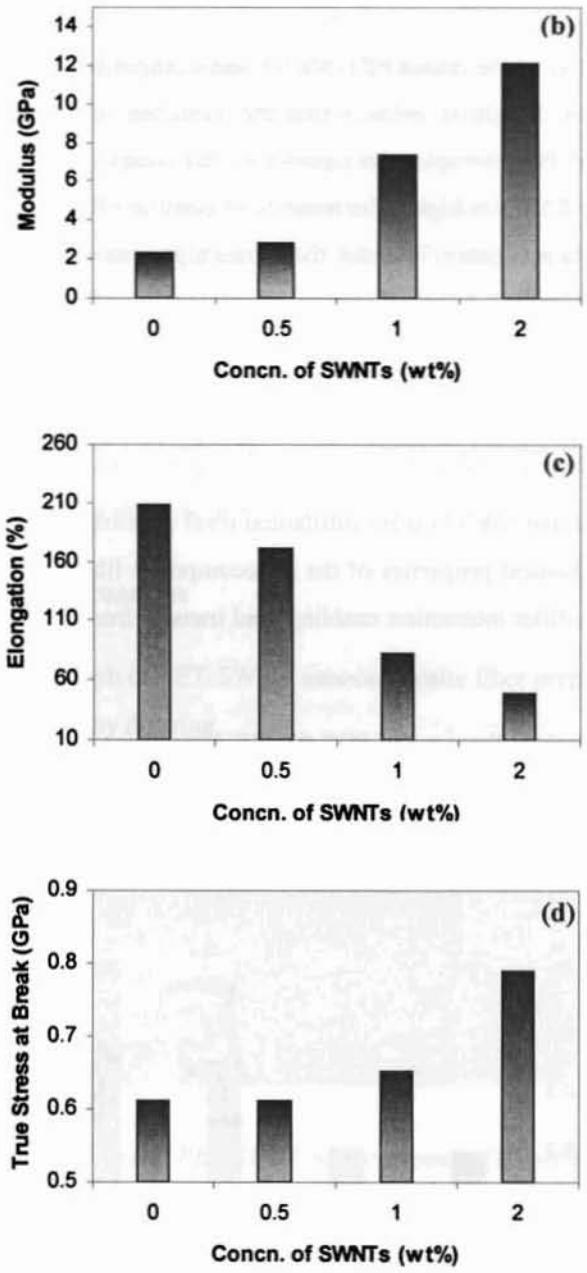

Fig. 5.4 Effect of SWNT concentration on the (b) modulus (c) elongation and (d) true stress at break of PET fiber

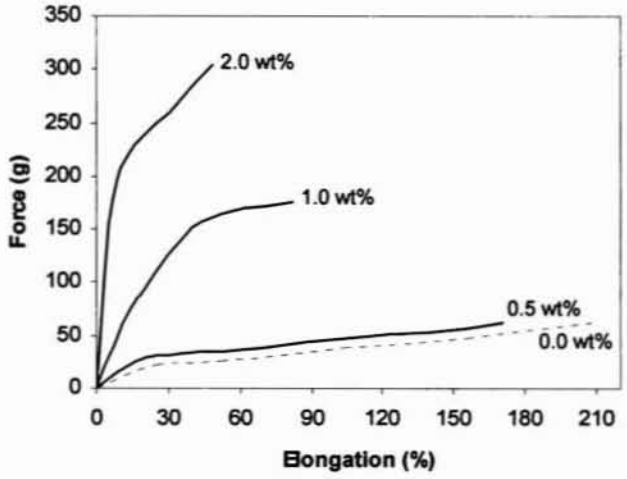

Fig. 5.5 Representative force-elongation plots of pristine PET and PET-SWNT nanocomposite fibers (draw ratio = 4)

5.3.2 Effect of draw ratio on the mechanical properties

Figure 5.6 shows the effect of increasing draw ratio on the mechanical properties of the filaments. As the draw ratio increases, so do the tenacity and modulus. This is mainly due to the increasing macromolecular alignment at higher draw ratios.[27] Elongation at break, however, is reduced at higher draw ratios.

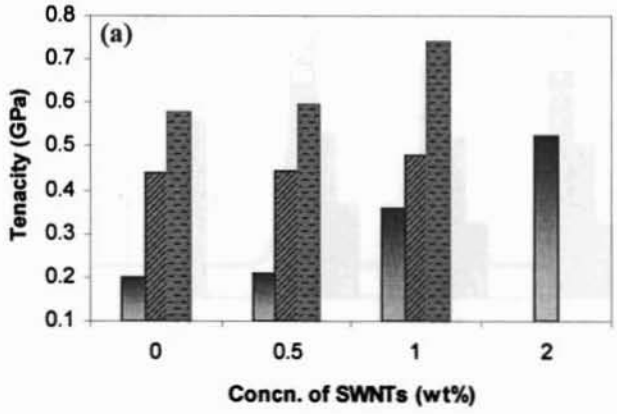

Fig. 5.6(a) Effect of draw ratio on the tenacity of PET-SWNT nanocomposite filaments

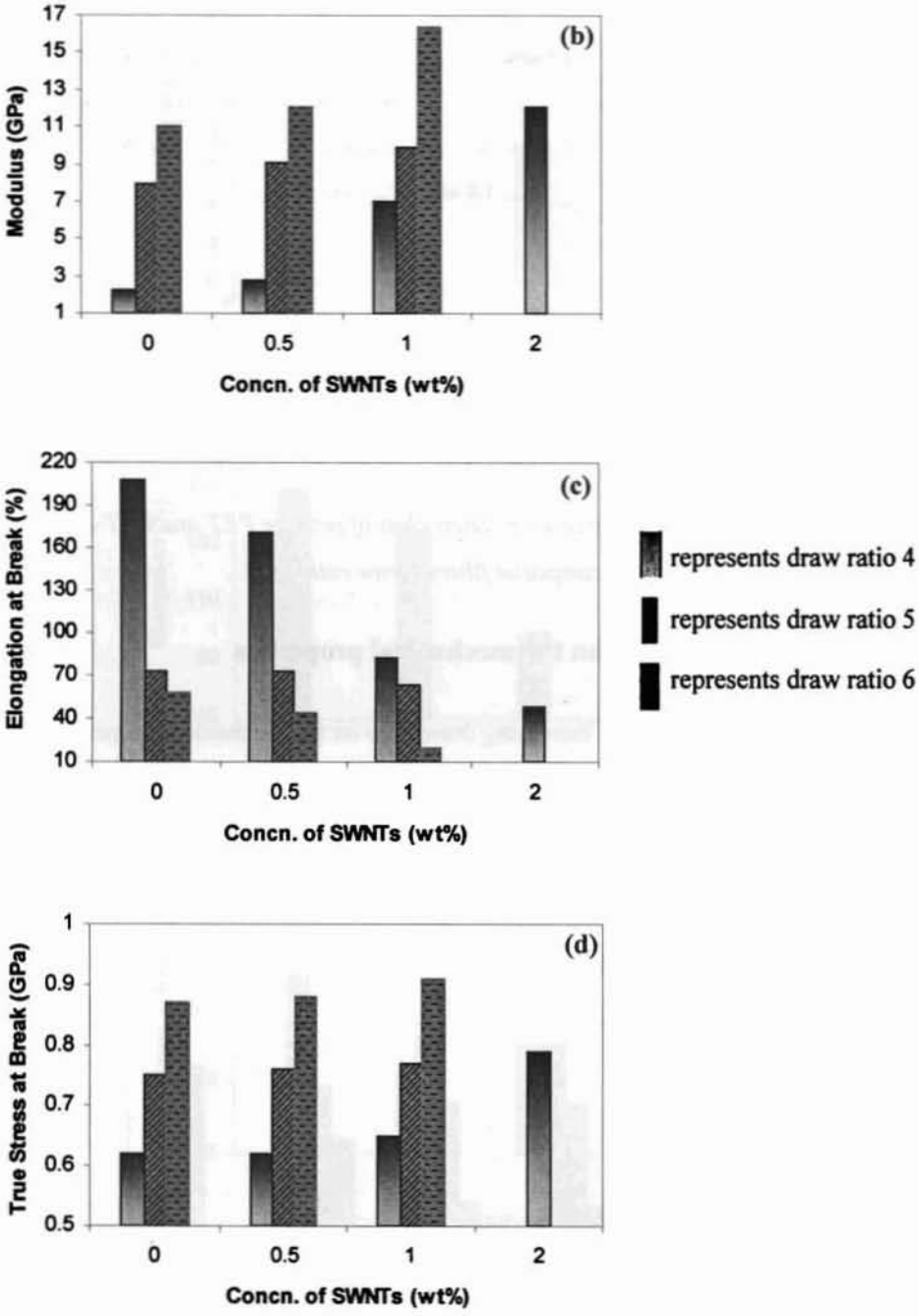

Fig. 5.6 Effect of draw ratio on the (b) modulus (c) elongation and (d) true stress at break of PET-SWNT nanocomposite filaments

5.3.3 Thermal stability

Temperature dependence of the weight loss characteristics (TGA) of PET-SWNT nanocomposite fibers is given in figure 5.7. The results indicate that the presence of SWNTs at a level of upto 2.0 wt% has no significant influence on the thermal stability of PET fiber. Typical DTG curves are given in figure 5.8.

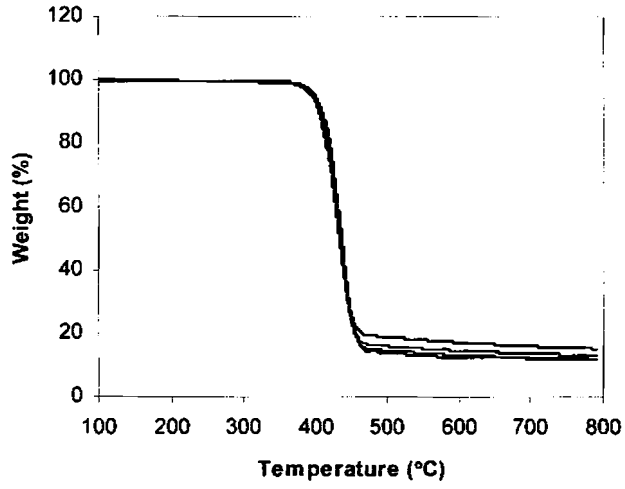

Fig. 5.7 TGA traces of neat PET (lowest curve) and PET-SWNT nanocomposite fibers

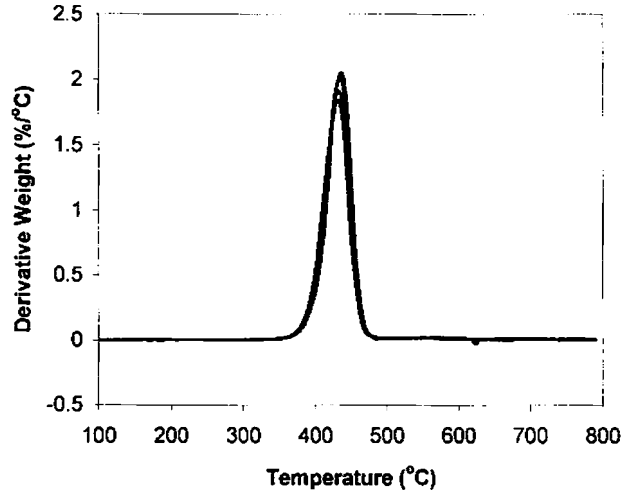

Fig. 5.8 Typical DTG traces of PET-SWNT nanocomposite fibers

5.4 Conclusions

PET-SWNT nanocomposite fibers have been prepared through melt spinning followed by subsequent drawing. The mechanical properties indicated that SWNTs provide significant reinforcement to PET fibers. The tenacity and modulus values of the fibers increased with draw ratio, the reason being the increased molecular orientation and crystallization induced by drawing. Thermogravimetric analysis revealed that the thermal stability of the fibers is not affected with SWNTs at low concentrations.

References

1. Carothers WH. J. Am. Chem. Soc. 1929;51:2548.
2. Gupta VB, Kothari VK, editors. Manufactured Fibre Technology. Chapman and Hall, London; 1997.
3. Gurudatt K, De P, Rakshit AK, Bardhan MK. J. Appl. Polym. Sci. 2003;90:3536.
4. Zeng J, Kumar S, Iyer S, Schiraldi DA, Gonzalez RI. High Performance Polymers 2005;17:403.
5. Jin X, Xiao C, An S, Jia G. J. Appl. Polym. Sci. 2006;102:4144.
6. Kim MS, Kim HK, Byun SW, Jeong SH, Hong YK, Joo JS, Song KT, Kim JK, Lee CJ, Lee JY. Synth. Met. 2002;126:233.
7. Cilffi N, Torsi L, Sabbatini L, Zambonin PG, Bleve-Zacheo T. J. Electroanal. Chem. 2000;488:42.
8. Huang CY, Wu CC. Euro. Polym. J. 2000;36:2729.
9. Asher PP. U.S. Pat. 5,952,099, 1999.
10. Yamada S. U.S. Pat. 4,743,505, 1988.
11. Hongwei L, Xushan G, Yan T. Chinese Journal of Materials Research 2002;17:444.

12. Junping Y, Xushan G, Yan T. Chinese Journal of Materials Research 2004;18:556.

13. Lee HJ, Oh SJ, Choi JY, Kim JW, Han J, Tan LS, Baek JB. Chem. Mater. 2005;17:5057.

14. Shin DH, Yoon KH, Kwon OH, Min BG, Hwang CI. J. Appl. Polym. Sci. 2006;99:900.

15. Xushan G, Yan T, Shuangyan H, Zhenfu G. Chemical Fibers International 2005;55:170.

16. Kumar S, Dang TD, Arnold FE, Bhattacharyya AR, Min BG, Zhang XF, Vaia RA, Park C, Adams WW, Hauge RH, Smalley RE, Ramesh S, Willis PA. Macromolecules 2002;35:9039.

17. Sandler JKW, Pegel S, Cadek M, Gojny F, van Es M, Lohmar J, Blau WJ, Schulte K, Windle AH, Shaffer MSP. Polymer 2004;45:2001.

18. Sreekumar TV, Liu T, Min BG, Guo H, Kumar S, Hauge RH, Smalley RE. Adv. Mater. 2004;16:58.

19. Bhattacharyya AR, Sreekumar TV, Liu T, Kumar S, Ericson LM, Hauge RH, Smalley RE. Polymer 2003;44:2373.

20. Kumar S, Doshi H, Srinivasrao M, Park JO, Schiraldi DA. Polymer 2002;43:1701.

21. Andrews R, Jacques D, Rao AM, Rantell T, Derbyshire F, Chen Y, Chen J, Haddon RC. Appl. Phys. Lett. 1999;75:1329.

22. Qian D, Dickey EC, Andrews R, Rantell T. Appl. Phys. Lett. 2000;76:20.

23. Haggenmueller R, Gommans HH, Rinzler AG, Fischer JE, Winey KI. Chem. Phys. Lett. 2000;330:219.

24. Néri W, Maugey M, Miaudet P, Derré A, Zakri C, Poulin P. Macromol. Rapid Commun. 2006;27:1035.

25. Ma H, Zeng J, Realff ML, Kumar S, Schiraldi DA. Compos. Sci. Technol. 2003;63:1617.

26. Siochi EJ, Working DC, Park C, Lillehei PT, Rouse JH, Topping CC, Bhattacharyya AR, Kumar S. Composites: Part B 2004;35:439.

27. Doi M, Edwards SF. The Theory of Polymer Dynamics. Oxford University Press; 1986.

Chapter 6

Natural rubber-SWNT nanocomposites

Fabrication and characterization*

Abstract

Natural rubber (NR) based nanocomposites have been prepared with single walled carbon nanotubes (SWNTs). The conventional mill mixing method is found to be not effective in efficiently dispersing the nanotubes in NR matrix. To rectify this problem and to get a better dispersion of SWNTs in the matrix, they have been dispersed in water through ultrasonication with the help of added surfactants and subsequently mixed with NR latex. Casting the compounded latex followed by curing gave good quality composite films with significantly improved properties. For example, the tensile strength and modulus of the composite film containing 2.0 phr SWNTs were, respectively, 56 % and 63 % higher in relation to pure NR. Electrical percolation threshold concentration of SWNTs in the NR matrix was found to be 1.5 phr. Thermogravimetric analysis indicated that the thermal stability of natural rubber remains unaffected in the presence of SWNTs at low concentrations.

---

*A part of the work described in this chapter has been presented at the *International Conference,* ***Asia Rub Tech Expo '06****, Nov 23-25, 2006, Cochin, India.*

6.1 Introduction: Natural rubber

Natural rubber (NR) is a high molecular weight polymer of isoprene (2-methyl 1,3-butadiene) (figure 6.1). It is commonly obtained from the latex of *Hevea Brasiliensis* tree and is the oldest known rubber and the most versatile one for fabrication into rubber products.[1]

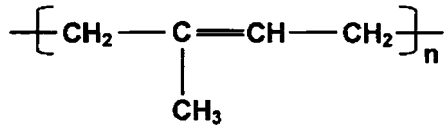

Fig. 6.1 Structure of natural rubber (Molecular weight of repeat unit: 68.12 g/mol) [NR is the cis isomer of polyisoprene, trans isomer is called, gutta percha]

The high and reversible deformability of natural rubber is of great industrial importance. However, its initial modulus and durability are low, and an additional reinforcing phase is required for practical use.[2-4] Carbon black and silica particles have been extensively used for this purpose.[5-9] In addition, $CaCO_3$, ZnO, MgO, talc, mica etc. have also been used.[10-17] Influence of these particulate fillers on the deformability of the polymer was earlier considered to be purely hydrodynamic. However, later it was proven that specific interactions between the filler and matrix is very important in imparting the reinforcement.[18-20]

Apart from the reinforcing effect, these fillers also provide some desirable aspects when incorporated into the rubber matrix. For example, historically, tyres have been compounded with a volume fraction, V_f of carbon black well above the percolation threshold ($V_f > 20$ %), which prevents the tyre from becoming charged with static electricity during use. However, the silica filled compounds which are nowadays being developed are electrically insulating, which results in a dangerous build up of static electricity which becomes a hazard, for example, during refueling. One solution is to find a filler that when included at small quantities would not adversely affect the reinforcing properties of silica but which would make the tyres conductive. Typically, the volume fraction of the filler to reach percolation threshold is determined by the

size, distribution and shape factor of the reinforcing media. Resulting from this, it has been reported that fillers with extremely high aspect ratios (1,000-10,000) such as carbon nanotubes have a much lower percolation threshold. Therefore, it might be possible to formulate a compound, which conducts and which has all other advantages of the 'green' tyre, by incorporating relatively small amounts of carbon nanotubes into the rubber compound.

Nanoparticles have been recently used to reinforce elastomers. For example, Stephen *et al.* have studied the properties of nanocomposites of layered silicates with natural rubber and carboxylated styrene butadiene rubber and their blends.[21] Liu *et al.* have studied the structure and properties of natural rubber-organoclay nanocomposites prepared by grafting and intercalating method in latex.[22] Indeed, there are several other reports in literature regarding the preparation and characterization of natural rubber based nanocomposites with various nanofillers.[23]

Carbon nanotubes also have been considered as attractive candidates for imparting several properties to elastomers. Frogley *et al.* have studied the mechanical properties of single walled carbon nanotube (SWNT) filled silicone rubber. They observed that SWNTs provide an unprecedented level of reinforcement to the rubber matrix.[24] Kueseng and Jacob have also studied the mechanical properties of natural rubber-carbon nanotube nanocomposites.[25] They prepared the nanocomposites by incorporating carbon nanotubes in a solution of rubber and subsequently evaporating the solvent. Their report claims that the initial modulus increased by upto 50 % in relation to pure NR at the nanotube concentration as low as 1.5 phr.

In this part of the work, the effect of incorporation of SWNTs on the mechanical, thermal and electrical conducting characteristics of natural rubber is investigated. Conductive rubber nanocomposites may be used instead of metallic conductors because the soft materials have the obvious advantage of flexibility and ability to absorb mechanical shock. In the first part, a conventional mill mixing method has been tried in order to incorporate the nanotubes in NR matrix and in the latter part, a latex stage mixing method has been explored.

6.2 Incorporation of SWNTs into NR matrix: Two-roll mill mixing

6.2.1 Materials and instrumentation

6.2.1.1 NR and its compounding ingredients

Natural Rubber, NR (ISNR 5, Mooney viscosity ML(1+4) @100 °C, 82.00) was supplied by Rubber Research Institute of India, Kottayam, India. SWNTs were purchased from CarboLex Inc. (Lexington, U.S.A) (section 2.2.1.2 of this thesis). Rest of the ingredients used in compounding were of commercial grade. The formulations used are given in table 6.1.

Table 6.1

Compounding recipe

Ingredients	Concentration (phr)					
	Mix A	Mix B	Mix C	Mix D	Mix E	Mix F
Natural rubber	100	100	100	100	100	100
Zinc oxide	5.0	5.0	5.0	5.0	5.0	5.0
Stearic acid	2.5	2.5	2.5	2.5	2.5	2.5
CBS	0.6	0.6	0.6	0.6	0.6	0.6
SWNTs	-	**0.1**	**0.3**	**0.5**	-	-
HAF black	-	-	-	-	**30**	-
Aromatic oil	-	5.0	5.0	5.0	5.0	5.0
Silica	-	-	-	-	-	**30**
DEG	-	-	-	-	-	1.5
Sulphur	2.5	2.5	2.5	2.5	2.5	2.5
Antioxidant	0.5	0.5	0.5	0.5	0.5	0.5

6.2.1.2 Mill mixing

The mixing was done using a laboratory size (16 × 33 cm) two-roll mixing mill (Santosh, SMX lab 613) at a friction ratio of 1:1.25. After complete mixing the stock

was passed six times through tight nip and finally sheeted out at a fixed nip gap. The samples were kept overnight for maturation.

6.2.1.3 Determination of cure characteristics

Cure characteristics were determined using a Rubber process analyser (RPA 2000, Alpha Technologies). The die type used was biconical and the die gap was 0.487. The optimum cure time of the samples was determined at 150 °C at a frequency of 50.0 cpm and a strain of 0.20 deg.

6.2.1.4 Differential scanning calorimetry

The effect of SWNTs on the glass transition temperature of NR was studied using a Differential scanning calorimeter (DSC Q-100, TA Instruments, section 2.2.4). Samples (approximately 10 mg) were equilibrated at $^{-}$85 °C, kept isothermally for 15 min and were then heated at 20 °C/min to ambient.

6.2.1.5 Compression molding

Blanks cut from unvulcanized sheets marked with the machine direction were vulcanized at a temperature of 150 ± 1 °C and at a pressure of 200 Kg cm^{-2} in an electrically heated hydraulic press (18 × 18 cm, Santosh, SMP- 50), to their respective optimum cure times. Rectangular moldings were cooled quickly in water at the end of each curing cycle and were used for subsequent property measurements.

6.2.1.6 Mechanical, thermal and electrical properties

Dumbbell shaped tensile and angle tear specimens were punched out from the vulcanized sheets and the mechanical properties were studied using a Shimadzu Universal testing machine (UTM, model- AG1, section 3.2.2) with a load cell of 10 kN capacity. The gauge length between the jaws at the start of each test was adjusted to 30 mm and the measurements were carried out at a cross-head speed of 500 mm/min. Average of atleast six sample measurements represents each data point.

Hardness of the 6 mm thick molded samples was measured using a Durometer (Zwick) and the results are expressed in Shore A units. Thermogravimetric analyser (TGA Q-50, TA Instruments) was used to study the effect of SWNTs on the thermal stability of NR (section 3.2.6). The D.C. electrical conductivity of the samples (rectangular strips of dimensions, 40 × 15 × 1.8 mm) was measured using a Keithley Nanovoltmeter using a standard four-probe electrode configuration (section 3.2.8).

6.2.2 Results and discussion

6.2.2.1 Cure characteristics

Cure time and scorch time of NR vulcanizates containing SWNTs at different concentrations is given in table 6.2. The data indicate that they remain unaffected with mill mixed SWNTs at low concentrations. The cure time and scorch time values of NR vulcanizates containing carbon black and silica at 30 phr are slightly reduced as compared with the gum compound.

Table 6.2

Cure characteristics of composites of NR with SWNTs, carbon black and silica

Sample	Cure time (min)	Scorch time (min)
Mix A	10.68	3.42
Mix B	10.23	3.53
Mix C	10.44	3.27
Mix D	10.46	3.70
Mix E	9.85	2.16
Mix F	9.87	2.77

6.2.2.2 Glass transition temperature

The data reported in table 6.3 indicate that SWNTs when incorporated through mill mixing upto a concentration of 0.5 phr have no significant influence on the glass transition temperature (T_g) of natural rubber.

Table 6.3

Glass transition temperature values of NR-SWNT, NR-carbon black and NR-silica composites

Sample	T_g (°C)
Mix A	-61.90
Mix B	-61.70
Mix C	-61.83
Mix D	-61.85
Mix E	-60.72
Mix F	-61.16

6.2.2.3 Mechanical and electrical properties

Mechanical properties of the NR-SWNT nanocomposites prepared through the conventional mill mixing method are given in table 6.4. The reported values are the average of atleast six measurements. The results indicate that mill mixed SWNTs at low weight fractions have no considerable effect in reinforcing NR. Even with the highest concentration of SWNTs (0.5 phr), the increase in tensile strength and modulus is marginal. Tear strength values as well as the elongation at break also show the same trend. In comparison, carbon black and silica filled composites at higher loading levels, exhibit significant improvement in mechanical properties. High abrasion furnace (HAF) carbon black at a loading level of 30 phr increases the tensile strength of NR by around 30 %. Modulus values also show a dramatic improvement.

Hardness of the rubber samples stays almost unaffected with SWNTs upto a concentration of 0.5 phr. A comparison is also made with conventional particulate fillers at a concentration of 30 phr. The hardness of the samples is significantly enhanced with these fillers at a high loading level. This is expected, because, as more filler particles get into the rubber, the elasticity of the rubber chains is reduced, resulting in more rigid vulcanizates.[26]

Table 6.4

Mechanical properties of composites of NR with SWNTs, carbon black and silica

Sample	Tensile strength (MPa)	Tensile modulus* (MPa)	Elongation at break (%)	Tear strength (N/mm)	Hardness (Shore A)
Mix A	20.39	1.10	1210.6	38.54	35.5
Mix B	20.81	1.10	1210.8	39.74	36.0
Mix C	21.41	1.12	1208.5	39.14	36.0
Mix D	21.94	1.27	1201.1	40.01	36.1
Mix E	26.72	4.64	850.6	99.18	51.0
Mix F	24.77	1.99	1139.8	59.10	45.0

*at 300 % elongation

Electrical conductivity measurements indicate that the samples other than carbon black filled NR have conductivity, an order of magnitude, 10^{-12} S cm^{-1}. Carbon black at a loading level of 30 phr can induce conductivity to the matrix polymer, an order of magnitude, 10^{-7} S cm^{-1}. It may be concluded that mill mixed SWNTs upto a concentration of 0.5 phr are not effective in forming a percolative network in the NR matrix.

6.2.2.4 Thermal stability

The effect of mill mixed SWNTs on the thermal stability of natural rubber is given in the table 6.5. The data indicate that, thermal stability of NR remains unaffected with SWNTs at low concentrations. A comparison is also made with the carbon black and silica filled samples. It is observed that the onset of thermal degradation for the samples with conventional fillers at a high concentration considerably increases as compared to that of pure NR.

Table 6.5

TGA data for NR-SWNT, NR-carbon black and NR-silica composites

Sample	Temp. at 10 % decomposition (°C)	Temp. at 50 % decomposition (°C)	Temp. at 90 % decomposition (°C)	Residue at 800 °C (%)
Mix A	340.54	383.48	440.96	5.56
Mix B	340.40	386.60	438.28	4.58
Mix C	342.82	388.52	441.14	4.38
Mix D	342.60	388.45	440.99	5.27
Mix E	355.50	402.34	-	24.01
Mix F	344.53	397.70	-	22.14

On the basis of the above results, it may be concluded that mill mixing is not an effective method to disperse carbon nanotubes efficiently in NR matrix. More over, since the minimum capacity of a laboratory-size mixing mill is 100 g, trials to study the effect of SWNTs at higher concentrations through this method are rather limited. In order to overcome these limitations, and to get a better dispersion of SWNTs in the NR matrix, a latex stage mixing is tried, the details of which are given in following sections.

6.3 NR-SWNT nanocomposites through latex stage mixing

In this part of the work, SWNTs have been dispersed in water by sonication with the help of added surfactants and subsequently mixed with natural rubber latex. The physical adsorption of surfactants/long chain polymers on SWNTs offers an attractive solution to prevent their agglomeration in solution. The advantage of this method is that it does not involve covalent or ionic interactions on SWNTs.[27] The surfactant or the polymer can either thread themselves onto or wrap themselves around the surfaces of SWNTs and will disrupt the van der Waals interactions which cause SWNTs to aggregate into bundles.[28] The effect of use of these kinds of surfactants has been reported elsewhere.[29-32]

The rubber latex is compounded as per standard recipe along with SWNT dispersions at different concentrations and the compounded latex mix is then cast onto glass trays and vulcanized.

6.3.1 Materials and methods

6.3.1.1 Latex, surfactants and compounding ingredients

Natural rubber latex: NR latex (Dry Rubber Content (DRC) = 60 %, Total Solids Content (TSC) = 61.2 %) was purchased from Njavallil latex, Cochin, India.

Surfactants: Sodium dodecyl benzene sulphonate ($C_{18}H_{29}NaO_3S$, hereafter referred as NaDDBS) was purchased from Loba Chemie. Sodium dodecyl sulphate ($C_{12}H_{25}NaO_4S$- hereafter referred as SDS) was purchased from Sisco Research Laboratories. Polyvinyl alcohol (PVA) was supplied by Fluka. Isooctyl phenoxy polyethoxy ethanol (commercially known as Criton X-100) and Sodium benzoate (C_6H_5COONa) was obtained from Central Drug House.

Compounding ingredients: The recipe for NR latex compounding is given in table 6.6. Aqueous dispersions of ZnO, ZDC and Sulphur (50 %) were prepared by ball milling (72 h) using stainless steel jars and ceramic balls. These dispersions contain small amounts of Sodium methylene bis naphthalene sulphonic acid (commercially known as Dispersol F), which helps to prevent reagglomeration of the dispersed particles. Potassium oleate was prepared by mixing stoichiometric amounts of Potassium hydroxide (dissolved in water) with Oleic acid at ~ 75 °C.

6.3.1.2 Preparation of the nanocomposites

Natural rubber latex was compounded as per the formulation given in table 6.6. Carbon nanotube dispersions have been prepared using a mechanical probe sonicator (13 mm, VibraCell Processor VC 750, operating at 40 % of the maximum power 750 W- figure 4.1 and section 4.2.3) by sonicating aqueous suspension of nanotubes along with the added surfactant for 20 min.

Table 6.6

Formulation for NR latex compounding

Ingredients	Amount (g)
Centrifuged latex (60 % DRC)	167.0
50 % ZnO dispersion	1.0
50 % ZDC dispersion	2.0
50 % Sulphur dispersion	3.0
10 % KOH solution	1.0
10 % Potassium oleate solution	1.0
20 % Vulcastab VL* solution	1.0

*Vulcastab VL- Polyethylene oxide condensate

The nanotube dispersions have been mixed with the compounded latex at various compositions so as to result SWNT concentrations of 0.5-2.0 phr in NR, and stirred well using a magnetic stirrer for ~ 30 min so as to achieve uniformity. The samples were cast onto flat glass trays in order to make films. They were kept overnight to remove excess water and then cured at 100 °C for 1 h in an oven.

6.3.1.3 Rheological experiments

Rheological experiments of the latex systems were carried out using a Haake Viscotester (model VT 550). Coaxial cylinder sensors according to ISO 3219 were used for the measurements. The experiments were done at 25 °C over a range of shear rates. Effect of temperature on the viscosity was also studied for two selected compositions.

Rest of the experimental techniques used and procedures adopted for this part of the work are mentioned in sections 6.2.1.4 and 6.2.1.6.

6.3.2 Results and discussion

To evaluate the competing stabilization characteristics of SWNT-dispersions, the dispersing power of five different surfactants: Sodium dodecyl benzene sulphonate

(NaDDBS), Sodium dodecyl sulphate (SDS), Polyvinyl alcohol (PVA), Isooctyl phenoxy polyethoxy ethanol (Criton X-100) and Sodium benzoate have been explored.

The first step toward stabilization was to find suitable concentration ratios of nanotubes to the surfactant. To this end, nanotubes were suspended in water with various surfactant concentrations and sonicated for 20 min. A ratio was deemed suitable when the nanotubes dispersed and did not get reaggregate after sonication. The optimum ratio of nanotubes to surfactant varied from 1:2 to 1:10 by weight for different surfactants. The SWNT-NaDDBS dispersion was by far the most stable; it remained dispersed for atleast six weeks. The optimum ratio in the case of NaDDBS was 1:5. Presumably, most of the surfactant in suspension adsorbed onto the nanotube surfaces. Neither sedimentation nor aggregation of nanotube bundles was observed in this case. By contrast we were unable to prepare nanotube dispersions that are stable with other additives. It is readily observed that the NaDDBS-nanotube dispersion is homogeneous, whereas the rest contain coagulated bundles of tubes at the bottom of their respective containers (figure 6.2).

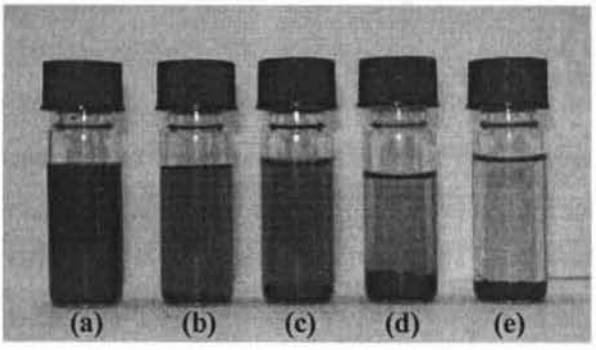

Fig. 6.2 Vials containing aqueous dispersions of SWNTs in (a) NaDDBS, (b) SDS, (c) PVA, (d) Criton X-100 and (e) Sodium Benzoate (Photograph taken after six weeks of the sample preparation)

Tube stabilization depends on the surfactant molecules that lie on the tube surface parallel to the cylindrical axis. It can be assumed that the alkyl chain groups of a surfactant molecule adsorb flat along the length of the tube instead of the diameter. It

has already been reported that NaDDBS disperses the tubes better than SDS because of its benzene rings and Criton X100 because of its slightly longer alkyl chain (figure 6.3).[33]

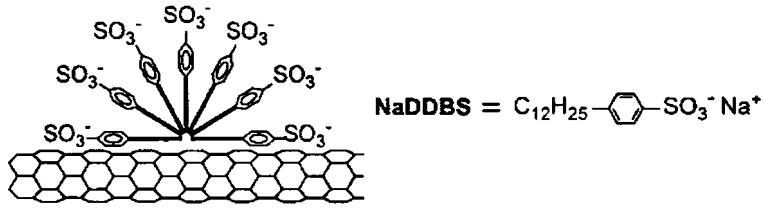

Fig. 6.3 Schematic representation of adsorption of NaDDBS onto the SWNT surface

The properties of natural rubber-SWNT nanocomposites prepared through latex compounding assisted with ultrasound (+surfactant) treatment are summarized in the following sections. Flow properties of the latex compounds are also investigated prior to making the films.

6.3.2.1 Rheology of latex compounds

Rheological behavior of latex compounds is industrially important as far as the manufacturing of latex goods is concerned. There have been many reports in literature regarding the rheological properties of various latex systems.[34,35] Understanding the flow behavior of latices having fillers can even help to study the matrix-filler interaction. In this part of the study, rheological behavior of natural rubber latex containing various amounts of carbon nanotubes was studied with reference to shear rate, concentration of nanotubes and the temperature of testing.

Figure 6.4 represents the plots of viscosity versus shear rate measured at 25 °C for the latex compounds at three selected composition of SWNTs. As expected, the viscosity of latices increases as a function of filler loading over the entire range of shear rate studied. This is attributed to the reinforcement that occurred in the system in the presence of carbon nanotubes. It is also observed from the figure that the viscosity of the SWNT reinforced NR latex samples decreases with increase of shear rate, representing pseudoplastic nature or in other words, shear thinning behavior. This effect is more predominant in the case of samples with high filler loadings.

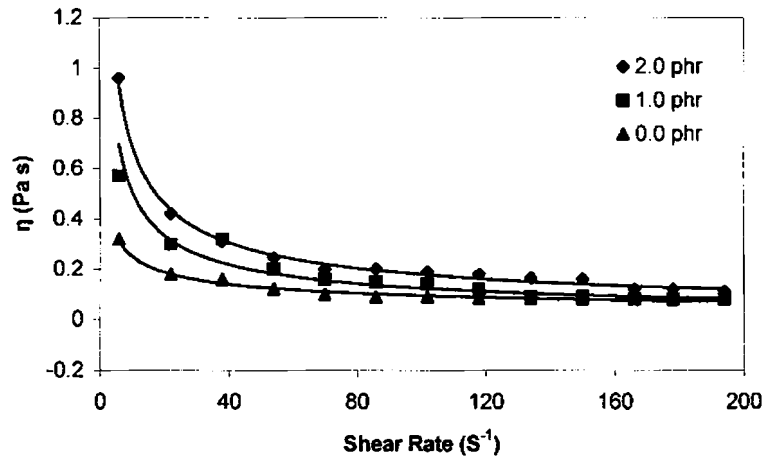

Fig. 6.4 Effect of shear rate on the viscosity of NR-SWNT latex compounds

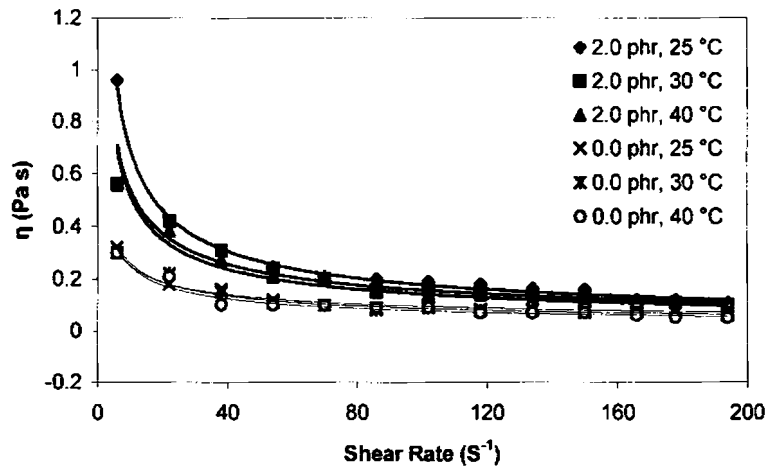

Fig. 6.5 Viscosity Vs. shear rate plots at different temperatures

Figure 6.5 indicates the effect of temperature on the viscosity of the latex systems. It is noticeable that the viscosity of the samples decreases with temperature over the entire range of shear rate tested, the effect of which is more predominant in the case of the NR-SWNT system as compared to pure NR latex system. These results are almost in agreement with those reported by Stephen *et al.* who studied the rheological behavior of latex systems of natural rubber containing layered silicates as nanofillers.[21]

6.3.2.2 Glass transition temperature

The DSC results for the glass transition temperature of NR and NR-SWNT nanocomposites prepared through latex stage mixing are given in table 6.7. The data indicate that the glass transition temperature of NR stays almost unaffected with SWNTs upto a concentration of 2.0 phr.

Table 6.7

Glass transition temperature values of NR-SWNT nanocomposites

Concentration of SWNTs (phr)	Glass transition temperature, T_g (°C)
0.0	-62.04
0.5	-62.68
1.0	-62.10
1.5	-62.61
2.0	-61.19

6.3.2.3 Mechanical properties

Mechanical properties of NR-SWNT nanocomposites prepared through latex stage mixing are summarized in figure 6.6. It is evident from the results, that SWNTs significantly increase the strength and modulus of natural rubber. For example, the tensile strength of NR increases by around 56 % with a nanotube concentration as low as 2.0 phr (figure 6.6 (a)). The tensile modulus of the NR-SWNT nanocomposite at this concentration is roughly 63 % higher as compared to that of pure rubber vulcanizate (figure 6.6 (b)). Tear strength is also higher by around 30 % as compared with pure rubber at SWNT fractions as low as 2.0 phr (figure 6.6 (d)). However, the elongation at break of the matrix reduces with increasing nanotube loading due to an embrittlement of the elastomer matrix (figure 6.6 (c)).

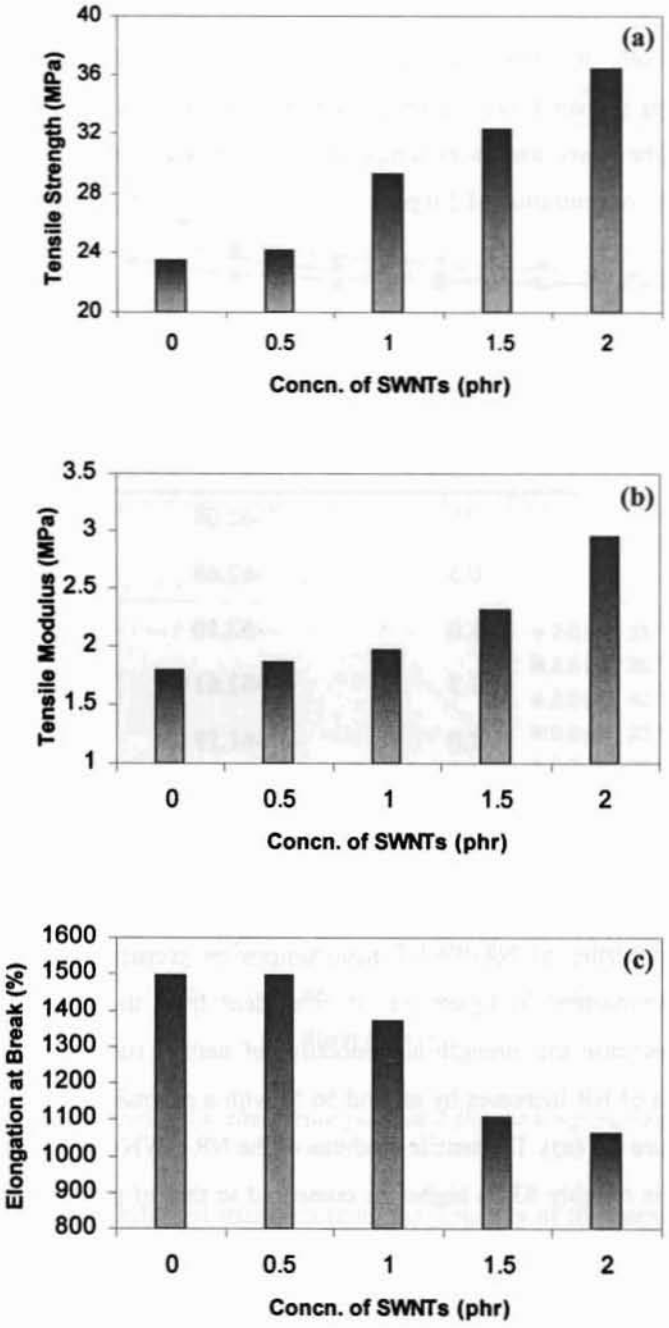

Fig. 6.6 Effect of SWNT concentration on the mechanical properties of NR-SWNT nanocomposites

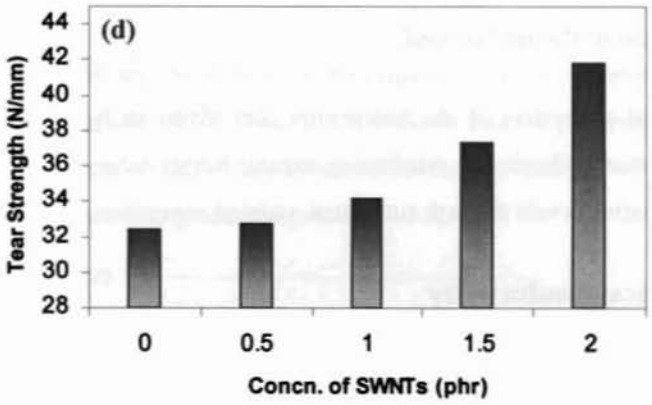

Fig. 6.6 (d) Tear strength of the nanocomposites as a function of SWNT concentration

These results are in agreement with those reported by Atieh *et al.* who dissolved both the nanotubes (by sonication) and the rubber in toluene to prepare the NR-MWNT nanocomposites.[36] Their paper reports a significant improvement in the tensile strength and modulus of natural rubber. Varghese *et al.* also adopted latex compounding method to prepare natural rubber based nanocomposites with layered silicates.[37] They observed that the nanocomposites exhibit significant enhancement in mechanical properties and thermal stability in relation to pure natural rubber.

Although its mechanism is not fully understood, there is a general agreement about the basic processes contributing to the reinforcement of filled elastomers.[38-40] In addition to the expected increase in the modulus resulting from the inclusion of rigid filler particles in the soft matrix, another contribution arises from the filler-rubber interactions, leading to additional cross-links in the network structure. The improved reinforcement observed in NR-SWNT nanocomposites is due to the interaction between SWNTs and the rubber matrix. An essential condition for this interaction is an efficient dispersion of the nanofillers in the matrix, which is accomplished through surfactant-assisted sonication. A good interface between the SWNTs and the rubber supports the material to withstand stress. As described in chapter 1, SWNTs are extremely strong materials compared to other types of fillers, thus making them good

candidates as nanofillers. Under a load, the matrix distributes the force to SWNTs, which carry most of the applied load.

The mechanical properties of the nanocomposites given in figure 6.6 indicate that SWNTs are indeed effective in reinforcing natural rubber when incorporated in latex stage at low loading levels through surfactant-assisted sonication.

6.3.2.4 Electrical conductivity

The room temperature D.C. electrical conductivity results of NR-SWNT nanocomposites are given in figure 6.7. It is obvious from the figure that SWNTs are effective in imparting electrical conductivity to the insulating rubber matrix.

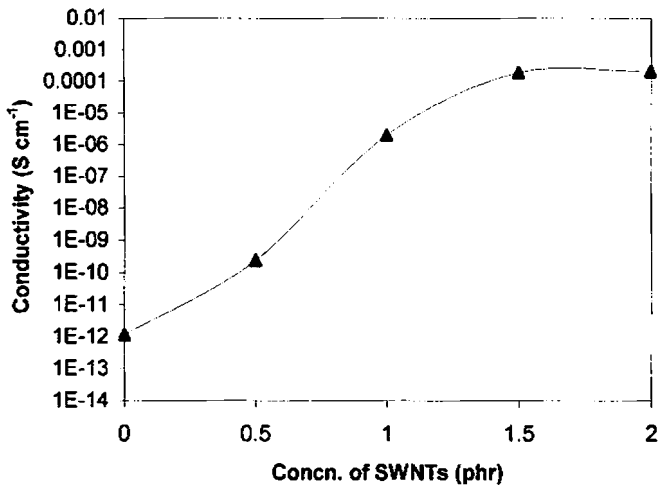

Fig. 6.7 Electrical conductivity of NR-SWNT nanocomposites

The conductivity of pure natural rubber is of the order of 10^{-12} S cm^{-1}. At concentrations exceeding 1.0 phr, the conductivity surpasses an order of magnitude of 10^{-6} S cm^{-1} and reaches percolation with a value of 10^{-4} S cm^{-1} at SWNT fractions exceeding 1.5 phr. These results are in good agreement with several literature reports regarding the carbon nanotubes-induced electrical conductivity in various insulating polymer matrices.[41,42]

6.3.2.5 Thermal stability

TGA plots of pure NR and NR-SWNT nanocomposites prepared through latex stage mixing are given in figure 6.8.[43-45] The results indicate that the presence of SWNTs at low weight fractions has no significant effect on the thermal stability of natural rubber. Typical DTG curves are also given in figure 6.9.

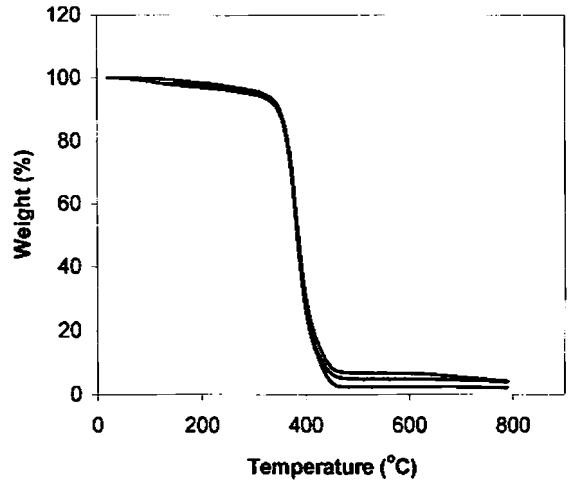

Fig. 6.8 Temperature dependence of the weight loss characteristics (TGA) of pure NR (lowest curve) and NR-SWNT nanocomposites (1.0 and 2.0 phr)

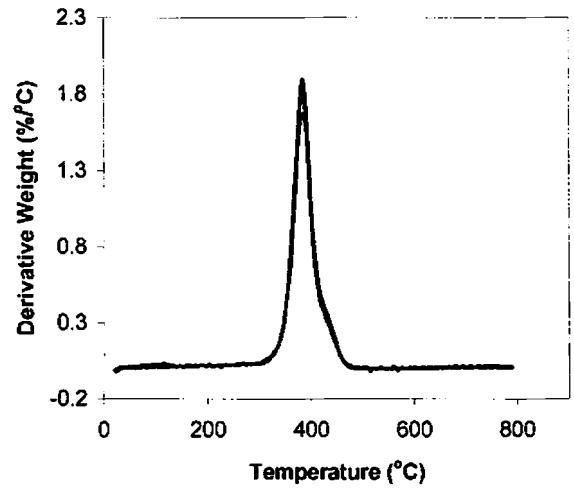

Fig. 6.9 Typical DTG traces of NR and NR-SWNT nanocomposites

6.3.2.6 Ageing resistance

The mechanical properties of NR-SWNT nanocomposites after thermal ageing (in an oven) at 100 °C for different time intervals are given in table 6.8. Samples designated as 0 h are unaged samples, those designated as 24 h and 48 h are samples that are aged, for 24 h and 48 h respectively. The data in table 6.8 are the average of atleast six measurements. It is noticeable from the results that SWNTs at concentrations of upto 2.0 phr have no significant influence on the thermal ageing of natural rubber.

Table 6.8

Ageing resistance of NR-SWNT nanocomposites

Concn. of SWNTs (phr)	Tensile strength (MPa)			Tensile modulus (MPa)		
	0 h	24 h	48 h	0 h	24 h	48 h
0.0	23.39	20.90	14.51	1.80	1.26	1.01
0.5	24.11	20.01	15.09	1.86	1.30	1.01
1.0	29.31	23.03	20.56	1.97	1.36	1.11
1.5	32.34	28.81	23.81	2.31	2.10	2.01
2.0	36.49	31.15	28.94	2.95	2.31	2.05

6.4 Conclusions

Natural rubber-single walled carbon nanotube nanocomposites have been prepared through conventional two-roll mill mixing as well as a latex stage mixing. The former method is not effective in improving the materials properties, whereas the latter provides dramatic improvement in the mechanical properties. SWNTs when incorporated to the NR matrix through latex stage mixing are found to be effective in imparting electrical percolation at low filler fractions. The thermal stability and ageing characteristics of NR stay almost unaffected with SWNTs at concentrations of upto 2.0 phr.

References

1. Blackley DC. Polymer Latices: Science and Technology. Vol. 2, Types of Latices, 2nd edition. Chapman and Hall; 1997.
2. Nielson LE. Mechanical Properties of Polymers and Composites. Marcel Dekker; 1974.
3. Kraus G. Reinforcement of Elastomers. Wiley; 1965.
4. Hundiwale DG, Kapadi UR, Desai MC, Bidkar SH. J. Appl. Polym. Sci. 2002;85:995.
5. Guth E. J. Appl. Phys. 1944;16:20.
6. Kurian T, De PP, Khastgir D, Tripathy DK, De SK, Peiffer DG. Polymer 1995;36:3875.
7. Yatsuyanagi F, Suzuki N, Ito M, Kaidou H. Polymer 2001;42:9523.
8. Alberola ND, Benzarti K, Bas C, Bomal Y. Polym. Compos. 2001;22:312.
9. Zhang A, Wang L, Lin Y, Mi X. J. Appl. Polym. Sci. 2006;101:1763.
10. Seto J. Rubber Chem. Technol. 1977;50:333.
11. Smit PPA. Rubber Chem. Technol. 1968;41:1194.
12. Ahmed S, Jones FR. J. Mater. Sci. 1990;25:4933.
13. Edwards DC. J. Mater. Sci. 1990;25:4175.
14. Wolff S. Rubber Chem. Technol. 1996;69:325.
15. Payne AR, Whittaker RE. Rubber Chem. Technol. 1971;44:440.
16. Janecek J. Rubber Chem. Technol. 1962;35:833.
17. Dizon ES, Hicks AE, Chirico VE. Rubber Chem. Technol. 1974;47:231.
18. Bokobza L, Rapoport O. J. Appl. Polym. Sci. 2002;85:2301.
19. Hepburn C. Plast. Rubber Int. 1984;9:11.
20. Parkinson D. Reinforcement of Rubber. Lakeman and Co.; 1957.

21. Stephen R, Alex R, Cherian T, Varghese S, Joseph K, Thomas S. J. Appl. Polym. Sci. 2006;101:2355.

22. Liu L, Luo Y, Jia D, Fu W, Guo B. J. Elast. Plast. 2006;38:147.

23. López-Manchado MA , Herrero B, Arroyo M. Polym. Int. 2004;53:1766.

24. Frogley MD, Ravich D, Wagner HD. Compos. Sci. Technol. 2003;63:1647.

25. Kueseng K, Jacob KI. Euro. Polym. J. 2006;42:220.

26. Imanah JE, Okieimen FE. J. Appl. Polym. Sci. 2003;90:3718.

27. Bandyopadhyay R, Roth EN, Regev O, Rozen RY. Nano Letters 2002;2:25.

28. Star A, Stoddart JF, Steuerman D, Diehl M, Boukai A, Wong EW, Yang X, Chung SW, Choi H, Heath JR. Angew. Chem. Int. Ed. 2001;40:1721.

29. Cui S, Canet R, Derre A, Couzi M, Delhaes P. Carbon 2003;41:797.

30. Gong X, Liu J, Baskaran S, Voise RD, Young JS. Chem. Mater. 2000;12:1049.

31. Moore VC, Strano MS, Haroz EH, Hauge RH, Smalley RE. Nano Letters 2003,3:1379.

32. Barraza HJ, Pompeo F, O'Rear EA, Resasco DE. Nano Letters 2002;2:22.

33. Islam MF, Rojas E, Bergey DM, Johnson AT, Yodh AG. Nano Letters 2003;3:269.

34. Varkey JT, Rao SS, Thomas S. J. Appl. Polym. Sci. 1996;62:2169.

35. Varkey JT, Thomas S, Rao SS. J. Appl. Polym. Sci. 1995;56:451.

36. Atieh MA, Girun N, Ahmadun FR, Guan GT, Mahdi ES, Baik DR. AZojono: J. Nanotech. Online 2005;1:1.

37. Varghese S, Karger-Kocsis J. Polymer 2003;44:4921.

38. Dannenberg EM. Rubber Chem. Technol. 1975;48:410.

39. Wagner MP. Rubber Chem. Technol. 1976;49:703.

40. Voet A. J. Polym. Sci.: Macromol. Rev. 1980;15:327.

41. Yue D, Liu Y, Shen Z, Zhang L. J. Mater. Sci. 2006;41:2541.

42. Ahir SV, Terentjev EM. in Polymeric Nanostructures and Their Applications, edited by Nalwa HS. American Scientific Publishers; 2006.

43. Mathew AP, Packirisamy S, Thomas S. Polymer Degradation and Stability 2001;72:423.

44. Sharif J, Yunus WMZW, Dahlan KH, Ahmad MH. J. Appl. Polym. Sci. 2006;100:353.

45. Manchado MAL, Herrero B, Arroyo M. Polym. Int. 2003;52:1070.

Chapter 7

Summary and Conclusions

Carbon nanotubes (CNTs) have been recognized as one of the stiffest structures ever made. Since carbon-carbon covalent bonds are one of the strongest in nature, it is reasonable that a unique structure based on a perfect arrangement of these bonds oriented along a particular axis produces an exceedingly strong material. The most important application of nanotubes based on their mechanical properties is as reinforcement in composites. Their excellent strength and modulus, coupled with relatively low density, make these materials ideal candidates for weight-efficient structures, and for the same reason, CNTs are considered to be the ultimate reinforcement in polymer-based composites. Apart from the reinforcing effect, they also impart certain additional attractive features such as electrical conductivity, to the matrices in which they are dispersed.

In the present investigation, an attempt has been made to modify the performance characteristics of polymers through the incorporation of single walled carbon nanotubes (SWNTs). Owing to their attractive inherent properties and wide use, a thermoplastic polyester [poly(ethylene terephthalate)- PET] and an elastomer [natural rubber- NR] were selected for the modification.

In the first part of the study, a simple melt compounding route was adopted for preparing PET-SWNT nanocomposites; the method being a versatile and commercially viable one. Differential scanning calorimetry studies revealed that SWNTs act as effective nucleating agents for PET melt crystallization. For example, the nanotubes at a concentration as low as 300 ppm enhanced the crystallization temperature (T_c) of PET during melt cooling by 10 °C. Because of the large surface area and reasonably good dispersion of SWNTs, their nucleation effect reached saturation at very low concentrations (0.03 wt%). They also reduced the melt's isothermal crystallization

time by more than 50 %. WAXD experiments indicated oriented crystallization of PET during cooling from randomized melts containing oriented SWNTs, supporting the hypothesis that SWNTs induce crystallization of PET chains along them. Comparison of the nucleation efficiency of the SWNTs with their traditional counterparts also revealed that they are promising candidates as nucleating agents for PET.

The improved mechanical and dynamic mechanical properties of the nanocomposites revealed that a small concentration of SWNTs can considerably reinforce PET. For example, SWNTs at a level of 1 wt% increased the strength of PET by about 25 % and modulus by over 50 %. Similarly, the dynamic modulii of the nanocomposites below glass transition increased substantially; with 1.0 wt% SWNTs, the storage modulus was increased by around 50 %. This is due to the stiffening effect of nanotubes and efficient stress transfer between the polymer matrix and SWNTs. The glass transition temperature, however, was not significantly affected by SWNTs at low concentrations. Thermogravimetric analysis and thermal expansion studies revealed that carbon nanotubes do not affect the thermal and dimensional stability of PET. The increased dynamic modulii of the nanocomposite melts (as revealed from melt rheology) indicated that the nanotubes are effectively entangled in the melt state also. In particular, the dynamic storage modulus of the nanocomposite melt at low frequencies increased 100 fold with 3.0 wt% SWNTs. Similarly, SWNTs were found to impart electrical conductivity to the PET matrix, which otherwise is an insulator.

To further improve the dispersion characteristics, PET-SWNT nanocomposites have been prepared through an ultrasound assisted dissolution-evaporation route. The enhancement in crystallization temperature of PET on dispersion of SWNTs through the latter method at a weight fraction as low as 0.3 % was roughly 24 °C. The observed increase in the T_c value on incorporation of SWNTs is almost double as compared to that for the melt route (12.5 °C) at the very same concentration. As expected, they could also impart electrical conductivity to the PET matrix, at concentrations still lower than those required in the melt route. For example, the percolation threshold concentration for conductivity is almost half the value in the solution route (1.0 wt%) in comparison with that in the melt route (2.0 wt%).

Since the melt compounding method produces sufficiently larger quantities of samples, they were further used for fabricating nanocomposite fibers. The mechanical properties of PET-SWNT nanocomposite fibers prepared through melt spinning and drawing indicated that SWNTs provide significant reinforcement to the polyester fiber matrix even at low loading fractions. For example, the tenacity and initial modulus of the composite fiber with 2.0 wt% SWNTs were, respectively, ~ 2.5 times and ~ 5 times higher as compared to pristine PET fiber prepared under identical conditions. However, the elongation was drastically reduced by the presence of SWNTs due to the embrittlement of the fiber matrix. The elongation of the nanocomposite fiber with 2.0 wt% SWNTs was reduced by ~ 75 % as compared to that of the pristine PET fiber. The tenacity and modulus values of the fibers increased with draw ratio, due to the increased molecular orientation achieved during drawing.

In the last part of the work, natural rubber (NR) based nanocomposites have been prepared with SWNTs. The nanotubes have been incorporated into the elastomer matrix through conventional mill mixing as well as a latex stage mixing. The former method resulted in composites with comparable materials properties in relation to pure NR vulcanizates, whereas the latter provided enormous improvement in the mechanical properties. For example, the tensile strength of NR increased by around 56 % with a nanotube concentration as low as 2.0 phr. The tensile modulus of the NR-SWNT nanocomposite at this concentration was roughly 63 % higher as compared to that of pure NR. However, the elongation at break of the matrix reduced with increasing nanotube loading. SWNTs when incorporated to the NR matrix through latex stage mixing were also found to be effective in imparting electrical conductivity at low weight fractions. The percolation threshold concentration was found to be 1.5 phr. On the other hand, thermal stability and ageing characteristics of the rubber matrix remained unaltered with SWNTs.

To conclude, single walled carbon nanotubes are proved to be promising candidates to modify the performance characteristics of poly(ethylene terephthalate) and natural rubber.

List of abbreviations and symbols

ABS	Acrylonitrile-butadiene-styrene (copolymer)
AFM	Atomic force microscopy
ARES	Advanced rheometric expansion system
BHET	Bishydroxyethyl terephthalate
CBS	N-cyclohexyl benzthiazyl-2-sulphenamide
CNFs	Carbon nanohorns
CNTs	Carbon nanotubes
CoMoCat	Cobalt molybdenum catalyst
CTE	Coefficient of thermal expansion
CVD	Chemical vapour deposition
DC	Direct current
DEG	Diethylene glycol
DMA	Dynamic mechanical analysis
DMT	Dimethyl terephthalate
DR	Draw ratio
DRC	Dry rubber content
DSC	Differential scanning calorimetry
DTG	Differential thermogravimetry
EG	Ethylene glycol
EMI	Electro magnetic interference
EVA	Ethylene-vinyl acetate (copolymer)
FETs	Field effect transistors
FOY	Fully oriented yarn
HAF	High abrasion furnace
HFIP	1,1,1,3,3,3-Hexafluro-2-propanol
HiPCO	High pressure carbon monoxide disproportionation
HOY	Highly oriented yarn
HRTEM	High resolution transmission electron microscopy
ISNR	Indian standard natural rubber

ISO	International organization for standardization
ITO	Indium tin oxide
LCD	Liquid crystal display
LCP	Liquid crystal polymer
LED	Light emitting diode
MFM	Magnetic force microscopy
MWNTs	Multi walled carbon nanotubes
NaDDBS	Sodium dodecyl benzene sulphonate
NASA	National aeronautics and space administration
NEC	National electric corporation
NR	Natural rubber
PAN	Polyacrylonitrile
PBO	Poly(p-phenylene benzobisoxazole)
PBT	Poly(butylene terephthalate)
PCDT	Poly(1,4-cyclohexane dimethylene terephthalate)
PE	Polyethylene
PEEK	Poly(ether ether ketone)
PEN	Poly(ethylene 2,6-naphthalate)
PET	Poly(ethylene terephthalate)
phr	Parts per hundred parts of rubber
PMMA	Poly(methyl methacrylate)
PmPV	Poly(p-phenlyene vinylene-co-2,5-dioctoxy-m-phenylene vinylene)
POY	Partially oriented yarn
PP	Polypropylene
PPV	Poly(p-phenylene vinylene)
PPy	Polypyrrole
PTFE	Poly(tetrafluoro ethylene)
PTT	Poly(trimethylene terephthalate)
PVA	Polyvinyl alcohol
RPA	Rubber process analyser
SDS	Sodium dodecyl sulphate
SEM	Scanning electron microscopy

SSP	Solid state polymerization
SWNTs	Single walled carbon nanotubes
TCE	1,1,2,2-Tetrachloroethane
TEM	Transmission electron microscopy
TGA	Thermogravimetric analysis
TMA	Thermo mechanical analysis
TPA	Terephthalic acid
TSC	Total solids content
UTM	Universal testing machine
WAXD	Wide angle X-ray diffraction
YAG	Yttrium aluminium garnet
ZDC	Zinc diethyl dithio carbamate

c	Concentration
G'	Storage modulus
G"	Loss modulus
I	Rate of nucleation
k	Boltzmann's constant
M_n	Number average molecular weight
t	Time
T	Temperature
T_c	Crystallization temperature
T_g	Glass transition temperature
T_m	Melting temperature
t_{peak}	Peak crystallization time
U*	Activation energy
V_f	Volume fraction
ΔF	Free energy
ΔH_c	Enthalpy of crystallization
ΔH_m	Enthalpy of melting
ΔS_m	Entropy of melting

ΔT	Degree of supercooling
$\Delta\Phi^*$	Free energy barrier for the formation of nucleus
γ_0	Strain amplitude
$\gamma(t)$	Oscillatory strain
ω	Frequency
σ	Surface energy
$\sigma(t)$	Linear shear stress
η_{rel}	Relative viscosity
$[\eta]$	Intrinsic viscosity
η^*	Complex viscosity

Publications and presentations

1. Carbon nanotubes induced crystallization of poly(ethylene terephthalate)
   K. Anoop Anand, U.S. Agarwal, Rani Joseph
   Polymer *2006;47:3976.*

2. Carbon nanotubes reinforced PET nanocomposite by melt-compounding
   K. Anoop Anand, U.S. Agarwal, Rani Joseph
   Journal of Applied Polymer Science *2006 (in press).*

3. PET-SWNT nanocomposites through ultrasound assisted dissolution-evaporation
   K. Anoop Anand, U.S. Agarwal, Rani Joseph
   European Polymer Journal *2006 (in press).*

4. PET-SWNT nanocomposite fibers through melt spinning
   K. Anoop Anand *et al.* (*to be submitted*).

5. Natural rubber-SWNT nanocomposites through latex compounding
   K. Anoop Anand *et al.* (*to be submitted*).

6. Anoop Anand K, U.S. Agarwal and Rani Joseph, *International Conference-* ***Asia Rub Tech Expo '06****, Nov 23-25, 2006, Cochin, India.*

7. Anoop Anand K, U.S. Agarwal and Rani Joseph, *International Conference on Nanoscience and Technology-* ***ICONSAT 2006****, March 16-18, 2006, India Habitat Center, New Delhi, India.*

8. Anand A, Agarwal U.S and Joseph R, *17th Annual General Meeting of Materials Research Society of India-* ***AGM-MRSI****, Feb 13-15, 2006, University of Lucknow, India.*

9. Anoop Anand K, Rani Joseph and U.S. Agarwal, *National Conference on Frontiers in Polymer Science and Technology-* ***POLYMER 2006****, Feb 10-12, 2006, Indian Association for the Cultivation of Science, Jadavpur, Kolkata, India.*

10. Anoop Anand K, U.S. Agarwal and Rani Joseph, *18th* ***Kerala Science Congress****, Jan 29-31, 2006, CESS, Thiruvananthapuram, India.*

11. Anoop Anand K, U.S. Agarwal and Rani Joseph, *58th Annual Session of Indian Institute of Chemical Engineers (IIChE), Indian Chemical Engineers Congress-* ***CHEMCON 2005****, Dec 14-17, 2005, Indian Institute of Technology, New Delhi, India.*

12. Anoop Anand K, U.S. Agarwal and Rani Joseph, *National Seminar on Emerging Trends and New Vistas in Chemistry-* ***EMTIC 2005****, Nov 29-30, 2005, Dept. of Chemistry, University of Calicut, India.*

13. Anoop Anand K, ***'Polymer Quest 2005'****, Nov 12-13, 2005, Rubber Technology Center, Indian Institute of Technology, Kharagpur, India* **(Award winning manuscript {Polymer nanocomposites} in All India Young Scientists' National Essay Competition).**

14. Anoop Anand K, ***'Polymer Quest 2003'****, Nov 1-2, 2003, Rubber Technology Center, Indian Institute of Technology, Kharagpur, India.*

Curriculum Vitae

G8999

Name	Anoop Anand K
Date of birth	10th May 1980
Nationality	Indian
Residential address	XV/19, Kuzhuppully, Parappukara, Thrissur (Dist.), Kerala – 680 310, India.

Academic records

M.Sc Chemistry... (April 2002, University of Calicut)

B.Sc Chemistry... (April 2000, University of Calicut)

Pre-Degree... (April 1997, University of Calicut)

S.S.L.C... (March 1995, State Board of Public Examinations)

After completing his Master's degree, Anoop joined the Dept. of Polymer Science and Rubber Technology (PSRT), Cochin University of Science and Technology (CUSAT), in a research project funded by *All India Council for Technical Education (AICTE),* Govt. of India. In May 2003, he registered for Ph.D (Faculty of Technology), under the supervision of Dr. Rani Joseph, Professor, PSRT, CUSAT and Dr. Uday S. Agarwal, Dept. of Chemical Engg. and Chemistry, Technical University of Eindhoven (TU/e), the Netherlands. In May 2004, Anoop was selected for a fellowship of the Dutch Government, supported by the collaboration between TU/e and PSRT/CUSAT under the MHO-NUFFIC programme. In May 2005, he joined as Research Fellow of a project funded by the *Department of Science and Technology (DST),* Govt. of India. After his Ph.D, Anoop will join as Research Associate at the Nanotechnology Centre of Amrita Institute of Medical Sciences and Research Centre, Cochin, on 01.01.2007.

UNIVERSITY LIBRARY
COCHIN UNIVERSITY OF SCIENCE AND TECHNOLOGY
Cochin - 682 022

The author may be reached at: anoopnair24@gmail.com/anoopnair24@hotmail.com